



HAL
open science

Divergent synthesis of 5',7'-difluorinated dihydroxanthene-hemicyanine fused near-infrared fluorophores

Shasha Zheng, Gu Lingyue, Michelle Jui Hsien Ong, Denis Jacquemin, Anthony Romieu, Jean-Alexandre Richard, Rajavel Srinivasan

► **To cite this version:**

Shasha Zheng, Gu Lingyue, Michelle Jui Hsien Ong, Denis Jacquemin, Anthony Romieu, et al.. Divergent synthesis of 5',7'-difluorinated dihydroxanthene-hemicyanine fused near-infrared fluorophores. *Organic & Biomolecular Chemistry*, 2019, 17 (17), pp.4291-4300. 10.1039/c9ob00568d. hal-02140853

HAL Id: hal-02140853

<https://hal.science/hal-02140853>

Submitted on 30 Dec 2021

HAL is a multi-disciplinary open access archive for the deposit and dissemination of scientific research documents, whether they are published or not. The documents may come from teaching and research institutions in France or abroad, or from public or private research centers.

L'archive ouverte pluridisciplinaire **HAL**, est destinée au dépôt et à la diffusion de documents scientifiques de niveau recherche, publiés ou non, émanant des établissements d'enseignement et de recherche français ou étrangers, des laboratoires publics ou privés.

Divergent Synthesis of 5',7'-Difluorinated Dihydroxanthene-Hemicyanine Fused Near-Infrared Fluorophores

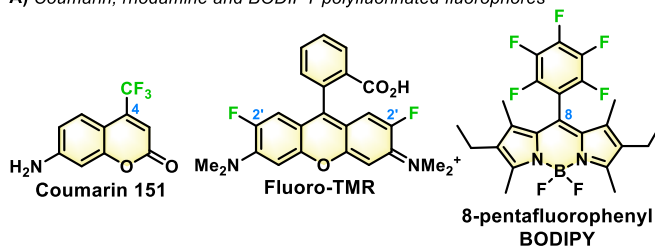
Shasha Zheng,^a Gu Lingyue,^a Michelle Jui Hsien Ong,^b Denis Jacquemin,^{*c} Anthony Romieu,^{*d,e} Jean-Alexandre Richard^{*b} and Rajavel Srinivasan^{*a}

We describe an expedient access to a 5',6',7'-trifluoro dihydroxanthene-hemicyanine fused scaffold in 2 steps and 54% overall yield from the corresponding salicylic aldehyde. A 6'-regioselective nucleophilic aromatic substitution (S_NAr) reaction with a wide range of nitrogen, sulfur or selenium nucleophiles then gives access to 16 near-infrared (NIR) fluorophores emitting in the 710-750 nm range. We also report the experimental and theoretical photophysical investigations of these unique optical agents that include the first series of 6'-heavy atom substituted dihydroxanthenes, extending the pool of polyfluorinated markers for biomedical and material applications.

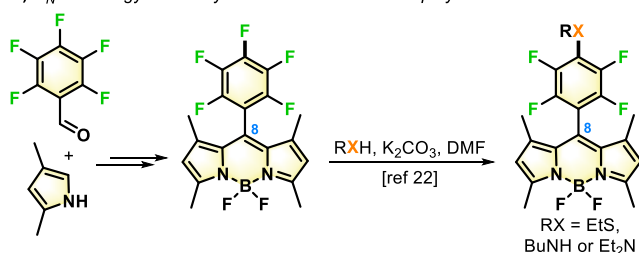
Introduction

In their quest to discover useful small molecules and organic materials, chemists resort to a variety of strategies to optimize their structure and function. One of them is the replacement of C-H bonds by C-F linkages which often provide specific and valuable properties (*e.g.*, small size of fluorine, high polarization and strength of the C-F bond, etc...)¹ beneficial for the development of pharmaceuticals,² agrochemicals,³ materials,⁴ and optical devices.⁵ The fluorine atom finds use in many applications like polytetrafluoroethylene polymers (*i.e.*, Teflon)⁶ and is currently estimated to be present in 25% of pharmaceuticals⁷ and agrochemicals.⁸ Fluorine is also useful for diagnostics with ¹⁸F positron emission tomography (PET)⁹ and magnetic resonance imaging (MRI),¹⁰ ¹⁹F nuclear magnetic resonance (NMR) analysis¹¹ or the synthesis and purification of organic molecules.¹² Because of its high sensitivity and attractive safety profile, fluorescence optical imaging is an indispensable technique in medical diagnosis and the

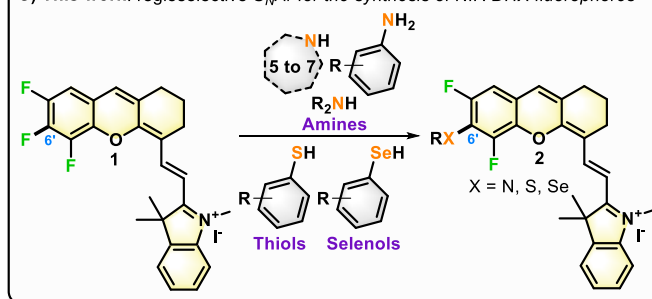
A) Coumarin, rhodamine and BODIPY polyfluorinated fluorophores



B) S_NAr strategy for the synthesis of functionalized polyfluorinated BODIPY



C) This work: regioselective S_NAr for the synthesis of NIR DHX fluorophores



Scheme 1 A) Representative polyfluorinated fluorophores; B) Nucleophilic aromatic substitution (S_NAr) of a pentafluorinated BODIPY fluorophore; C) Proposed regioselective, late-stage S_NAr for the synthesis of 5',7'-difluoro DHX-hemicyanine fused dyes **2**.

^a S. Zheng, G. Lingyue, Prof. R. Srinivasan
School of Pharmaceutical Science and Technology (SPST), Tianjin University,
Building 24, 92 Weijin Road, Nankai District, Tianjin, 300072 P. R. China
E-mail: rajavels@tju.edu.cn

^b Dr. J.-A. Richard
Organic Chemistry
Institute of Chemical and Engineering Sciences (ICES), Agency for Science,
Technology and Research (A*STAR)
8 Biomedical Grove, Neuros, #07-01, Singapore 138665
E-mail: jean_alexandre@ices.a-star.edu.sg

^c Prof. D. Jacquemin
Chimie Et Interdisciplinarité, Synthèse, Analyse, Modélisation (CEISAM), UMR
CNRS no. 6230, BP 92208, Université de Nantes, 2, Rue de la Houssinière, 44322
Nantes Cedex 3, France
E-mail: Denis.Jacquemin@univ-nantes.fr

^d Prof. A. Romieu
ICMUB, UMR 6302, CNRS, Univ. Bourgogne Franche-Comté
9, Avenue Alain Savary, 21078 Dijon cedex, France
E-mail: anthony.romieu@u-bourgogne.fr

^e Prof. A. Romieu
Institut Universitaire de France
1, Rue Descartes, Bâtiment MONGE, 75231 Paris, France

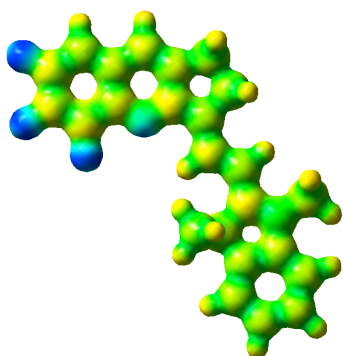
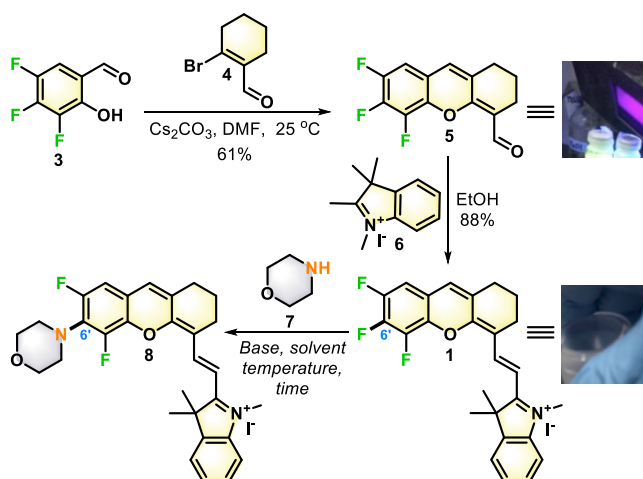


Fig. 1 Representation of the DFT electrostatic potential of the model compound **1**. Blue/yellow regions correspond the most negatively/positively charged regions, see computational details.

introduction of fluorine atoms within the core structure of organic-based fluorophores is an appealing concept for improving the performances of these small-molecule markers.¹³ For instance, the attachment of polyfluorinated tags on rhodamines,¹⁴ oxazine and squaraine dyes¹⁵ has been performed and polyfluorinated cyanines have been reported to form *J*-aggregates in fluoruous solvents.¹⁶ Coumarins, xanthene,¹⁷ BODIPY¹⁸ and cyanine dyes^{19, 20} bearing fluorine atoms have also been prepared and feature improved optical properties compared to their non-fluorinated counterparts (Scheme 1A). [¹⁸F]-radiolabelled far-red and NIR-emitting bimodal cyanine dyes have also been described.²¹ In this context, the efficiency of the nucleophilic aromatic substitution (S_NAr) reactions reported by the McClenaghan²² and Wiehe²³ groups where a nucleophile regioselectively attacks the *meso*-pentafluorinated ring of a BODIPY fluorophore attracted our attention (Scheme 1B). In this case, the spectral signatures of the penta- and tetrafluorinated fluorophores were highly similar and we wondered if we could perform a similar site-specific transformation on a different fluorophore where the replacement of fluorine atom by a heteroatom would positively influence its photophysical properties. In particular, we aimed at developing polyfluorinated fluorophores on a scaffold emitting in the near-infrared (NIR) because of the advantages long wavelengths provide when used in biological systems.²⁴ To the best of our knowledge, such fluorinated NIR fluorophores have seldom been described²⁵ and we decided to explore the reactivity of the dihydroxanthene (DHX) skeleton²⁶ since its structural modularity and attractive emission profile makes it an interesting alternative to other more conventional and popular cyanine dyes.²⁷ Leveraging on a methodology we previously developed to synthesize DHX cores,²⁸ we aimed at preparing a polyfluorinated precursor to perform a late-stage, regioselective diversification giving access to a wide range of polyfluorinated analogues. We therefore prepared the trifluorinated dihydroxanthene precursor **1** and demonstrated that a wide range of nitrogen, sulfur and selenium nucleophiles could regioselectively displace the 6'-F position to lead to unique 6-heterosubstituted NIR 5',7'-difluorinated DHX-hemicyanine fused dyes **2** (Scheme 1C). We evaluated the spectral properties of these long-wavelength fluorinated xanthene-like fluorophores either in simulated physiological conditions or in organic media and performed Time-Dependent Density Functional Theory (TD-DFT) computations to get insights into their unusual electronic absorption properties.



Entry	Base (3 eq.)	Solvent	T (°C)	Time (h)	Yield (%) ^[a]
1	–	Morpholine	80	16	0
2	Pyridine	DMSO	25	12	0
3	Pyridine	DMSO	80	12	57
4	<i>i</i> -Pr ₂ NEt	DMSO	80	12	49
5	<i>i</i> -Pr ₂ NEt	H ₂ O	80	16	0
6	Pyridine	DMF	80	12	61 ^[b]
7	–	Pyridine	80	8	61
8	–	Pyridine	40	16	0
9	Pyridine	1,4-dioxane	40	12	4

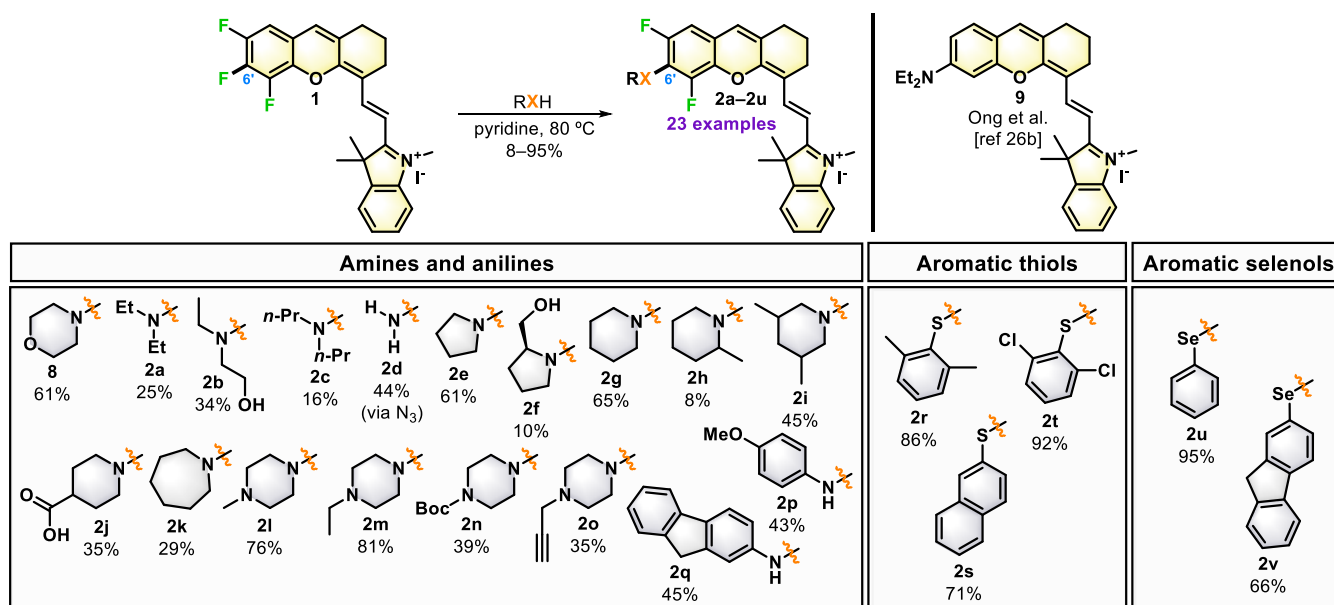
[a] Yield recorded after purification by silica-gel chromatography. [b] Incomplete conversion.

Scheme 2 Synthesis of the 5',6',7'-trifluoro DHX-hemicyanine fused dye precursor **1** and optimization of the late-stage S_NAr reaction.

Results and discussion

Late-stage S_NAr for the synthesis of a library of 5',7'-difluoro dihydroxanthene-hemicyanine fused fluorophores

Before addressing the synthetic aspect of the study, we wondered if computation could provide us any intelligence regarding the feasibility of such a 6'-regioselective S_NAr reaction. We first investigated the electrostatic potential of the molecule but it was inconclusive because all C-F functions showed very similar potential. We therefore turned to conceptual DFT to determine which one of the 5'-, 6'- or 7' carbon atoms was the most electrophilic by comparing the natural charges determined on the DHX molecule **1** in its neutral and charged counterparts. The change of charge is twice larger on the 6' carbon (-0.039e) as compared to 7' and 5' which undergo smaller variations of -0.017e and -0.010e, respectively, confirming that the 6' position is the most reactive toward nucleophiles (Fig. 1). Consequently, we performed the synthesis of the bright yellow trifluorinated precursor **5** which we prepared in one step (Cs₂CO₃, DMF) and 61% yield from the reaction between 3,4,5-trifluoro-2-hydroxybenzaldehyde **3** (prepared from the Duff formylation of 2,3,4-trifluorophenol, see ESI[†]) and 6-bromocyclohex-1-ene-1-carbaldehyde **4**. The formation of the deep blue-colored dye **1** was then achieved in 88% yield in the presence of the Fisher's base 1,2,3,3-tetramethyl-3H-indol-1-ium iodide **6** in EtOH. Having



Scheme 3 Scope of the late-stage S_NAr for the synthesis of 5',7'-difluoro DHX-hemicyanine fused dyes **2a-2v** and **8**.

successfully synthesised the advanced intermediate **1** in gram scale, we assessed our hypothesis regarding the late-stage, 6'-regioselective S_NAr reaction. Using morpholine (5 equiv.) as model nitrogen nucleophile, we detected no product when we carried out the reaction in this cyclic secondary amine as solvent or in DMSO at room temperature in the presence of pyridine (Scheme 2, entries 1-2). However, we were delighted to observe the product formation in 57% yield when we performed the same reaction at 80 °C for 12 h (Scheme 2, entry 3). The reaction not only cleanly led to mono-substituted product and was selective for the anticipated 6'-position. Encouraged by this result, we screened a panel of solvents, bases and temperatures to optimize the transformation. Replacing pyridine by Hünig's base resulted in a slight drop of product formation in DMSO (49% yield) and no product in water (Scheme 2, entries 4-5). Using pyridine in DMF provided a good 61% yield but under these conditions, the isolation of the pure product was challenging because of incomplete conversion (Scheme 2, entry 6). We also obtained the best yield of 61% when we carried out the reaction in a sealed tube with neat pyridine at 80 °C for 8 h (Scheme 2, entry 7). In contrast, no product formed at 40 °C, a trend confirmed using 1,4-dioxane as solvent which showed the importance of temperature for the efficiency of the reaction (Scheme 2, entry 8-9). With this set of optimised reaction conditions in hand, we then tested an array of nucleophiles including aliphatic and aromatic amines, morpholine, piperazines, 5-, 6-, and 7-membered nitrogen containing saturated heterocycles, aryl thiols and selenols (Scheme 3). While the reaction with bis-alkylated amines provided fluorophores **2a-2c** in moderate yields (16-34% yield), the use of NaN₃ as a nucleophile provided the resulting azido product which undergoes formal reduction during purification to furnish the aniline derivative **2d** (44% yield). The S_NAr reaction was also successful with pyrrolidine **2e** and piperidine **2g** (61%, and 65%, respectively) but the yield dropped for substituted pyrrolidine **2f** (10%), piperidines **2h-2j** (8%, 45% and 35%, respectively) as

well as for the 7-membered ring azepane **2k** (29% yield), showing a sensitivity of the reaction for the steric hindrance of the amine nucleophile. *N*-Alkylated piperazines **2l-2o** were also tolerated (35-81% yield) as well as less nucleophilic aromatic amines 4-methoxyaniline **2p** and 2-aminofluorene **2q** (43% and 45%, respectively). The influence of the nucleophilicity was investigated with the use of thiophenols and aromatic selenols which showed increased yields (95% and 66% yield for **2u** and **2v**) even for sterically hindered *o*-disubstituted 2,6-dimethylthiophenol **2r** (86% yield) and 2,6-dichlorothiophenol **2t** (92% yield). We underline that some of the substrates obtained are bifunctional (*i.e.*, **2b**, **2f**, **2j**, **2n** and **2o**) and could be post-synthetically derivatised for further functionalization (*e.g.*, introduction of polar groups for water solubility) or conjugation to (bio)molecular partners.

Photophysical properties of the 5',7'-difluoro dihydroxanthene-hemicyanine fused fluorophores

We evaluated the photophysical properties of our library of 23 difluoro-DHX-hemicyanine fused dyes **2a-2v** and **8** in different media including phosphate buffered saline (PBS) with 5% (w/v) bovine serum albumin (BSA) as simulated body fluid (only for the less hydrophobic derivatives),²⁹ EtOH, and CHCl₃ (Table 1, Fig. 2 for Abs/Ex/Em spectra of **2a** and **2e** in CHCl₃ and in PBS + 5% BSA, see ESI[†] for Abs/Ex/Em spectra of **2d**, **2g**, **2k** and **8**). All 6'-substituted DHX derivatives display an intense absorption band in the far-red and/or NIR region. However, compared to non-fluorinated parent compounds previously studied by us,^{28b} this main band, assigned to the S₀-S₁ electronic transition, is much broader and structureless with no clear vibronic structure observable. For instance, *N,N*-diethyl derivatives **2a** and **9** exhibit full-width half maximum (FWHM), Δλ_{1/2 max} in the range 139-167 nm and 36-51 nm respectively, depending on the solvent used for spectral measurements (Fig. 2). As confirmed

Table 1 Photophysical properties of 5',7'-difluoro DHX-hemicyanine fused dyes **1**, **2a-v** and **8** at 25 °C. For structures, see Scheme 3.

entry	dye	Abs λ_{\max} [nm] ^[a]			Em λ_{\max} [nm] ^[c]			ϵ [M ⁻¹ cm ⁻¹]			Stokes' shift [cm ⁻¹]			Φ_F [%] ^[d]		
		CHCl ₃	EtOH	PBS ^[b]	CHCl ₃	EtOH	PBS ^[b]	CHCl ₃	EtOH	PBS ^[b]	CHCl ₃	EtOH	PBS ^[b]	CHCl ₃	EtOH	PBS ^[b]
1	1	552 ^{br} 578 ^{br}	543 ^{br}	—	—	—	—	38 000 37 850	36 000	—	—	—	—	—	—	—
2	2a	639 ^{br}	616 ^{br}	614 ^{br}	738	730	729	37 800	38 750	32 000	2099	2535	2569	4	1.5	1
3	2b	606 ^{br}	619 ^{br}	—	735	731	—	32 850	32 950	—	2896	2475	—	3	1	—
4	2c	643 ^{br} 696 ^{br}	622 ^{br}	—	738	732	—	40 100 32 600	36 600	—	2002 818	2416	—	4	1	—
5	2d	629 ^{br} 684 ^{br}	633 ^{br} 690 ^{br}	—	709	718	—	56 550 56 150	51 600 61 200	—	1794 515	1870 565	—	2	2	—
6	2e	665 ^{br} 721 ^{br}	651 ^{br} 707 ^{br}	655 ^{br} 717 ^{br}	747	743	742	42 300 68 300	39 700 48 150	31 200 40 200	1651 483	1902 685	1790 470	9.5	4.5	3
7	2f	658 ^{br} 720 ^{br}	646 ^{br} 702 ^{br}	650 ^{br} 707 ^{br}	748	738	740	22 300 27 800	23 350 24 000	19 700 19 700	1829 520	1930 695	1871 631	6	3	1.5
8	2g	640 ^{br} 689 ^{br}	621 ^{br}	624 ^{br}	740	732	726	33 550 28 550	31 900	25 450	2111 1000	2442	2251	5	1.5	1
9	2h	610 ^{br}	595 ^{br}	—	741	731	—	26 850	26 650	—	2898	3127	—	2.5	1	—
10	2i	639 ^{br} 686 ^{br}	612 ^{br}	619 ^{br}	741	733	726	43 350 36 300	43 600	32 600	2154 1082	2697	2381	4	1.5	1
11	2j	634 ^{br}	620 ^{br}	619 ^{br}	731	729	733	45 400	40 700	33 750	2093	2411	2512	3	1.5	1
12	2k	651 ^{br} 709 ^{br}	632 ^{br}	634 ^{br}	741	738	729	41 350 41 400	37 900	30 850	1866 609	2272	2055	6	2	1.5
13	2l	619 ^{br}	611 ^{br}	—	728	720	—	24 700	27 700	—	2419	2478	—	1.5	1	—
14	2m	619 ^{br}	612 ^{br}	—	726	720	—	31 450	34 400	—	2381	2451	—	1	1	—
15	2n	626 ^{br}	608 ^{br}	—	725	728	—	40 450	37 650	—	2181	2711	—	2	1	—
16	2o	629 ^{br} 642 ^{br}	614 ^{br} 645 ^{br}	—	731	723	—	43 650 43 600	42 300 39 650	—	2218	2455	—	2	1	—
17	2p	696 ^{br}	696 ^{br}	—	—	—	—	38 050	37 600	—	—	—	—	—	—	—
18	2q	642 ^{br}	642 ^{br}	—	—	—	—	33 700	31 400	—	—	—	—	—	—	—
19	2r	574 ^{br} 605 ^{br}	563 ^{br} 587 ^{br}	—	—	—	—	37 300 40 450	36 500 35 900	—	—	—	—	—	—	—
20	2s	568 ^{br} 593 ^{br}	557 ^{br}	—	—	—	—	32 450 32 450	33 300	—	—	—	—	—	—	—
21	2t	569 ^{br} 600 ^{br}	560 ^{br}	—	—	—	—	43 800 45 550	43 050	—	—	—	—	—	—	—
22	2u	568 ^{br} 595 ^{br}	557 ^{br}	—	—	—	—	32 950 34 050	34 000	—	—	—	—	—	—	—
23	2v	599 ^{br}	560 ^{br}	—	—	—	—	39 350	36 050	—	—	—	—	—	—	—
24	8	624 ^{br}	610 ^{br}	—	727	725	—	45 850	40 000	—	2270	2600	—	2	1	—

^a Assigned to S₀-S₁ transition (see Fig. 2 and the Supporting Information for selected examples of Abs spectra). ^b PBS buffer containing 5% BSA. ^c Excitation at 615 nm. ^d Determined at 25 °C by using sulfoindocyanine dye Cy 5.0 (Φ_F = 20% in PBS, λ_{ex} = 615 nm) as standard.⁴⁰

by TD-DFT calculations (*vide infra*), the presence of two ortho-fluorine atoms within **2a** could prevent the presence in solution of a single absorbing species in which the electron-donating NEt₂ group and DHX chromophore are co-planar and full-conjugated. The sole difluoro-DHX-hemicyanine fused dye for which the behavior of the absorption spectrum is relatively similar to that of the corresponding non-fluorinated analog is the *N*-pyrrolidinyl derivative **2e**. Thus, the size and geometry of its azolidine ring are probably optimal to avoid adverse steric interferences with fluorine atoms which are at the origin of multiple conformers (rotation around the C6'-N bond) in solution, and hence broader spectra. As anticipated, all 6'-*N,N*-dialkylamino DHX-hemicyanine hybrids **2a-2o** and **8** show an emission peak in the NIR region, with the maximum in the 709-747 nm range depending on the solvent used and the nature of nitrogen substituents. The good match between the absorption and excitation spectra of **2e** confirms the presence of a single absorbing/emissive species in all tested media. As expected, this trend is not observed for the fluorinated fluorophores

existing as a mixture of multiple conformers, such as **2a**. The lower values of fluorescence quantum yield than those obtained with non-fluorinated fluorophores (*e.g.*, Φ_F of **9** is 30% and 10% in CHCl₃ and in PBS + 5% BSA respectively)^{28b} could be due to the intramolecular charge transfer from electron-rich heteroatom to DHX core and are in line with the prominence of non-radiative decay processes intertwined with the conformational equilibrium previously put forward. Complete extinction of the NIR emission is obtained through the introduction of an *N*-aryl substituent or aryl thiol/selenol moieties (compounds **2p-2v**, see ESI[†] for selected examples of Abs spectra). For these latter hetero-functionalizations, the lack of a substituent with a good electron-donating ability and/or the spin-orbit (heavy-atom) effects promoting triplet state formation relative to fluorescence, are reasonable assumptions to explain this quenching.³⁰ These readily accessible long-wavelength chromophores would therefore be interesting candidates to be used as dark quencher molecules for the

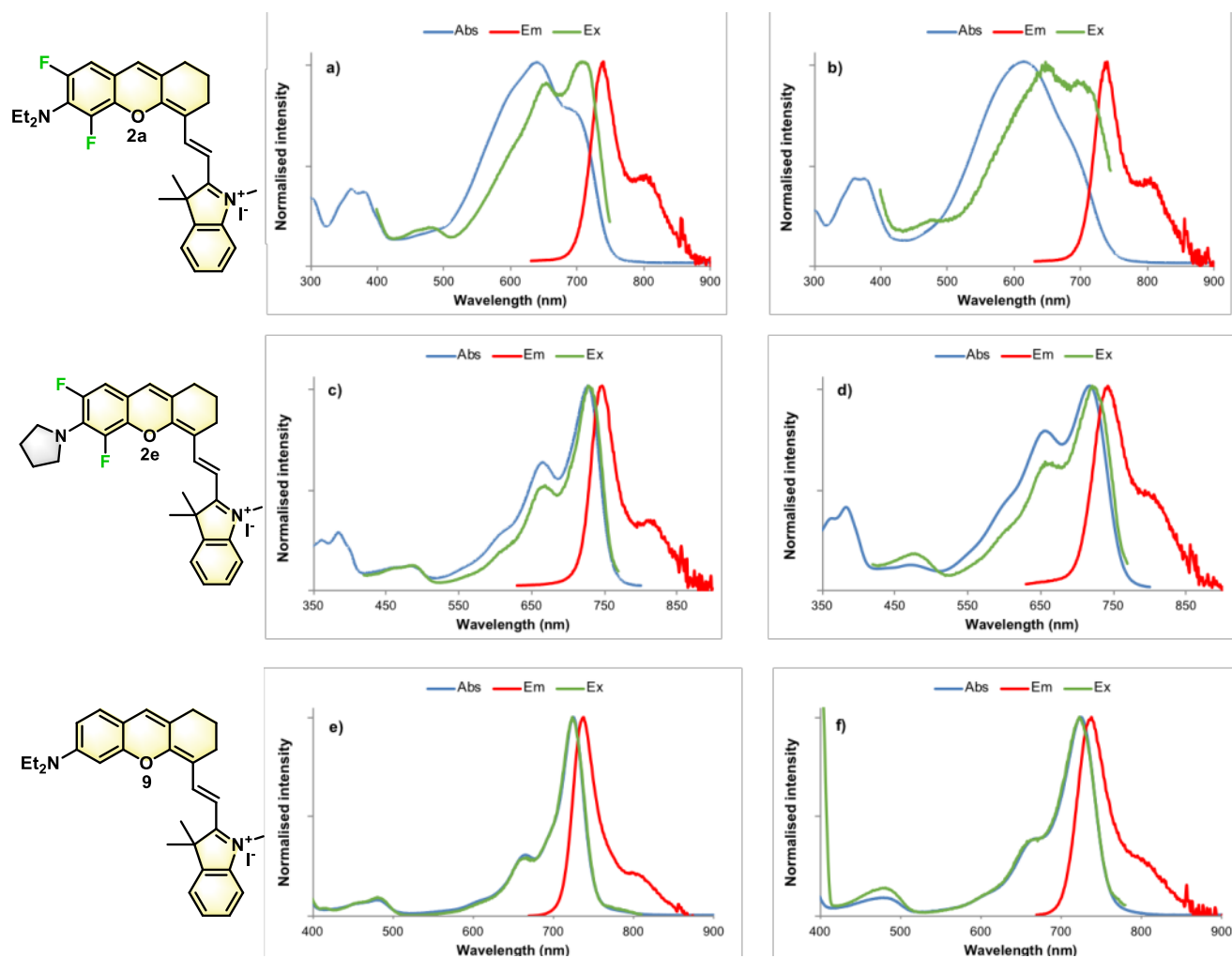


Fig. 2 Normalised absorption, emission (excitation at 615 nm for **a-d** and 650 nm for **e-f**) and excitation (emission at 760 nm for **a-d**, 830 nm for **e** or 800 nm for **f**) spectra of fluorinated *N,N*-dialkylamino-DHX NIR fluorophores **2a** (a in CHCl₃ and b in PBS + 5% BSA), **2e** (c in CHCl₃ and d in PBS + 5% BSA), and non-fluorinated parent NIR fluorophore **9** (e in CHCl₃ and f in PBS + 5% BSA). For the excitation spectrum of **9** in PBS + 5% BSA, a peak at 400 nm ($\lambda_{ex}/2$) assigned to Rayleigh scattering is observed. See Experimental section for details about these measurements.

construction of NIR fluorescent probes based on Förster resonance energy transfer (FRET) mechanism.³¹

TD-DFT computation for selected 5',7'-difluoro dihydroxanthene-hemicyanine fused fluorophores

The density difference plots for two representative examples, **8** and **2e**, are displayed in Fig. 3. Consistently with our previous work,³² we observe a clear π - π^* character for the electronic transition with changes of opposite sign on the vicinal carbon atoms of the hemicyanine moiety. As expected, the pushing *N,N*-dialkylamino group plays the role of a donor (nitrogen in blue in Fig. 3). We have then used theory to investigate the impact of the electron-donating group on the photophysical properties, and in particular, the broadness of the observed electronic absorption spectra (Table 2, *vide supra*). For **8**, we could locate two non-equivalent true minima, differing by the relative twist of the donor group with respect to the plane of the core of the dye, on both the ground (S_0) and excited (S_1) state potential energy surfaces. For the S_0 state, the dihedral

angle between the two subsystems is vastly different (24° and 67°), but the computed free energy difference between the two structures is negligible (< 1 kcal/mol), implying a fast conversion between the two (*i.e.*, a series of intermediate states). As expected, the computed absorption energies vastly differ for these two compounds (by ca. 0.3 eV at the CC2 level). In contrast, when going to the S_1 state, the most planar molecule (now with a 32° dihedral) becomes significantly more stable (by 3.2 kcal/mol). This theoretical result is in line with the experimental trends that show a broad absorption, but a standard emission for **8**. The computed 0-0 energies for the two species are 1.667 and 1.898 eV, logically bracketing the experimental value. For **2d**, we found only one conformation for the NH₂ group with a twist of the NH bond, with respect to the dye's plane, of 20° and 8° in S_0 and S_1 , respectively. There is therefore limited flexibility and the absorption spectrum is tight. The theoretical 0-0 energy is 1.803 eV, very close to the experimental value of 1.783 eV. For **2e**, we started with the pyrrolidiny group either perfectly in the plane of the dye or twisted, but both optimizations led to the in-plane structure in

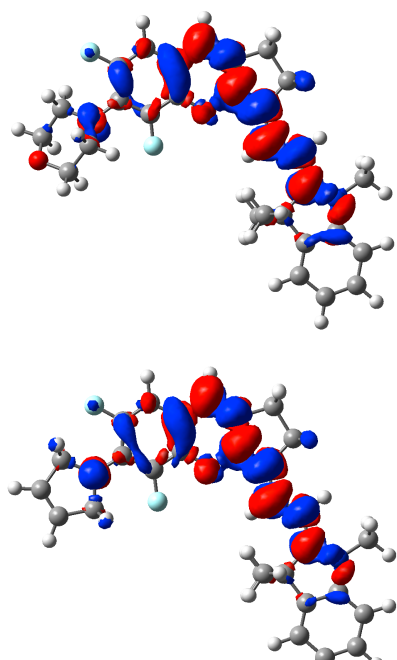


Fig. 3 Density difference plot [$\Delta\rho=\rho(S_1)-\rho(S_0)$] obtained for **8** (top) and **2e** (bottom). The blue and red regions indicate loss and gain of electronic density upon absorption, respectively. Contour threshold: 8×10^{-4} au.

both the S_0 and S_1 states. The computed 0-0 energy (1.655 eV) is strongly red-shifted compared **2d**, which is perfectly consistent with the experimental trend (0-0 of 1.690 eV). For **2g**, starting with a planar and perpendicular conformation of the side group, we obtained two slightly different minima, both showing similar twisting angles of 25° (S_0) and ca. 35° (S_1). For both conformers, the relative free energies are almost equal (differences < 1 kcal/mol) and the same holds for the 0-0 energies: 1.622 and 1.645 eV. These values do not agree so well with the experimental value of 1.722 eV. For **2a**, we could find several orientations of the NEt_2 donor groups all inside a 1 kcal/mol window (relative S_0 free energies), with however significantly different absorption maxima, explaining the broad spectra (see Table 2). In the excited-state, different twisting angles are still obtained depending on the conformers but they present more alike fluorescence energies. The 0-0 energies obtained are very similar to **2g**, which is consistent with experiment, though the 0-0 energies are undershot, as in the previous case. Finally, for **2k** we could also find two different conformers but as for **2g** they do present very similar spectroscopic signatures, which is consistent with the relatively small width at half maximum observed experimentally for **2k**.

Conclusions

In summary, we have developed a divergent access to 6'-heterosubstituted 5',7'-difluoro dihydroxanthene-hemicyanine fused dyes through a 6'-selective and effective $S_N\text{Ar}$ reaction. Conceptual DFT allowed us to predict the regioselectivity of the displacement of an aryl fluoride moiety which exclusively led to the 6'-substitution. The transformation was successful using a wide range of amino, thio, and seleno nucleophiles and provided either fluorophores emitting in the 710-750 nm range

Table 2. Comparison of the experimental and theoretical optical properties of the 5',7'-difluoro DHX-hemicyanine fused dyes. In several cases, different conformers (conf.) are obtained. The theoretical results have been obtained at the CC2//CAM-B3LYP level of theory (see Experimental Section for details).

dye	conf.	λ_{abs} [the] [nm]	λ_{abs} [exp] [nm]	λ_{fl} [the] [nm]	λ_{fl} [exp] [nm]	0-0 [the] [eV]	0-0 [exp] [eV]
2a	a	673	639 (br)	775	738	1.640	1.727
	b	643		783		1.629	
	c	671		777		1.632	
2d	—	600	684	713	709	1.803	1.783
2f	—	671	721	770	747	1.655	1.671
2g	a	653	689	784	740	1.622	1.722
	b	649		782		1.645	
2k	a	679	709	789	741	1.613	1.701
	b	679		782		1.633	1.633
8	Planar	630	624 (br)	770	727	1.667	1.771

in aqueous and organic media or non-emissive NIR chromophores potentially usable as NIR fluorescence quenchers. The various broadness of the absorption and emission spectra have been correlated to the presence (or absence) of several conformers of similar energies. As a general rule, bis-fluorination of DHX scaffold led to a drop of fluorescence efficiency compared to the parent non-fluorinated fluorophores, even if a "hit" photoactive compound bearing a pyrrolidinyl as N,N -dialkylamino electron-donating group and exhibiting a good fluorescence quantum yield of 10% in CHCl_3 , was identified. We hope that the attractive features of this $S_N\text{Ar}$ -based functionalization procedure (*i.e.*, simplicity and ease of implementation) will encourage its further use in the conversion of DHX-hemicyanine hybrid scaffolds to reaction-based small-molecule fluorescent probes and promote their use in other biomedical applications.^{27, 33}

Experimental

See ESI⁺ for the details about sections "General", "Instruments and methods", and all experimental and spectral data associated with synthesised compounds.

Synthesis

5',6',7'-Trifluoro-2,3-dihydro-1H-xanthene-4-carbaldehyde (5) To 2-hydroxyl-3,4,5-trifluoro-benzaldehyde **3** (528 mg, 3 mmol, 1 equiv) and Cs_2CO_3 (978 mg, 3 mmol, 1 equiv) in DMF (15 mL) was added 6-bromocyclohex-1-ene-1-carbaldehyde (**4**) (2.26 g, 12 mmol, 4 equiv) and the mixture was stirred at 25°C for 56 h. The reaction mixture was filtered and concentrated *in vacuo*. Purification by flash-column chromatography on silica gel (10% EtOAc in petroleum ether) afforded 5',6',7'-trifluoro-2,3-dihydro-1H-xanthene-4-carbaldehyde **5** as a yellow solid (483 mg, 61%). ^1H NMR (400.0 MHz, CDCl_3): δ = 10.35 (s, 1H), 6.78 (m, 1H), 6.53 (s, 1H), 2.59 (t, J = 5.8 Hz, 2H), 2.45 (t, J = 6.1 Hz, 2H), 1.73 (m, 2H) ppm; ^{19}F NMR (376.5 MHz, CDCl_3): δ = -140.7 (m, 1F), -155.2 (m, 1F), -155.8 (m, 1F) ppm; ^{13}C NMR (100.0

MHz, CDCl₃): δ = 188.1, 157.9, 146.9 (ddd, J_{C-F} = 2.1 Hz, J_{C-F} = 11.1 Hz, $^1J_{C-F}$ = 246.6 Hz), 140.6 (ddd, J_{C-F} = 12.1 Hz, J_{C-F} = 16.9 Hz, $^1J_{C-F}$ = 254.2 Hz), 139.8 (ddd, J_{C-F} = 4.0 Hz, J_{C-F} = 12.5 Hz, $^1J_{C-F}$ = 253.8 Hz), 137.4 (m), 131.5 (d, J_{C-F} = 2.9 Hz), 123.6 (dd, J_{C-F} = 3.1 Hz, J_{C-F} = 5.7 Hz), 117.1 (m), 115.2 (d, J_{C-F} = 0.9 Hz), 107.8 (dd, J_{C-F} = 3.7 Hz, J_{C-F} = 19.6 Hz), 30.1, 21.5, 20.0 ppm; HRMS (ESI+): m/z calcd for C₁₄H₉F₃O₂ [M + Na]⁺ 289.0447, found 289.0450.

5',6',7'-Trifluoro DHX-hemicyanine fused dye precursor (1) To 5,6,7-trifluoro-2,3-dihydro-1*H*-xanthen-4-carbaldehyde **5** (265 mg, 0.99 mmol, 1 equiv) in EtOH (2 mL) was added 1,2,3,3-tetramethyl-3*H*-indol-1-ium iodide **6** (300 mg, 0.99 mmol, 1 equiv) and the solution was refluxed at 80 °C for 4 h. The reaction mixture was concentrated and the crude product was purified by flash-column chromatography on silica gel (1% MeOH in CH₂Cl₂) to afford compound **1** as a dark blue solid (483 mg, 88%). ¹H NMR (400.0 MHz, DMSO-*d*₆): δ = 8.50 (d, J = 15.6 Hz, 1H), 7.82 (m, 2H), 7.56 (m, 3H), 7.18 (s, 1H), 6.83 (d, J = 15.6 Hz, 1H), 4.01 (s, 3H), 2.70 (m, 4H), 1.82 (m, 2H), 1.74 (s, 6H) ppm; ¹⁹F NMR (376.5 MHz, DMSO-*d*₆): δ = -140.2 (m, 1F), -156.1 (m, 1F), -157.6 (d, J_{F-F} = 19.4 Hz, 1F) ppm; ¹³C NMR (100.0 MHz, DMSO-*d*₆): δ = 180.0, 156.0, 146.8 (dd, J_{C-F} = 10.2 Hz, $^1J_{C-F}$ = 244.2 Hz), 145.3, 143.1, 142.5, 140.6 (m), 140.4 (ddd, J_{C-F} = 11.9 Hz, J_{C-F} = 17.1 Hz, $^1J_{C-F}$ = 253.0 Hz), 138.0 (m), 131.9, 129.4, 128.8, 127.2, 123.3, 118.5 (dd, J_{C-F} = 3.1 Hz, J_{C-F} = 9.2 Hz), 115.5, 114.8, 109.6 (d, J_C = 2.8 Hz), 109.4, 51.6, 34.1, 29.2, 27.1, 23.9, 20.1 ppm; HRMS (ESI+): m/z calcd for C₂₆H₂₃F₃NO⁺ [M]⁺ 422.1763, found 422.1707.

General procedure for the synthesis of NIR 5',7'-difluoro DHX-hemicyanine fused dyes 2a-2v and 8: To intermediate **1** (220 mg, 0.4 mmol, 1 equiv) in pyridine (1 mL) was added the respective nucleophile (2 mmol, 5 equiv) and the mixture was heated at 80 °C for 12 h in a sealed tube. After cooling down to r.t., the reaction mixture was concentrated *in vacuo* and directly purified by flash-column chromatography on silica gel (1% MeOH in CH₂Cl₂) to afford the corresponding blue products **2a-2v** and **8**.

Computational details

We have followed a computational protocol developed especially for the *nor*-DHX-hemicyanine fused dyes and detailed in a previous published publication.³² We refer the interested reader to that earlier work for details and justification of this protocol that combines TD-DFT and second-order CC (CC2) methods. All DFT and TD-DFT calculations were performed with the Gaussian16 program,³⁴ applying both a tightened self-consistent field convergence criterion (10⁻⁹-10⁻¹⁰ a.u.) and an improved optimization threshold (10⁻⁵ a.u. on average residual forces). The ground (S₀) and excited (S₁) state structures of all dyes have been optimised at the CAM-B3LYP/6-311G(2d,p) level,³⁵ and the minima nature of all structures was confirmed using analytical calculations of the Hessian. These structural and vibrational parameters have been obtained in solution (CHCl₃), and the medium effects were evaluated with the well-known Polarizable Continuum Model (PCM)³⁶ applying the Linear-Response (LR)³⁷ formalism in its the *equilibrium* limit. The zero-point energies of both states was computed at this same PCM-CAM-B3LYP/6-311G(2d,p) level. We next determined the total and transition energies at the PCM-(TD)-CAM-B3LYP/6-311++G(2df,2pd) level in both gas-phase and in solution, using the same LR-PCM model for the latter, considering both the non-equilibrium and equilibrium limits. CC2/*aug-cc-pVTZ* total

and transition energies have been computed in the gas-phase on the DFT and TD-DFT structures with the Turbomole package.³⁸ We applied the Resolution-of-Identity (RI-V) approximation during all calculations and selected default Turbomole convergence thresholds.

To obtain the 0-0 energies, we applied the following equation:³⁹

$$E^{0-0} = E_{\text{gas}}^{\text{adia}}[\text{CC2}] + \Delta E_{\text{LR}(\text{eq})}^{\text{ZPVE}}[\text{TDDFT}] + E_{\text{LR}(\text{eq})}^{\text{adia}}[\text{TDDFT}] - E_{\text{gas}}^{\text{adia}}[\text{TDDFT}] + E_{\text{LR}(\text{neq})}^{\text{abso}}[\text{TDDFT}] - E_{\text{LR}(\text{eq})}^{\text{abso}}[\text{TDDFT}]$$

in which we use the so-called adiabatic energies and correct them for zero-point vibrational effects as well as for *non-equilibrium* solvation effects. This protocol was shown to deliver accurate results for *nor*-DHX dyes.³²

Photophysical properties

UV-visible spectra were obtained either on a Varian Cary 50 scan (single-beam) or an Agilent Technologies 60 (single-beam) spectrophotometer by using a rectangular quartz cell (Hellma, 100-QS, 45 × 12.5 × 12.5 mm, pathlength: 10 mm, chamber volume: 3.5 mL), at 25 °C (using a temperature control system combined with water circulation). Fluorescence spectra (emission/excitation spectra) were recorded with an HORIBA Jobin Yvon Fluorolog spectrophotometer (software FluorEssence) at 25 °C (using a temperature control system combined with water circulation), using a standard fluorometer cell (Labbox, LB Q, light path: 10 mm, width: 10 mm, chamber volume: 3.5 mL). Emission spectra were recorded in the range 630-900 nm after excitation at 615 nm (shutter: Auto Open, excitation slit = 5 nm and emission slit = 5 nm). Excitation spectra were recorded in the range 400-750 nm or 400-770 nm after emission at 760 nm or 800 nm (shutter: Auto Open, excitation slit = 12 nm and emission slit = 5 nm). All fluorescence spectra were corrected until 850 nm. Fluorescence quantum yields were measured at 25 °C by a relative method using sulfoindocyanine dye Cy 5.0 (ϕ_F = 20% in PBS) as a standard (dilution by a factor of 3 between absorption and fluorescence measurements).⁴⁰ The following equation was used to determine the relative fluorescence quantum yield:

$$\phi_F(x) = (A_s/A_x)(F_x/F_s)(n_x/n_s)^2\phi_F(s)$$

where A is the absorbance (in the range of 0.01-0.1 A.U.), F is the area under the emission curve, n is the refractive index of the solvents (at 25 °C) used in measurements, and the subscripts s and x represent standard and unknown, respectively. The following refractive index values were used: 1.479 for DMSO, 1.446 CHCl₃, 1.361 EtOH, 1.337 for PBS (100 mM phosphate + 150 mM NaCl, pH 7.4) and PBS + 5% BSA. Stock solutions (1.0 mg/mL) of 5',7'-difluoro DHX-hemicyanine fused NIR dyes were prepared in DMSO (RPE, for analysis, Carlo Erba) and subsequently diluted with CHCl₃, EtOH or PBS + 5% BSA for UV-vis absorption and fluorescence measurements.

Conflicts of interest

The authors declare no conflict of interest.

Acknowledgements

This work is supported by SPST, Tianjin University (P.R. China), ICES, A*STAR (Singapore), and the CNRS, Université de Bourgogne and

Conseil Régional de Bourgogne through the "Plan d'Actions Régional pour l'Innovation (PARI) and the "Fonds Européen de Développement Régional (FEDER)" programs. Financial support from Institut Universitaire de France (IUF, 2013-2018), Institut Français de Singapour (PHC Merlion grant, 2015, 5.04.15) and GDR CNRS "Agents d'Imagerie Moléculaire" (AIM) 2037 are also greatly acknowledged. The authors thank Ms Doris Tan (ICES, Singapore) and Dr. Quentin Bonnin (IR CNRS, PACSMUB, Dijon, France) for the recording of HRMS spectra. A. R. thanks the "Plateforme d'Analyse Chimique et de Synthèse Moléculaire de l'Université de Bourgogne" (PACSMUB, <http://www.wpcm.fr>) for access to spectroscopy instrumentation. This work used the computational resources of the CCIPL (Centre de Calcul Intensif des Pays de la Loire) installed in Nantes.

Notes and references

- 1 D. O'Hagan, *Chem. Soc. Rev.*, 2008, **37**, 308.
- 2 (a) H.-J. Böhm, D. Banner, S. Bendels, M. Kansy, B. Kuhn, K. Müller, U. Obst-Sander and M. Stahl, *ChemBioChem*, 2004, **5**, 637; (b) K. Müller, C. Faeh and F. Diederich, *Science*, 2007, **317**, 1881; (c) W. K. Hagmann, *J. Med. Chem.*, 2008, **51**, 4359; (d) S. Purser, P. R. Moore, S. Swallow and V. Gouverneur, *Chem. Soc. Rev.*, 2008, **37**, 320; (e) D. O'Hagan, *J. Fluorine Chem.*, 2010, **131**, 1071; (f) E. P. Gillis, K. J. Eastman, M. D. Hill, D. J. Donnelly and N. A. Meanwell, *J. Med. Chem.*, 2015, **58**, 8315; (g) N. A. Meanwell, *J. Med. Chem.*, 2018, **61**, 5822.
- 3 (a) P. Jeschke, *ChemBioChem*, 2004, **5**, 570; (b) P. Jeschke, *Pest Manage. Sci.*, 2010, **66**, 10; (c) S. Jeanmart, A. J. F. Edmunds, C. Lamberth and M. Pouliot, *Bioorg. Med. Chem.*, 2016, **24**, 317.
- 4 R. Berger, G. Resnati, P. Metrangolo, E. Weber and J. Hulliger, *Chem. Soc. Rev.*, 2011, **40**, 3496.
- 5 F. Babudri, G. M. Farinola, F. Naso and R. Ragni, *Chem. Commun.*, 2007, 1003.
- 6 D. Anton, *Adv. Mater.*, 1998, **10**, 1197.
- 7 (a) J. Wang, M. Sánchez-Roselló, J. L. Aceña, C. del Pozo, A. E. Sorochinsky, S. Fustero, V. A. Soloshonok and H. Liu, *Chem. Rev.*, 2014, **114**, 2432; (b) Y. Zhou, J. Wang, Z. Gu, S. Wang, W. Zhu, J. L. Aceña, V. A. Soloshonok, K. Izawa and H. Liu, *Chem. Rev.*, 2016, **116**, 422.
- 8 T. Fujiwara and D. O'Hagan, *J. Fluorine Chem.*, 2014, **167**, 16.
- 9 (a) L. Cai, S. Lu and V. W. Pike, *Eur. J. Org. Chem.*, 2008, 2853; (b) D. van der Born, A. Pees, A. J. Poot, R. V. A. Orru, A. D. Windhorst and D. J. Vugts, *Chem. Soc. Rev.*, 2017, **46**, 4709.
- 10 I. Tirotta, V. Dichiarante, C. Pigliacelli, G. Cavallo, G. Terraneo, F. B. Bombelli, P. Metrangolo and G. Resnati, *Chem. Rev.*, 2015, **115**, 1106.
- 11 (a) H. Chen, S. Viel, F. Ziarelli and L. Peng, *Chem. Soc. Rev.*, 2013, **42**, 7971; (b) E. N. G. Marsh and Y. Suzuki, *ACS Chem. Biol.*, 2014, **9**, 1242.
- 12 (a) D. P. Curran, *Angew. Chem. Int. Ed.*, 1998, **37**, 1174; (b) D. P. Curran and Z. Luo, *J. Am. Chem. Soc.*, 1999, **121**, 9069; (c) D. P. Curran, *Synlett*, 2001, 1488; (d) W. Zhang, *Tetrahedron*, 2003, **59**, 4475.
- 13 M. Matsui, in *Functional Dyes*, Elsevier Science, Amsterdam, 2006, pp. 257.
- 14 D. K. Kölmel, B. Rudat, D. M. Braun, C. Bednarek, U. Schepers and S. Bräse, *Org. Biomol. Chem.*, 2013, **11**, 3954.
- 15 E. M. Sletten and T. M. Swager, *J. Am. Chem. Soc.*, 2014, **136**, 13574.
- 16 W. Cao and E. M. Sletten, *J. Am. Chem. Soc.*, 2018, **140**, 2727.
- 17 (a) V. N. Belov, M. L. Bossi, J. Fölling, V. P. Boyarskiy and S. W. Hell, *Chem. Eur. J.*, 2009, **15**, 10762; (b) G. Y. Mitronova, V. N. Belov, M. L. Bossi, C. A. Wurm, L. Meyer, R. Medda, G. Moneron, S. Bretschneider, C. Eggeling, S. Jakobs and S. W. Hell, *Chem. Eur. J.*, 2010, **16**, 4477; (c) K. Kolmakov, V. N. Belov, J. Bierwagen, C. Ringemann, V. Müller, C. Eggeling and S. W. Hell, *Chem. Eur. J.*, 2010, **16**, 158; (d) Z. R. Woydziak, L. Fu and B. R. Peterson, *J. Org. Chem.*, 2012, **77**, 473; (e) H. Schill, S. Nizamov, F. Bottanelli, J. Bierwagen, V. N. Belov and S. W. Hell, *Chem. Eur. J.*, 2013, **19**, 16556.
- 18 (a) B. J. Littler, M. A. Miller, C.-H. Hung, R. W. Wagner, D. F. O'Shea, P. D. Boyle and J. S. Lindsey, *J. Org. Chem.*, 1999, **64**, 1391; (b) M. A. H. Alamiry, A. C. Benniston, J. Hagon, T. P. L. Winstanley, H. Lemmetyinen and N. V. Tkachenko, *RSC Adv.*, 2012, **2**, 4944; (c) M. Hecht, T. Fischer, P. Dietrich, W. Kraus, A. B. Descalzo, W. E. S. Unger and K. Rurack, *ChemistryOpen*, 2013, **2**, 25.
- 19 (a) J. Lenaerts, G. Verlinden, L. Van Vaeck, R. Gijbels, I. Geuens and P. Callant, *Langmuir*, 2001, **17**, 7332; (b) B. R. Renikuntla, H. C. Rose, J. Eldo, A. S. Waggoner and B. A. Armitage, *Org. Lett.*, 2004, **6**, 909; (c) G. L. Silva, V. Ediz, D. Yaron and B. A. Armitage, *J. Am. Chem. Soc.*, 2007, **129**, 5710.
- 20 Cooper, M. E.; Gardner, N. J.; Laughton, P. G. (Amersham, GB). US Patent 7,767,829 B2, 2010.
- 21 (a) R. Ting, T. A. Aguilera, J. L. Crisp, D. J. Hall, W. C. Eckelman, D. R. Vera and R. Y. Tsien, *Bioconjugate Chem.*, 2010, **21**, 1811; (b) T. Priem, C. Bouteiller, D. Camporese, X. Brune, J. Hardouin, A. Romieu and P.-Y. Renard, *Org. Biomol. Chem.*, 2013, **11**, 469; (c) E. A. Rodríguez, Y. Wang, J. L. Crisp, D. R. Vera, R. Y. Tsien and R. Ting, *Bioconjugate Chem.*, 2016, **27**, 1390; (d) F.-F. An, H. Kommidi, N. Chen and R. Ting, *Int. J. Mol. Sci.*, 2017, **18**, 1214.
- 22 G. Vives, C. Giansante, R. Bofinger, G. Raffy, A. D. Guerzo, B. Kauffmann, P. Batat, G. Jonusauskas and N. D. McClenaghan, *Chem. Commun.*, 2011, **47**, 10425.
- 23 H. R. A. Golf, H.-U. Reissig and A. Wiehe, *Org. Lett.*, 2015, **17**, 982.
- 24 (a) R. Weissleder and U. Mahmood, *Radiology*, 2001, **219**, 316; (b) J. V. Frangioni, *Curr. Opin. Chem. Biol.*, 2003, **7**, 626; (c) I. Martinić, S. V. Eliseeva and S. Petoud, *J. Lumin.*, 2017, **189**, 19.
- 25 O. Galangau, C. Dumas-Verdes, R. Méallet-Renault and G. Clavier, *Org. Biomol. Chem.*, 2010, **8**, 4546.
- 26 For mono-fluorinated phenol-based DHX fluorophores with a lowered pKa value promoting a strong NIR emissive phenolate form at physiological pH, see: (a) Q. Yang, C. Jia, Q. Chen, W. Du, Y. Wang and Q. Zhang, *J. Mater. Chem. B*, 2017, **5**, 2002; (b) X. Zhu, L. Yuan, X. Hu, L. Zhang, Y. Liang, S. He, X.-B. Zhang and W. Tan, *Sens Actuators B Chem.*, 2018, **259**, 219.
- 27 H. Chen, B. Dong, Y. Tang and W. Lin, *Acc. Chem. Res.*, 2017, **50**, 1410.
- 28 (a) J.-A. Richard, *Org. Biomol. Chem.*, 2015, **13**, 8169; (b) M. J. H. Ong, R. Srinivasan, A. Romieu and J.-A. Richard, *Org. Lett.*, 2016, **18**, 5122; (c) A. Romieu and J.-A. Richard, *Tetrahedron Lett.*, 2016, **57**, 317; (d) M. J. H. Ong, S. Debieu, M. Moreau, A. Romieu and J.-A. Richard, *Chem. Asian J.*, 2017, **12**, 936.
- 29 J. Pauli, M. Grabolle, R. Brehm, M. Spieles, F. M. Hamann, M. Wenzel, I. Hilger and U. Resch-Genger, *Bioconjugate Chem.*, 2011, **22**, 1298.
- 30 M. R. Detty, P. N. Prasad, D. J. Donnelly, T. Ohulchanskyy, S. L. Gibson and R. Hilf, *Bioorg. Med. Chem.*, 2004, **12**, 2537.
- 31 T. Myochin, K. Hanaoka, S. Iwaki, T. Ueno, T. Komatsu, T. Terai, T. Nagano and Y. Urano, *J. Am. Chem. Soc.*, 2015, **137**, 4759.
- 32 C. Azarias, M. Ponce-Vargas, I. Navizet, P. Fleurat-Lessard, A. Romieu, B. Le Guennic, J.-A. Richard and D. Jacquemin, *Phys. Chem. Chem. Phys.*, 2018, **20**, 12120.

- 33 For selected examples of small molecule theranostics based on DHX-hemicyanine hybrids or related NIR fluorophores, see: (a) X. Wu, M. Yu, B. Lin, H. Xing, J. Han and S. Han, *Chem. Sci.*, 2015, **6**, 798; (b) F. Kong, Z. Liang, D. Luan, X. Liu, K. Xu and B. Tang, *Anal. Chem.*, 2016, **88**, 6450; (c) B. Zhou, Y. Li, G. Niu, M. Lan, Q. Jia and Q. Liang, *ACS Appl. Mater. Interfaces*, 2016, **8**, 29899.
- 34 M. J. Frisch, G. W. Trucks, H. B. Schlegel, G. E. Scuseria, M. A. Robb, J. R. Cheeseman, G. Scalmani, V. Barone, G. A. Petersson, H. Nakatsuji, X. Li, M. Caricato, A. V. Marenich, J. Bloino, B. G. Janesko, R. Gomperts, B. Mennucci, H. P. Hratchian, J. V. Ortiz, A. F. Izmaylov, J. L. Sonnenberg, D. Williams-Young, F. Ding, F. Lipparini, F. Egidi, J. Goings, B. Peng, A. Petrone, T. Henderson, D. Ranasinghe, V. G. Zakrzewski, J. Gao, N. Rega, G. Zheng, W. Liang, M. Hada, M. Ehara, K. Toyota, R. Fukuda, J. Hasegawa, M. Ishida, T. Nakajima, Y. Honda, O. Kitao, H. Nakai, T. Vreven, K. Throssell, J. A. Montgomery Jr., J. E. Peralta, F. Ogliaro, M. J. Bearpark, J. J. Heyd, E. N. Brothers, K. N. Kudin, V. N. Staroverov, T. A. Keith, R. Kobayashi, J. Normand, K. Raghavachari, A. P. Rendell, J. C. Burant, S. S. Iyengar, J. Tomasi, M. Cossi, J. M. Millam, M. Klene, C. Adamo, R. Cammi, J. W. Ochterski, R. L. Martin, K. Morokuma, O. Farkas, J. B. Foresman and D. J. Fox, Gaussian 16 Revision A.03, Gaussian Inc., Wallingford CT, 2016.
- 35 T. Yanai, D. P. Tew and N. C. Handy, *Chem. Phys. Lett.*, 2004, **393**, 51.
- 36 J. Tomasi, B. Mennucci and R. Cammi, *Chem. Rev.*, 2005, **105**, 2999.
- 37 R. Cammi and B. Mennucci, *J. Chem. Phys.*, 1999, **110**, 9877.
- 38 TURBOMOLE V6.6 2014, a development of University of Karlsruhe and Forschungszentrum Karlsruhe GmbH, 1989–2007, TURBOMOLE GmbH, since 2007, available from <http://www.turbomole.com>, accessed 13 June 2016.
- 39 Note that Eq(3) in Ref. 32 was incorrect, but the calculations in that earlier work have been actually performed with this (correct) formalism.
- 40 R. B. Mujumdar, L. A. Ernst, S. R. Mujumdar, C. J. Lewis and A. S. Waggoner, *Bioconjugate Chem.*, 1993, **4**, 105.

Table of contents

1. General.....	S2
2. Instruments and methods.....	S2
3. Experimental Section	S2
3.1 Preparation of Intermediate 1	S2
3.2 Preparation of Substrate E	S4
3.3 General procedure for the S _N Ar reaction.....	S5
4. References.....	S15
5. ¹ H, ¹⁹ F and ¹³ C NMR spectra of synthesized compounds	S16
6. High-performance liquid chromatography (HPLC) separations	S57
7. UV-visible absorption spectra of compound 1 and non-fluorescent 5',7'-difluoro-DHX-hemicyanine fused dyes.....	S67
8. Absorption, excitation and emission spectra of selected 5',7'-difluoro-6'-amino-DHX-hemicyanine fused dyes.....	S68

Supporting Information

1. General

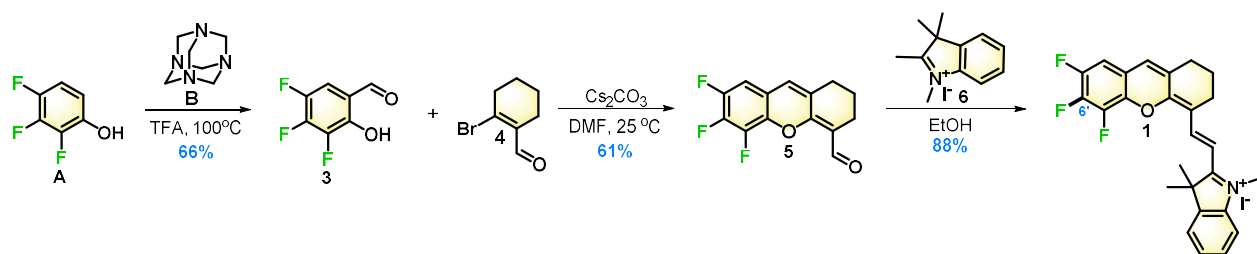
Chemicals, reagents and solvents were purchased from commercial vendors and used without further purification. Trifluoroacetic acid (TFA), dichloromethane (DCM), dimethylformamide (DMF), ethyl acetate (EtOAc), petroleum ether (b.p. 40-60 °C), acetonitrile (MeCN), dimethyl sulfoxide (DMSO), methanol (MeOH), ethanol (EtOH), and pyridine used in this work were reagent grade. Bovine serum albumin (BSA, heat shock fraction, pH 7, $\geq 98\%$) was provided by Sigma-Aldrich. The HPLC-gradient grade CH₃CN used for HPLC-MS analyses was obtained from Carlo Erba. Formic acid (FA, puriss p.a., ACS reagent, reagent grade, Ph. Eur., $\geq 98\%$) was provided by Sigma-Aldrich. All aq. buffers used in this work (PBS and aq. mobile-phases for HPLC) were prepared using water purified with a PURELAB Ultra system from ELGA (purified to 18.2 M Ω .cm). Thin-layer chromatography (TLC) was carried on pre-coated glass plates with 0.2 mm silica gel and visualized under UV (254 nm) and/or potassium permanganate (KMnO₄) stain. Flash-column chromatography was performed using Silica gel 60 (200–400 mesh) with specified eluents.

2. Instruments and methods

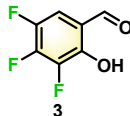
¹H, ¹³C and ¹⁹F NMR spectra were recorded on Bruker Avance 400 MHz or 600 MHz spectrometers. Chemical shifts (δ) are reported in parts per million (ppm) and residual non-deuterated solvent peaks were used as internal reference (proton δ 7.26 and carbon δ 77.16 for CDCl₃ and proton δ 2.50 and carbon δ 39.5 for DMSO-*d*₆). ¹H NMR coupling constants (*J*) are reported in Hertz (Hz). The following abbreviations were used in reporting multiplicities: s (singlet), d (doublet), t (triplet), m (multiplet), dd (doublet of doublets), ddd (doublet of doublet of doublets) and br (broad). High-resolution mass spectra (HRMS) were recorded on either a Q-ToF micro (Bruker Compass Data Analysis 4.0) spectrometer or a Thermo LTQ Orbitrap XL apparatus, both equipped with an ESI analytical source. HPLC-MS analyses were performed on a Thermo-Dionex Ultimate 3000 instrument (pump + autosampler at 20 °C + column oven at 25 °C) equipped with a diode array detector (Thermo-Dionex DAD 3000-RS) and a MSQ Plus single quadrupole mass spectrometer (low-resolution mass (LRMS) analyses through electrospray ionization (ESI) source).

3. Experimental Section

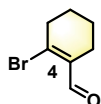
3.1 Preparation of Intermediate 1



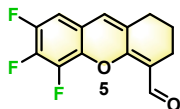
Scheme S1 Synthetic route towards Intermediate 1



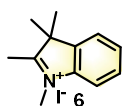
2-Hydroxy-3,4,5-trifluoro-benzaldehyde 3. To 2,3,4-trifluorophenol **A** (148 mg, 1 mmol, 1 equiv.) in TFA (2 mL) was added hexamethylenetetramine **B** (350 mg, 2.5 mmol, 2.5 equiv.). The mixture was stirred at room temperature (r.t.) for ~10 min until observation of a clear solution. The resulting solution was refluxed at 100 °C for 13 h and cooled down to r.t. Deionized water (2 mL) and conc. H₂SO₄ (370 μL) were added and the mixture was further stirred at r.t. for 18 h. The reaction mixture was extracted with DCM (3 x 20 mL) and the combined organic layers were dried over anhydrous Na₂SO₄, filtered and concentrated *in vacuo*. Purification by flash-column chromatography on silica gel (100% Petroleum ether) afforded 2-hydroxy-3,4,5-trifluoro-benzaldehyde **3** as a white solid (117 mg, 66%). ¹H NMR (400.0 MHz, CDCl₃): δ = 11.05 (s, 1H), 9.83 (s, 1H), 7.27 (m, 1H) ppm; ¹⁹F NMR (376.5 MHz, CDCl₃): δ = -144.4 (dd, *J* = 9.0, 21.1 Hz, 1F), -145.2 (m, 1F), -155.3 (d, *J* = 18.3 Hz, 1F) ppm; ¹³C NMR (100.0 MHz, CDCl₃): δ = 194.7, 148.2 (m), 145.7 (ddd, *J*_{C-F} = 12.3 Hz, *J*_{C-F} = 16.2 Hz, ¹*J*_{C-F} = 262.0 Hz), 144.4 (ddd, *J*_{C-F} = 1.2 Hz, *J*_{C-F} = 10.8 Hz, ¹*J*_{C-F} = 245.4 Hz), 140.4 (ddd, *J*_{C-F} = 2.6 Hz, *J*_{C-F} = 11.8 Hz, ¹*J*_{C-F} = 254.5 Hz), 115.7 (m), 114.0 (ddd, *J*_{C-F} = 1.9 Hz, *J*_{C-F} = 3.7 Hz, *J*_{C-F} = 18.1 Hz) ppm; MS (EI⁺): *m/z* calcd for C₇H₃F₃O₂ [M]⁺ 176.0085, found 176.0000.



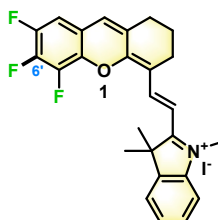
6-Bromocyclohex-1-ene-1-carbaldehyde 4. To a mixture of DMF (23.5 mL, 306 mmol, 3 equiv.) and CHCl₃ (100 mL) at 0 °C was added PBr₃ (24.2 mL, 255 mmol, 2.5 equiv.) portionwise under an atmosphere of N₂. After 1.5 h, cyclohexanone (10.5 mL, 102 mmol, 1 equiv.) was added and the mixture was stirred at r.t. overnight. The resulting solution was poured onto ice and then solid NaHCO₃ was slowly added until pH ~ 7. The aqueous layer was extracted with CH₂Cl₂ and the organic layer was washed with water. The combined organic layers were dried over anhydrous Na₂SO₄ and concentrated. The yellow mixture was purified by flash-column chromatography on silica gel (100% Petroleum ether) and 6-Bromocyclohex-1-ene-1-carbaldehyde **4** was obtained as a pale yellow liquid (13.6 g, 72%). ¹H NMR (400.0 MHz, CDCl₃): δ = 10.01 (s, 1H), 2.74 (m, 2H), 2.26 (m, 2H), 1.75 (m, 2H), 1.68 (m, 2H). The spectral data matched with the reference.¹



5',6',7'-Trifluoro-2,3-dihydro-1H-xanthene-4-carbaldehyde 5. To 2-hydroxy-3,4,5-trifluoro-benzaldehyde **3** (528 mg, 3 mmol, 1 equiv.) and Cs₂CO₃ (978 mg, 3 mmol, 1 equiv.) in DMF (15 mL) was added 6-bromocyclohex-1-ene-1-carbaldehyde **4** (2.26 g, 12 mmol, 4 equiv.) and the mixture was stirred at 25 °C for 56 h. The reaction mixture was filtered and concentrated *in vacuo*. Purification by flash-column chromatography on silica gel (10% EtOAc in petroleum ether) afforded 5',6',7'-Trifluoro-2,3-dihydro-1H-xanthene-4-carbaldehyde **5** as a yellow solid (483 mg, 61%). ¹H NMR (400.0 MHz, CDCl₃): δ = 10.35 (s, 1H), 6.78 (m, 1H), 6.53 (s, 1H), 2.59 (t, *J* = 5.8 Hz, 2H), 2.45 (t, *J* = 6.1 Hz, 2H), 1.73 (m, 2H) ppm; ¹⁹F NMR (376.5 MHz, CDCl₃): δ = -140.7 (m, 1F), -155.2 (m, 1F), -155.8 (m, 1F) ppm; ¹³C NMR (100.0 MHz, CDCl₃): δ = 188.1, 157.9, 146.9 (ddd, *J*_{C-F} = 2.1 Hz, *J*_{C-F} = 11.1 Hz, ¹*J*_{C-F} = 246.6 Hz), 140.6 (ddd, *J*_{C-F} = 12.1 Hz, *J*_{C-F} = 16.9 Hz, ¹*J*_{C-F} = 254.2 Hz), 139.8 (ddd, *J*_{C-F} = 4.0 Hz, *J*_{C-F} = 12.5 Hz, ¹*J*_{C-F} = 253.8 Hz), 137.4 (m), 131.5 (d, *J*_{C-F} = 2.9 Hz), 123.6 (dd, *J*_{C-F} = 3.1 Hz, *J*_{C-F} = 5.7 Hz), 117.1 (m), 115.2 (d, *J*_{C-F} = 0.9 Hz), 107.8 (dd, *J*_{C-F} = 3.7 Hz, *J*_{C-F} = 19.6 Hz), 30.1, 21.5, 20.0 ppm; HRMS (ESI⁺): *m/z* calcd for C₁₄H₉F₃O₂ [M + Na]⁺ 289.0447, found 289.0450.

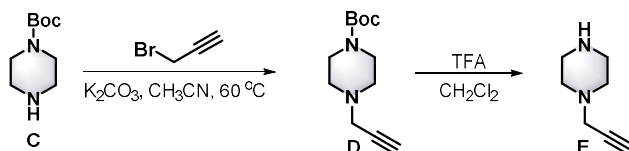


1,2,3,3-tetramethyl-3H-indol-1-ium iodide 6. To 2,3,3-trimethyl-3H-indole (32 mL, 200 mmol, 1 equiv.) in CH₃CN (200 mL) was added iodomethane (14 mL, 228 mmol, 2.28 equiv.) portion-wise and the solution was refluxed overnight. The precipitate was filtered and washed with Et₂O and dried *in vacuo* to afford 1,2,3,3-tetramethyl-3H-indol-1-ium iodide **6** as a light pink solid (56.5 g, 94%). ¹H NMR (400.0 MHz, DMSO-*d*₆): δ = 7.91 (m, 1H), 7.82 (m, 1H), 7.62 (m, 2H), 3.97 (s, 3H), 2.76 (s, 3H), 1.53 (s, 3H) ppm; ¹³C NMR (100.0 MHz, DMSO-*d*₆): δ = 196.5, 142.6, 142.1, 129.8, 129.3, 123.8, 115.6, 54.4, 35.1, 22.2, 14.5 ppm. The spectral data matched with the reference.²



5',6',7'-trifluoro DHX-hemicyanine fused dye precursor 1. To 5',6',7'-Trifluoro-2,3-dihydro-1H-xanthene-4-carbaldehyde **5** (265 mg, 0.99 mmol, 1 equiv.) in EtOH (2 mL) was added 1,2,3,3-tetramethyl-3H-indol-1-ium iodide **6** (300 mg, 0.99 mmol, 1 equiv.) and the solution was refluxed at 80 °C for 4 h. The reaction mixture was concentrated and the crude product was purified by flash-column chromatography on silica gel (1% MeOH in CH₂Cl₂) to afford compound **1** as a dark blue solid (483 mg, 88%). ¹H NMR (400.0 MHz, DMSO-*d*₆): δ = 8.50 (d, *J* = 15.6 Hz, 1H), 7.82 (m, 2H), 7.56 (m, 3H), 7.18 (s, 1H), 6.83 (d, *J* = 15.6 Hz, 1H), 4.01 (s, 3H), 2.70 (m, 4H), 1.82 (m, 2H), 1.74 (s, 6H) ppm; ¹⁹F NMR (376.5 MHz, DMSO-*d*₆): δ = -140.2 (m, 1F), -156.1 (m, 1F), -157.6 (d, *J*_{F-F} = 19.4 Hz, 1F) ppm; ¹³C NMR (100.0 MHz, DMSO-*d*₆): δ = 180.0, 156.0, 146.8 (dd, *J*_{C-F} = 10.2 Hz, ¹*J*_{C-F} = 244.2 Hz), 145.3, 143.1, 142.5, 140.6 (m), 140.4 (ddd, *J*_{C-F} = 11.9 Hz, *J*_{C-F} = 17.1 Hz, ¹*J*_{C-F} = 253.0 Hz), 138.0 (m), 131.9, 129.4, 128.8, 127.2, 123.3, 118.5 (dd, *J*_{C-F} = 3.1 Hz, *J*_{C-F} = 9.2 Hz), 115.5, 114.8, 109.6 (d, *J*_{C-F} = 2.8 Hz), 109.4, 51.6, 34.1, 29.2, 27.1, 23.9, 20.1 ppm; HRMS (ESI⁺): *m/z* calcd for C₂₆H₂₃F₃NO⁺ [M]⁺ 422.1763, found 422.1707; HPLC (system A): *t*_R = 4.8 min (purity >99% at 600 nm); LRMS (ESI⁺, recorded during RP-HPLC analysis): *m/z* 422.2 [M]⁺ (100), calcd for C₂₆H₂₃F₃NO⁺ 422.2; UV-vis (recorded during the HPLC analysis): λ_{max} = 541 nm (broad peak).

3.2. Preparation of Substrate E

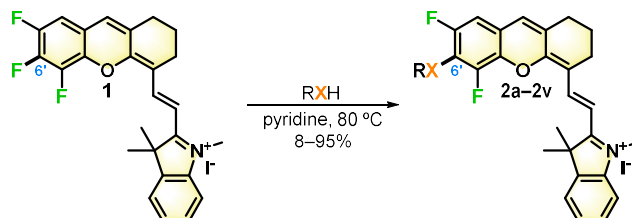


Scheme S2 Synthesis of substrate E

To 1-(tert-Butyloxycarbonyl)piperazine **C** (3.7 g, 20 mmol, 1 equiv.) in CH₃CN (80 mL) were added 3-bromopropyne (1.9 mL, 22 mmol, 1.1 equiv.) and K₂CO₃ (4.1 g, 30 mmol, 1.5 equiv.) and the mixture was stirred at 60 °C for 2 h. After cooling down to r.t., the solvent was removed under reduced pressure. The residue was washed with water and extracted

in DCM. Purification by flash-column chromatography on silica gel (20% EtOAc in petroleum ether) afforded tert-butyl 4-(prop-2-yn-1-yl)piperazine-1-carboxylate **D**. The latter was dissolved in DCM (25 mL), TFA (25 mL) was added and the mixture was stirred at r.t. for 3 h. The reaction mixture was washed with sat. aqueous NaHCO₃ solution and extracted with EtOAc. After concentration *in vacuo*, 1-(prop-2-yn-1-yl)piperazine **E** was obtained as a yellow solid (1.2 g, 48%). ¹H NMR (400.0 MHz, DMSO-*d*₆): δ = 3.20 (d, *J* = 2.2 Hz, 2H), 3.09 (t, *J* = 2.4 Hz, 1H), 2.71 (brs, 4H), 2.36 (brs, 4H) ppm. The spectrum matched with the corresponding reference.³

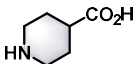
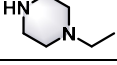
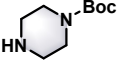
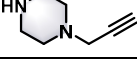
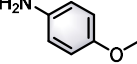
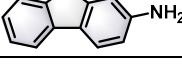
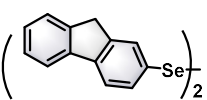
3.3 General procedure for the S_NAr reaction

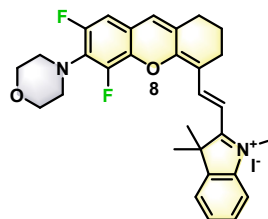


General procedure for the synthesis of NIR DHX-hemicyanine fused dyes **8 and **2a-2u**.** To intermediate **1** (220 mg, 0.4 mmol, 1 equiv.) in pyridine (1 mL) was added the respective nucleophile (2 mmol, 5 equiv.) and the mixture was heated at 80 °C for 12 h in a sealed tube. After cooling down to r.t., the reaction mixture was concentrated *in vacuo* and directly purified by flash-column chromatography on silica gel (1% MeOH in CH₂Cl₂) to afford the corresponding blue products **2a-2u**.

Table 1 The product and corresponding nucleophiles

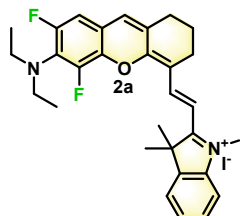
Nucleophiles (RXH)	Product	Yields
	8	61%
	2a	25%
	2b	34%
	2c	16%
NaN ₃	2d	44%
	2e	61%
	2f	65%
	2g	8%
	2h	45%

	2i	35%
	2j	29%
	2k	76%
	2l	81%
	2m	39%
	2n	35%
	2o	43%
	2p	45%
	2q	86%
	2r	71%
	2s	92%
	2t	95%
	2u	66%

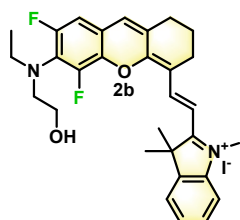


8: 61% yield; Dark green solid; $^1\text{H NMR}$ (400.0 MHz, $\text{DMSO-}d_6$): δ = 8.54 (d, J = 15.4 Hz, 1H), 7.83 (d, J = 7.3 Hz, 1H), 7.74 (d, J = 7.9 Hz, 1H), 7.57 (dd, J = 7.3, 7.5 Hz, 1H), 7.50 (t, J = 7.4 Hz, 1H), 7.26 (m, 2H), 6.71 (d, J = 15.4 Hz, 1H), 3.95 (s, 3H), 3.73 (t, J = 4.2 Hz, 4H), 3.26 (brs, 4H), 2.70 (m, 4H), 1.82 (m, 2H), 1.74 (s, 6H) ppm; $^{19}\text{F NMR}$ (376.5 MHz, $\text{DMSO-}d_6$): δ = -124.3 (m, 1F), -146.5 (s, 1F) ppm; $^{13}\text{C NMR}$ (100.0 MHz, $\text{DMSO-}d_6$): δ = 179.2, 157.9, 153.3 (dd, $J_{\text{C-F}}$ = 5.9 Hz, $^1J_{\text{C-F}}$ = 243.8 Hz), 144.3 (dd, $J_{\text{C-F}}$ = 7.6 Hz, $^1J_{\text{C-F}}$ = 247.9 Hz), 145.2, 142.8, 142.6, 138.6 (dd, $J_{\text{C-F}}$ = 1.6 Hz, $J_{\text{C-F}}$ = 10.1 Hz), 130.3 (dd, $J_{\text{C-F}}$ = 9.0 Hz, $J_{\text{C-F}}$ = 14.5 Hz), 130.0, 129.7, 129.4, 128.3, 123.3, 117.0 (d, $J_{\text{C-F}}$ = 11.0

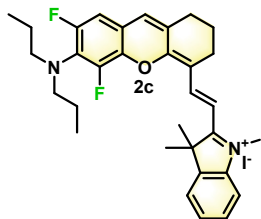
(Hz), 115.0, 114.3, 109.1 (dd, $J_{C-F} = 2.2$ Hz, $J_{C-F} = 24.3$ Hz), 107.6, 67.1, 51.4, 51.2, 33.7, 29.1, 27.4, 23.9, 20.2 ppm; HRMS (ESI+): m/z calcd for $C_{30}H_{31}F_2N_2O_2^+$ $[M]^{+\circ}$ 489.2348, found 489.2343; HPLC (system A): $t_R = 4.8$ min (purity 100% at 600 nm); LRMS (ESI+, recorded during RP-HPLC analysis): m/z 489.2 $[M]^{+\circ}$ (100), calcd for $C_{30}H_{31}F_2N_2O_2^+$ 489.2; UV-vis (recorded during the HPLC analysis): $\lambda_{max} = 602$ nm (broad peak).



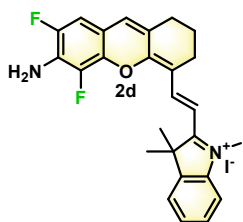
2a: 25% yield; Dark green solid; 1H NMR (400.0 MHz, DMSO- d_6): $\delta = 8.58$ (d, $J = 15.3$ Hz, 1H), 7.82 (d, $J = 7.3$ Hz, 1H), 7.73 (d, $J = 7.9$ Hz, 1H), 7.57 (dd, $J = 7.5, 7.7$ Hz, 1H), 7.50 (t, $J = 7.4$ Hz, 1H), 7.26 (m, 2H), 6.70 (d, $J = 15.3$ Hz, 1H), 3.94 (s, 3H), 3.26 (q, $J = 7.0$ Hz, 4H), 2.70 (m, 4H), 1.82 (m, 2H), 1.74 (s, 6H), 1.05 (t, $J = 7.0$ Hz, 6H) ppm; ^{19}F NMR (376.5 MHz, DMSO- d_6): $\delta = -123.2$ (m, 1F), -145.0 (s, 1F) ppm; ^{13}C NMR (100.0 MHz, DMSO- d_6): $\delta = 178.7, 157.5, 154.4$ (dd, $J_{C-F} = 5.8$ Hz, $^1J_{C-F} = 244.3$ Hz), 145.4 (dd, $J_{C-F} = 9.2$ Hz, $^1J_{C-F} = 248.1$ Hz), 144.8, 142.3, 142.1, 138.0 (dd, $J_{C-F} = 1.3$ Hz, $J_{C-F} = 10.5$ Hz), 129.6, 129.4, 128.9 - 128.6 (m), 128.8, 127.7, 122.7, 116.8 (d, $J_{C-F} = 11.6$ Hz), 114.4, 113.7, 108.3 (dd, $J_{C-F} = 2.0$ Hz, $J_{C-F} = 24.5$ Hz), 106.9, 50.7, 46.4, 33.1, 28.6, 26.9, 23.4, 19.8, 13.2 ppm; HRMS (ESI+): m/z calcd for $C_{30}H_{33}F_2N_2O^+$ $[M]^{+\circ}$ 475.2555, found 475.2552; HPLC (system A): $t_R = 5.4$ min (purity 99% at 600 nm); LRMS (ESI+, recorded during RP-HPLC analysis): m/z 474.9 $[M]^{+\circ}$ (100), calcd for $C_{30}H_{33}F_2N_2O^+$ 475.3; UV-vis (recorded during the HPLC analysis): $\lambda_{max} = 598$ nm (broad peak).



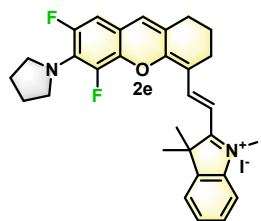
2b: 34% yield; Dark green solid; 1H NMR (400.0 MHz, CD $_3$ OD): $\delta = 8.80$ (d, $J = 15.2$ Hz, 1H), 7.69 (d, $J = 7.3$ Hz, 1H), 7.62 (d, $J = 7.9$ Hz, 1H), 7.56 (dd, $J = 7.1, 7.6$ Hz, 1H), 7.50 (t, $J = 7.3$ Hz, 1H), 7.21 (s, 1H), 7.06 (dd, $J_{H-F} = 1.1$ Hz, $J_{H-F} = 11.6$ Hz, 1H), 6.66 (d, $J = 15.2$ Hz, 1H), 3.93 (s, 3H), 3.68 (t, $J = 6.0$ Hz, 2H), 3.42 (m, 4H), 2.76 (m, 4H), 1.94 (m, 2H), 1.83 (s, 6H), 1.14 (t, $J = 7.1$ Hz, 3H) ppm; ^{19}F NMR (376.5 MHz, CD $_3$ OD): $\delta = -123.7$ (m, 1F), -145.3 (s, 1F) ppm; ^{13}C NMR (100.0 MHz, CD $_3$ OD): $\delta = 180.8, 160.5, 156.7$ (dd, $J_{C-F} = 5.9$ Hz, $^1J_{C-F} = 245.3$ Hz), 147.6, 147.4 (dd, $J_{C-F} = 8.0$ Hz, $^1J_{C-F} = 248.2$ Hz), 143.8, 143.7, 140.1 (dd, $J_{C-F} = 2.1$ Hz, $J_{C-F} = 10.9$ Hz), 131.7 (t, $J_{C-F} = 2.9$ Hz), 131.5 (dd, $J_{C-F} = 10.1$ Hz, $J_{C-F} = 15.6$ Hz), 131.3, 130.4, 129.2, 123.9, 118.6 (d, $J_{C-F} = 11.3$ Hz), 116.4, 114.4, 109.4 (dd, $J_{C-F} = 3.1$ Hz, $J_{C-F} = 24.9$ Hz), 107.2, 61.4, 55.9 (t, $J_{C-F} = 3.3$ Hz), 52.5, 33.4, 30.4, 28.1, 25.1, 21.7, 14.0 ppm; HRMS (ESI+): m/z calcd for $C_{30}H_{33}F_2N_2O_2^+$ $[M]^{+\circ}$ 491.2505, found 491.2488; HPLC (system A): $t_R = 4.7$ min (purity >99% at 600 nm); LRMS (ESI+, recorded during RP-HPLC analysis): m/z 491.0 $[M]^{+\circ}$ (100), calcd for $C_{30}H_{33}F_2N_2O_2^+$ 491.2; UV-vis (recorded during the HPLC analysis): $\lambda_{max} = 598$ nm (broad peak).



2c: 16% yield; Dark green solid; $^1\text{H NMR}$ (400.0 MHz, CD_3OD): δ = 8.78 (d, J = 15.1 Hz, 1H), 7.69 (d, J = 7.3 Hz, 1H), 7.62 (d, J = 7.9 Hz, 1H), 7.56 (dd, J = 7.4, 7.8 Hz, 1H), 7.49 (t, J = 7.4 Hz, 1H), 7.22 (s, 1H), 7.06 (dd, $J_{\text{H-F}}$ = 1.0 Hz, $J_{\text{H-F}}$ = 11.6 Hz, 1H), 6.66 (d, J = 15.2 Hz, 1H), 3.94 (s, 3H), 3.27 (t, J = 7.0 Hz, 4H), 2.75 (m, 4H), 1.94 (brs, 2H), 1.83 (s, 6H), 1.56 (m, 4H), 0.91 (t, J = 7.3 Hz, 6H) ppm; $^{19}\text{F NMR}$ (376.5 MHz, CD_3OD): δ = -123.8 (m, 1F), -145.9 (s, 1F) ppm; $^{13}\text{C NMR}$ (100.0 MHz, CD_3OD): δ = 180.7, 160.5, 156.5 (dd, $J_{\text{C-F}}$ = 6.0 Hz, $^1J_{\text{C-F}}$ = 245.2 Hz), 147.5, 147.1 (dd, $J_{\text{C-F}}$ = 7.9 Hz, $^1J_{\text{C-F}}$ = 247.8 Hz), 143.8, 143.7, 140.1 (dd, $J_{\text{C-F}}$ = 1.7 Hz, $J_{\text{C-F}}$ = 10.6 Hz), 131.8 (m), 131.8, 130.4, 129.1, 123.9, 118.2 (d, $J_{\text{C-F}}$ = 1.3 Hz), 116.4, 114.5, 109.5 (d, $J_{\text{C-F}}$ = 24.6 Hz), 107.2, 56.1 (t, $J_{\text{C-F}}$ = 3.3 Hz), 52.4, 33.7, 30.4, 28.1, 25.1, 22.7, 21.6, 11.8 ppm; HRMS (ESI⁺): m/z calcd for $\text{C}_{32}\text{H}_{37}\text{F}_2\text{N}_2\text{O}^+$ $[\text{M}]^{\text{+}}$ 503.2868, found 503.2868; HPLC (system A): t_{R} = 5.7 min (purity >99% at 600 nm); LRMS (ESI⁺, recorded during RP-HPLC analysis): m/z 503.1 $[\text{M}]^{\text{+}}$ (100), calcd for $\text{C}_{32}\text{H}_{37}\text{F}_2\text{N}_2\text{O}^+$ 503.3; UV-vis (recorded during the HPLC analysis): λ_{max} = 615 nm (broad peak).

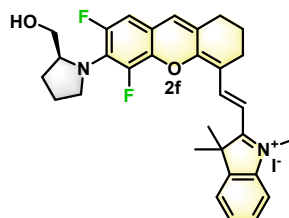


2d: 44% yield; Dark green solid; $^1\text{H NMR}$ (600.0 MHz, $\text{DMSO-}d_6$): δ = 8.58 (d, J = 14.9 Hz, 1H), 7.76 (d, J = 7.4 Hz, 1H), 7.64 (d, J = 8.0 Hz, 1H), 7.53 (dd, J = 7.5, 7.9 Hz, 1H), 7.43 (t, J = 7.5 Hz, 1H), 7.41 (s, 1H), 7.26 (d, $J_{\text{H-F}}$ = 10.5 Hz, 1H), 6.60 (brs, 2H), 6.54 (d, J = 15.0 Hz, 1H), 3.84 (s, 3H), 2.71 (t, J = 5.8 Hz, 2H), 2.67 (t, J = 6.0 Hz, 2H), 1.82 (m, 2H), 1.72 (s, 6H) ppm; $^{19}\text{F NMR}$ (376.5 MHz, $\text{DMSO-}d_6$): δ = -133.2 (m, 1F), -157.4 (d, $J_{\text{F-F}}$ = 11.4 Hz, 1F) ppm; $^{13}\text{C NMR}$ (100.0 MHz, $\text{DMSO-}d_6$): δ = 177.0, 159.4, 147.6 (dd, $J_{\text{C-F}}$ = 7.4 Hz, $^1J_{\text{C-F}}$ = 239.5 Hz), 144.0, 142.3, 141.7, 138.6 (d, $J_{\text{C-F}}$ = 8.0 Hz), 137.1 (dd, $J_{\text{C-F}}$ = 8.7 Hz, $^1J_{\text{C-F}}$ = 240.4 Hz), 133.0, 130.4 (dd, $J_{\text{C-F}}$ = 12.7 Hz, $J_{\text{C-F}}$ = 18.5 Hz), 128.7, 126.7, 125.4, 122.6, 113.9, 112.9, 109.6 (d, $J_{\text{C-F}}$ = 10.2 Hz), 107.8 (d, $J_{\text{C-F}}$ = 20.9 Hz), 104.3, 50.0, 32.4, 28.2, 27.2, 23.4, 19.9 ppm; HRMS (ESI⁺): m/z calcd for $\text{C}_{26}\text{H}_{25}\text{F}_2\text{N}_2\text{O}^+$ $[\text{M}]^{\text{+}}$ 419.1929, found 419.1916; HPLC (system A): t_{R} = 4.6 min (purity 99% at 600 nm); LRMS (ESI⁺, recorded during RP-HPLC analysis): m/z 419.0 $[\text{M}]^{\text{+}}$ (100), calcd for $\text{C}_{26}\text{H}_{25}\text{F}_2\text{N}_2\text{O}^+$ 419.2; UV-vis (recorded during the HPLC analysis): λ_{max} = 620 and 671 nm (broad peak).

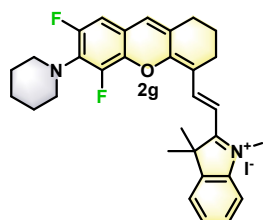


2e: 61% yield; Dark green solid; $^1\text{H NMR}$ (400.0 MHz, CD_3OD): δ = 8.72 (d, J = 14.9 Hz, 1H), 7.64 (d, J = 7.4 Hz, 1H), 7.52 (m, 2H), 7.43 (m, 1H), 7.27 (s, 1H), 7.02 (d, $J_{\text{H-F}}$ = 13.6 Hz, 1H), 6.50 (d, J = 14.9 Hz, 1H), 3.84 (s, 3H), 3.74 (brs, 4H), 2.74 (m, 4H), 1.95 (m, 6H), 1.79 (s, 6H) ppm; $^{19}\text{F NMR}$ (376.5 MHz, CD_3OD): δ = -126.0 (m, 1F), -153.1 (s, 1F) ppm; $^{13}\text{C NMR}$ (100.0 MHz, CD_3OD): δ = 179.3, 162.0, 151.6 (dd, $J_{\text{C-F}}$ = 8.1 Hz, $^1J_{\text{C-F}}$ = 243.5 Hz), 146.6, 143.9, 143.4, 141.4 (d, $J_{\text{C-F}}$ = 11.0 Hz), 141.3 (dd, $J_{\text{C-F}}$ = 9.4 Hz, $^1J_{\text{C-F}}$ = 243.2 Hz), 134.2, 131.9 (dd, $J_{\text{C-F}}$ = 8.3 Hz, $J_{\text{C-F}}$ = 14.4 Hz),

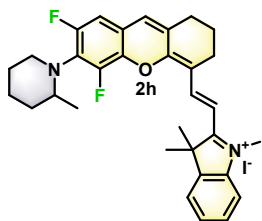
130.3, 128.4, 128.1, 123.8, 116.2, 113.7, 113.4 (d, J_{C-F} = 11.3 Hz), 110.0 (d, J_{C-F} = 25.3 Hz), 105.1, 53.1 (t, J_{C-F} = 6.4 Hz), 51.9, 33.0, 30.9, 30.1, 28.4, 26.9, 21.8 ppm; HRMS (ESI+): m/z calcd for $C_{30}H_{31}F_2N_2O^+$ $[M]^{+\circ}$ 473.2399, found 473.2386; HPLC (system A): t_R = 5.5 min (purity 98% at 600 nm); LRMS (ESI+, recorded during RP-HPLC analysis): m/z 473.2 $[M]^{+\circ}$ (100), calcd for $C_{30}H_{31}F_2N_2O^+$ 473.2; UV-vis (recorded during the HPLC analysis): λ_{max} = 647 and 701 nm (broad peak).



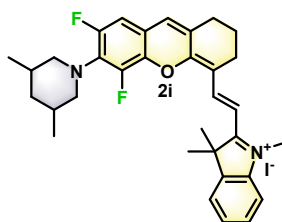
2f: 10% yield; Dark blue solid; Purification using semi-preparative RP-HPLC; 1H NMR (400.0 MHz, CD_3OD): δ = 8.79 (d, J = 15.0 Hz, 1H), 7.65 (d, J = 7.4 Hz, 1H), 7.59–7.48 (m, 2H), 7.48–7.43 (m, 1H), 7.26 (d, J = 1.6 Hz, 1H), 7.05 (dd, J = 13.0, 2.0 Hz, 1H), 6.55 (d, J = 15.0 Hz, 1H), 4.38 (m, J = 7.5 Hz, 1H), 4.00–3.90 (m, 1H), 3.86 (s, 3H), 3.65–3.42 (m, 3H), 2.75 (dt, J = 20.5, 6.4 Hz, 4H), 2.23–2.17 (m, J = 7.3, 3.9 Hz, 1H), 2.10–2.02 (m, 1H), 1.98–1.88 (m, J = 12.5, 4.9 Hz, 4H), 1.81 (d, J = 3.2 Hz, 6H); ^{13}C NMR (100.0 MHz, CD_3OD): δ = 179.8, 161.5, 147.0, 143.7, 143.4, 133.3, 130.2, 129.0, 128.5, 123.6, 116.0, 115.1, 115.0, 113.8, 109.6, 109.4, 105.5, 64.7, 63.0, 54.2, 52.0, 32.8, 30.1, 29.5, 28.1, 26.0, 24.9, 21.6 ppm; IR (film) ν_{max} = 3386, 2925, 2861, 1686, 1636, 1600, 1565, 1536, 1503, 1459, 1402, 1366, 1307, 1292, 1270, 1237, 1202, 1171, 1114, 1065, 1043, 1020, 929, 837 cm^{-1} ; HRMS (ESI+): m/z calcd for $C_{31}H_{33}F_2N_2O_2^+$ $[M]^{+\circ}$ 503.2505, found 503.2500; HPLC (system A): t_R = 4.8 min (purity 98% at 600 nm); LRMS (ESI+, recorded during RP-HPLC analysis): m/z 503.3 $[M]^{+\circ}$ (100), calcd for $C_{31}H_{33}F_2N_2O_2^+$ 503.3; UV-vis (recorded during the HPLC analysis): λ_{max} = 637 and 691 nm (broad peak).



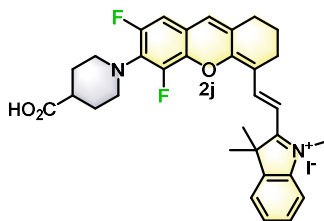
2g: 65% yield; Dark green solid; 1H NMR (400.0 MHz, $CDCl_3$): δ = 8.69 (d, J = 15.1 Hz, 1H), 7.46 (m, 4H), 6.97 (s, 1H), 6.82 (m, 2H), 4.16 (s, 3H), 3.31 (brs, 4H), 2.90 (t, J = 6.0 Hz, 2H), 2.72 (t, J = 5.4 Hz, 2H), 1.96 (m, 2H), 1.81 (s, 6H), 1.72 (m, 4H), 1.66 (m, 2H) ppm; ^{19}F NMR (376.5 MHz, CD_3OD): δ = -125.1 (d, J_{H-F} = 6.4 Hz, 1F), -147.1 (s, 1F) ppm; ^{13}C NMR (100.0 MHz, CD_3OD): δ = 180.7, 160.7, 155.3 (dd, J_{C-F} = 6.8 Hz, $^1J_{C-F}$ = 245.0 Hz), 147.5, 145.8 (dd, J_{C-F} = 7.0 Hz, $^1J_{C-F}$ = 247.2 Hz), 143.8, 143.7, 140.4 (m), 133.6 (dd, J_{C-F} = 9.1 Hz, J_{C-F} = 14.7 Hz), 132.0, 130.8, 130.4, 129.1, 123.9, 117.6 (d, J_{C-F} = 11.0 Hz), 116.4, 114.4, 109.6 (dd, J_{C-F} = 2.8 Hz, J_{C-F} = 24.4 Hz), 106.9, 53.7 (t, J_{C-F} = 3.8 Hz), 52.4, 33.4, 30.3, 28.1, 27.9, 25.4, 25.1, 21.7 ppm; HRMS (ESI+): m/z calcd for $C_{31}H_{33}F_2N_2O^+$ $[M]^{+\circ}$ 487.2555, found 487.2524; HPLC (system A): t_R = 5.5 min (purity 100% at 600 nm); LRMS (ESI+, recorded during RP-HPLC analysis): m/z 487.2 $[M]^{+\circ}$ (100), calcd for $C_{31}H_{33}F_2N_2O^+$ 487.3; UV-vis (recorded during the HPLC analysis): λ_{max} = 613 nm (broad peak).



2h: 8% yield; Dark green solid; $^1\text{H NMR}$ (400.0 MHz, CD_3OD): δ = 8.80 (d, J = 15.2 Hz, 1H), 7.70 (d, J = 7.3 Hz, 1H), 7.64 (d, J = 7.9 Hz, 1H), 7.57 (dd, J = 7.3, 7.9 Hz, 1H), 7.51 (t, J = 7.5 Hz, 1H), 7.19 (s, 1H), 7.06 (d, $J_{\text{H-F}}$ = 11.0 Hz, 1H), 6.69 (d, J = 15.3 Hz, 1H), 3.95 (s, 3H), 3.42 (m, 1H), 3.26 (m, 1H), 3.08 (m, 1H), 2.76 (m, 4H), 1.94 (m, 2H), 1.84 (s, 7H), 1.70 (m, 3H), 1.56 (m, 2H), 1.04 (d, J = 6.3 Hz, 3H) ppm; $^{19}\text{F NMR}$ (376.5 MHz, CD_3OD): δ = -123.7 (m, 1F), -145.3 (s, 1F) ppm; $^{13}\text{C NMR}$ (100.0 MHz, CD_3OD): δ = 181.1, 160.0, 157.9 (d, $^1J_{\text{C-F}}$ = 245.2 Hz), 148.7 (d, $^1J_{\text{C-F}}$ = 251.5 Hz), 147.7, 143.9, 143.7, 139.8 (d, $J_{\text{C-F}}$ = 10.5 Hz), 132.3 (dd, $J_{\text{C-F}}$ = 16.6 Hz, $J_{\text{C-F}}$ = 27.1 Hz), 132.1, 131.0, 130.4, 129.3, 120.1 (d, $J_{\text{C-F}}$ = 10.2 Hz) 116.6, 114.7, 109.4 (d, $J_{\text{C-F}}$ = 25.3 Hz), 107.9, 56.0, 52.6, 35.2, 30.9, 30.4, 28.1, 27.9, 25.1, 24.0, 21.6, 19.5 ppm; HRMS (ESI⁺): m/z calcd for $\text{C}_{32}\text{H}_{35}\text{F}_2\text{N}_2\text{O}^+$ $[\text{M}]^{\oplus}$ 501.2712, found 501.2707; HPLC (system A): t_{R} = 5.6 min (purity >99% at 600 nm); LRMS (ESI⁺, recorded during RP-HPLC analysis): m/z 501.1 $[\text{M}]^{\oplus}$ (100), calcd for $\text{C}_{32}\text{H}_{35}\text{F}_2\text{N}_2\text{O}^+$ 501.3; UV-vis (recorded during the HPLC analysis): λ_{max} = 589 nm (broad peak).

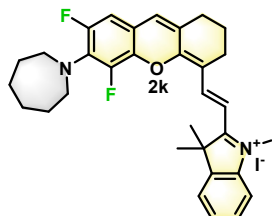


2i: 45% yield; Dark green solid; $^1\text{H NMR}$ (400.0 MHz, $\text{DMSO-}d_6$): δ = 8.52 (d, J = 15.3 Hz, 1H), 7.82 (d, J = 7.3 Hz, 1H), 7.74 (d, J = 7.9 Hz, 1H), 7.56 (dd, J = 7.1, 7.5 Hz, 1H), 7.48 (t, J = 7.5 Hz, 1H), 7.27 (s, 1H), 7.22 (m, 1H), 6.68 (d, J = 15.3 Hz, 1H), 3.94 (s, 3H), 3.26 (d, J = 10.8 Hz, 2H), 2.64 (m, 6H), 1.78 (m, 12H), 0.86 (d, J = 6.5 Hz, 6H) ppm; $^{19}\text{F NMR}$ (376.5 MHz, $\text{DMSO-}d_6$): δ = -124.2 (m, 1F), -146.9 (s, 1F) ppm; $^{13}\text{C NMR}$ (100.0 MHz, $\text{DMSO-}d_6$): δ = 178.4, 157.6, 152.7 (dd, $J_{\text{C-F}}$ = 6.1 Hz, $^1J_{\text{C-F}}$ = 243.4 Hz), 144.5, 143.6 (dd, $J_{\text{C-F}}$ = 7.5 Hz, $^1J_{\text{C-F}}$ = 247.1 Hz), 142.2, 142.1, 138.1 (dd, $J_{\text{C-F}}$ = 1.5 Hz, $J_{\text{C-F}}$ = 10.2 Hz), 130.7 (dd, $J_{\text{C-F}}$ = 9.4 Hz, $J_{\text{C-F}}$ = 14.7 Hz), 129.6, 129.0, 128.8, 127.6, 122.7, 115.7 (d, $J_{\text{C-F}}$ = 11.3 Hz), 114.4, 113.7, 108.4 (dd, $J_{\text{C-F}}$ = 1.7 Hz, $J_{\text{C-F}}$ = 24.3 Hz), 106.7, 58.0, 50.6, 41.3, 33.1, 31.4, 28.5, 26.9, 23.5, 19.7, 18.9 ppm; HRMS (ESI⁺): m/z calcd for $\text{C}_{33}\text{H}_{37}\text{F}_2\text{N}_2\text{O}^+$ $[\text{M}]^{\oplus}$ 515.2868, found 515.2853; HPLC (system A): t_{R} = 5.9 min (purity 98% at 600 nm); LRMS (ESI⁺, recorded during RP-HPLC analysis): m/z 514.9 $[\text{M}]^{\oplus}$ (100), calcd for $\text{C}_{33}\text{H}_{37}\text{F}_2\text{N}_2\text{O}^+$ 515.3; UV-vis (recorded during the HPLC analysis): λ_{max} = 515 nm (broad peak).

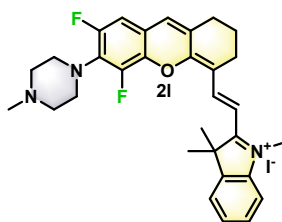


2j: 35% yield; Dark green solid; $^1\text{H NMR}$ (400.0 MHz, CD_3OD): δ = 8.80 (d, J = 15.3 Hz, 1H), 7.69 (d, J = 7.3 Hz, 1H), 7.62 (d, J = 7.8 Hz, 1H), 7.56 (dd, J = 7.2, 8.0 Hz, 1H), 7.50 (t, J = 7.4 Hz, 1H), 7.20 (s, 1H), 7.06 (d, $J_{\text{H-F}}$ = 11.6 Hz, 1H), 6.65 (d, J = 15.2 Hz, 1H), 3.92 (s, 3H), 3.51 (d, J = 12.6 Hz, 2H), 3.25 (t, J = 11.7 Hz, 2H), 2.76 (m, 4H), 2.54 (m, 1H), 2.03 (m, 2H), 1.94 (m, 2H), 1.85 (m, 8H) ppm; $^{19}\text{F NMR}$ (376.5 MHz, CD_3OD): δ = -125.4 (m, 1F), -147.6 (s, 1F) ppm; $^{13}\text{C NMR}$ (100.0 MHz, CD_3OD): δ = 180.8, 178.7, 160.6, 155.3 (dd, $J_{\text{C-F}}$ = 6.1 Hz, $^1J_{\text{C-F}}$ = 244.7 Hz), 147.6, 146.0 (dd,

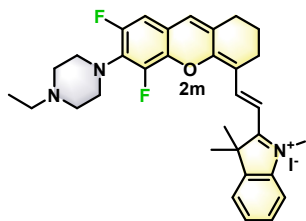
$J_{C-F} = 7.6$ Hz, $^1J_{C-F} = 247.4$ Hz), 143.8, 143.7, 140.2 (dd, $J_{C-F} = 2.2$ Hz, $J_{C-F} = 10.7$ Hz), 133.0 (dd, $J_{C-F} = 9.5$ Hz, $J_{C-F} = 14.9$ Hz), 131.8, 131.1, 130.4, 129.2, 123.9, 118.0 (d, $J_{C-F} = 11.4$ Hz), 116.4, 114.4, 109.6 (dd, $J_{C-F} = 2.0$ Hz, $J_{C-F} = 24.5$ Hz), 107.1, 52.5, 52.1 (t, $J_{C-F} = 3.6$ Hz), 42.0, 33.4, 30.4, 30.3, 28.1, 25.1, 21.7 ppm; HRMS (ESI+): m/z calcd for $C_{32}H_{33}F_2N_2O_3^+$ $[M]^{+\circ}$ 531.2454, found 531.2461; HPLC (system A): $t_R = 4.8$ min (purity >99% at 600 nm); LRMS (ESI+, recorded during RP-HPLC analysis): m/z 530.8 $[M]^{+\circ}$ (100), calcd for $C_{32}H_{33}F_2N_2O_3^+$ 531.3; UV-vis (recorded during the HPLC analysis): $\lambda_{max} = 608$ nm (broad peak).



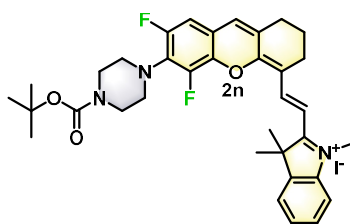
2k: 29% yield; Dark green solid; 1H NMR (400.0 MHz, CD_3OD): $\delta = 8.79$ (d, $J = 15.1$ Hz, 1H), 7.68 (d, $J = 7.2$ Hz, 1H), 7.60 (d, $J = 7.5$ Hz, 1H), 7.55 (ddd, $J = 1.2, 7.3, 7.9$ Hz, 1H), 7.48 (dt, $J = 1.2, 7.2$ Hz, 1H), 7.23 (s, 1H), 7.05 (dd, $J_{H-F} = 1.7$ Hz, $J_{H-F} = 12.3$ Hz, 1H), 6.62 (d, $J = 15.1$ Hz, 1H), 3.91 (s, 3H), 3.51 (t, $J = 5.6$ Hz, 4H), 2.76 (m, 4H), 1.94 (m, 2H), 1.83 (m, 10H), 1.74 (m, 4H) ppm; ^{19}F NMR (376.5 MHz, CD_3OD): $\delta = -125.3$ (t, $J_{H-F} = 9.0$ Hz, 1F), -146.5 (s, 1F) ppm; ^{13}C NMR (100.0 MHz, CD_3OD): $\delta = 180.4, 161.0, 154.9$ (d, $^1J_{C-F} = 242.7$ Hz), 147.4, 145.3 (d, $^1J_{C-F} = 246.5$ Hz), 143.8, 143.7, 140.6 (m), 134.4 (dd, $J_{C-F} = 9.9$ Hz, $J_{C-F} = 15.0$ Hz), 132.4, 130.4, 130.2, 128.9, 123.9, 116.6 (d, $J_{C-F} = 11.1$ Hz), 116.3, 114.2, 109.7 (d, $J_{C-F} = 25.3$ Hz), 106.6, 55.1 (t, $J_{C-F} = 4.1$ Hz), 52.3, 33.4, 31.0, 30.3, 28.8, 28.2, 25.1, 21.7 ppm; HRMS (ESI+): m/z calcd for $C_{32}H_{35}F_2N_2O^+$ $[M]^{+\circ}$ 501.2712, found 501.2713; HPLC (system A): $t_R = 5.7$ min (purity 98% at 600 nm); LRMS (ESI+, recorded during RP-HPLC analysis): m/z 501.1 $[M]^{+\circ}$ (100), calcd for $C_{32}H_{35}F_2N_2O^+$ 501.3; UV-vis (recorded during the HPLC analysis): $\lambda_{max} = 598$ nm (broad peak).



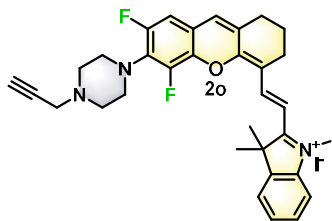
2l: 76% yield; Dark green solid; 1H NMR (400.0 MHz, CD_3OD): $\delta = 8.77$ (d, $J = 15.4$ Hz, 1H), 7.70 (d, $J = 7.2$ Hz, 1H), 7.64 (d, $J = 7.8$ Hz, 1H), 7.57 (dd, $J = 7.2, 7.6$ Hz, 1H), 7.51 (dd, $J = 7.3, 7.2$ Hz, 1H), 7.17 (s, 1H), 7.12 (d, $J_{H-F} = 10.6$ Hz, 1H), 6.71 (d, $J = 15.3$ Hz, 1H), 3.95 (s, 3H), 3.63 (brs, 4H), 3.42 (brs, 4H), 2.96 (s, 3H), 2.76 (m, 4H), 1.94 (m, 2H), 1.82 (s, 6H) ppm; ^{19}F NMR (376.5 MHz, CD_3OD): $\delta = -125.9$ (m, 1F), -146.5 (s, 1F) ppm; ^{13}C NMR (100.0 MHz, CD_3OD): $\delta = 179.7, 158.2, 153.8$ (dd, $J_{C-F} = 5.2$ Hz, $^1J_{C-F} = 245.3$ Hz), 146.2, 144.9 (m), 142.4, 142.2, 138.4 (dd, $J_{C-F} = 2.3$ Hz, $J_{C-F} = 10.7$ Hz), 130.7, 129.1, 128.9, 128.6 (dd, $J_{C-F} = 10.5$ Hz, $J_{C-F} = 15.5$ Hz), 127.9, 122.4, 118.2 (d, $J_{C-F} = 10.9$ Hz), 115.1, 113.2, 108.3 (dd, $J_{C-F} = 3.0$ Hz, $J_{C-F} = 24.3$ Hz), 106.5, 54.0, 51.1, 48.1, 42.8, 32.2, 28.9, 26.5, 23.5, 20.0 ppm; MS (ESI+): m/z calcd for $C_{31}H_{34}F_2N_3O^+$ $[M]^{+\circ}$ 502.2670, found 502.2658; HPLC (system A): $t_R = 3.6$ min (purity >99% at 600 nm); LRMS (ESI+, recorded during RP-HPLC analysis): m/z 272.3 $[2M + H + CH_3CN]^{2+}$ (100) and 502.1 $[M]^{+\circ}$ (45), calcd for $C_{31}H_{34}F_2N_3O^+$ 502.3; UV-vis (recorded during the HPLC analysis): $\lambda_{max} = 591$ nm (broad peak).



2m: 81% yield; Dark green solid; ^1H NMR (400.0 MHz, CD_3OD): δ = 8.78 (d, J = 15.3 Hz, 1H), 7.69 (d, J = 7.4 Hz, 1H), 7.63 (d, J = 7.8 Hz, 1H), 7.56 (ddd, J = 0.9, 7.4, 8.0 Hz, 1H), 7.50 (dt, J = 0.7, 7.4 Hz, 1H), 7.17 (s, 1H), 7.10 (dd, $J_{\text{H-F}} = 1.8$ Hz, $J_{\text{H-F}} = 11.6$ Hz, 1H), 6.68 (d, J = 15.3 Hz, 1H), 3.94 (s, 3H), 3.55 (t, J = 4.4 Hz, 4H), 3.12 (brs, 4H), 2.98 (m, 2H), 2.76 (m, 4H), 1.94 (m, 2H), 1.82 (s, 6H), 1.31 (t, J = 7.3 Hz, 3H) ppm; ^{19}F NMR (376.5 MHz, CD_3OD): δ = -125.7 (m, 1F), -146.9 (s, 1F) ppm; ^{13}C NMR (100.0 MHz, $\text{DMSO-}d_6$): δ = 179.2, 157.8, 153.3 (dd, $J_{\text{C-F}} = 4.6$ Hz, $^1J_{\text{C-F}} = 243.7$ Hz), 144.4 (dd, $J_{\text{C-F}} = 7.6$ Hz, $^1J_{\text{C-F}} = 247.7$ Hz), 145.2, 142.8, 142.6, 138.6 (m), 130.1, 129.9 (m), 129.6, 129.4, 128.3, 123.3, 117.1 (d, $J_{\text{C-F}} = 12.1$ Hz), 115.0, 114.3, 109.1 (d, $J_{\text{C-F}} = 24.6$ Hz), 107.7, 52.6, 51.9, 51.2, 49.9, 33.7, 29.1, 27.4, 23.9, 20.2, 11.2 ppm; MS (ESI⁺): m/z calcd for $\text{C}_{32}\text{H}_{36}\text{F}_2\text{N}_3\text{O}^+$ $[\text{M}]^+$ 516.2826, found 516.2890; HPLC (system A): $t_{\text{R}} = 3.7$ min (purity >99% at 600 nm); LRMS (ESI⁺, recorded during RP-HPLC analysis): m/z 279.3 $[\text{2M} + \text{H} + \text{CH}_3\text{CN}]^{2+}$ (100) and 516.1 $[\text{M}]^+$ (30), calcd for $\text{C}_{32}\text{H}_{36}\text{F}_2\text{N}_3\text{O}^+$ 516.3; UV-vis (recorded during the HPLC analysis): $\lambda_{\text{max}} = 592$ nm (broad peak).

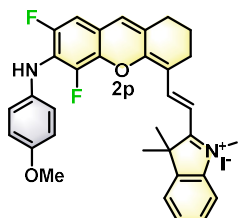


2n: 39% yield; Dark green solid; ^1H NMR (400.0 MHz, $\text{DMSO-}d_6$): δ = 8.56 (d, J = 15.2 Hz, 1H), 7.80 (d, J = 7.2 Hz, 1H), 7.74 (d, J = 7.9 Hz, 1H), 7.57 (dd, J = 7.5, 7.6 Hz, 1H), 7.50 (dd, J = 7.3, 7.4 Hz, 1H), 7.26 (m, 2H), 6.71 (d, J = 15.4 Hz, 1H), 3.94 (s, 3H), 3.47 (brs, 4H), 3.21 (brs, 4H), 2.70 (m, 4H), 1.82 (m, 2H), 1.75 (s, 6H), 1.43 (s, 9H) ppm; ^{19}F NMR (376.5 MHz, $\text{DMSO-}d_6$): δ = -124.1 (m, 1F), -146.0 (s, 1F) ppm; ^{13}C NMR (100.0 MHz, $\text{DMSO-}d_6$): δ = 178.7, 157.3, 153.7, 152.7 (d, $^1J_{\text{C-F}} = 244.3$ Hz), 144.8, 143.9 (d, $J_{\text{C-F}} = 247.8$ Hz), 142.3, 142.0, 138.0 (d, $J_{\text{C-F}} = 10.0$ Hz), 129.9 - 129.8 (m), 129.6, 129.0, 128.8, 127.7, 122.6, 116.6 (d, $J_{\text{C-F}} = 11.2$ Hz), 114.5, 113.7, 108.5 (d, $J_{\text{C-F}} = 23.7$ Hz), 107.1, 79.0, 50.6, 50.4, 33.1, 28.9, 28.5, 28.0, 26.9, 23.4, 19.7 ppm; HRMS (ESI⁺): m/z calcd for $\text{C}_{35}\text{H}_{40}\text{F}_2\text{N}_3\text{O}_3^+$ $[\text{M}]^+$ 588.3032, found 588.3021; HPLC (system A): $t_{\text{R}} = 5.4$ min (purity 97% at 600 nm); LRMS (ESI⁺, recorded during RP-HPLC analysis): m/z 588.3 $[\text{M}]^+$ (100), calcd for $\text{C}_{35}\text{H}_{40}\text{F}_2\text{N}_3\text{O}_3^+$ 588.3; UV-vis (recorded during the HPLC analysis): $\lambda_{\text{max}} = 602$ nm (broad peak).

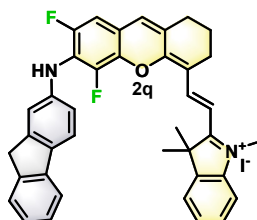


2o: 35% yield; Dark green solid; ^1H NMR (600.0 MHz, $\text{DMSO-}d_6$): δ = 8.56 (d, J = 14.9 Hz, 1H), 7.82 (d, J = 7.4 Hz, 1H), 7.74 (d, J = 8.0 Hz, 1H), 7.57 (dd, J = 7.6, 7.8 Hz, 1H), 7.50 (t, J = 7.4 Hz, 1H), 7.25 (m, 2H), 6.70 (d, J = 15.3 Hz, 1H), 3.94 (s, 3H), 3.38 (brs, 2H), 3.30 (brs, 4H), 3.21 (brs, 1H), 2.71 (brs, 2H), 2.68 (brs, 2H), 2.61 (brs, 4H), 1.82 (m, 2H), 1.75 (s, 6H) ppm; ^{19}F NMR (376.5 MHz, $\text{DMSO-}d_6$): δ = -124.2 (s, 1F), -146.3 (s, 1F) ppm; ^{13}C NMR (100.0 MHz,

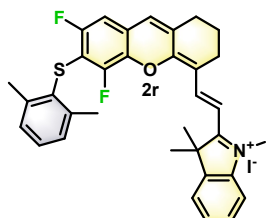
DMSO-*d*₆): δ = 178.7, 157.5, 152.7 (d, $^1J_{C-F}$ = 243.7 Hz), 144.7, 143.7 (dd, J_{C-F} = 7.8 Hz, $^1J_{C-F}$ = 247.0 Hz), 142.2, 142.0, 138.0 (d, J_{C-F} = 9.2 Hz), 130.0 (dd, J_{C-F} = 8.4 Hz, J_{C-F} = 11.3 Hz), 129.3(br), 128.8, 127.6, 122.6, 116.2 (d, J_{C-F} = 11.0 Hz), 114.4, 113.6, 108.5 (d, J_{C-F} = 24.5 Hz), 106.9, 78.9, 75.9, 51.5, 50.6, 50.3, 46.1, 33.0, 28.5, 26.9, 23.4, 19.7 ppm; HRMS (ESI⁺): *m/z* calcd for C₃₃H₃₄F₂N₃O⁺ [M]⁺ 526.2664, found 526.2644; HPLC (system A): *t*_R = 3.9 min (purity 99% at 600 nm); LRMS (ESI⁺, recorded during RP-HPLC analysis): *m/z* 284.3 [2M + H + CH₃CN]⁺ (100) and 526.0 [M]⁺ (55), calcd for C₃₃H₃₄F₂N₃O⁺ 526.3; UV-vis (recorded during the HPLC analysis): λ_{\max} = 591 nm (broad peak).



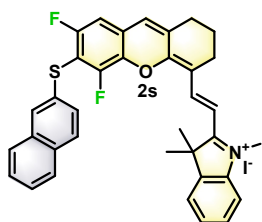
2p: 43% yield; Dark green solid; ¹H NMR (600.0 MHz, CDCl₃): δ = 8.67 (d, *J* = 15.3 Hz, 1H), 7.52 (m, 1H), 7.44 (m, 3H), 7.00 (m, 3H), 6.92 (d, *J*_{H-F} = 10.0 Hz, 1H), 6.89 (m, 2H), 6.84 (d, *J* = 14.9 Hz, 1H), 5.89 (brs, 1H), 4.15 (s, 3H), 3.83 (s, 3H), 2.91 (t, *J* = 6.1 Hz, 2H), 2.74 (t, *J* = 5.7 Hz, 2H), 1.96 (m, 2H), 1.74 (s, 6H) ppm; ¹⁹F NMR (376.5 MHz, CD₃OD): δ = -128.0 (m, 1F), -147.3 (s, 1F) ppm; ¹³C NMR (100.0 MHz, CD₃OD): δ = 180.1, 161.1, 157.2, 152.4 (dd, J_{C-F} = 6.5 Hz, $^1J_{C-F}$ = 244.1 Hz), 147.1, 143.6, 143.5, 140.5 (dd, J_{C-F} = 2.0 Hz, J_{C-F} = 9.2 Hz), 136.4, 132.9, 130.2, 129.6, 128.7, 126.9 (dd, J_{C-F} = 10.1 Hz, J_{C-F} = 16.5 Hz), 123.7, 121.9, 116.1, 115.4 (d, J_{C-F} = 10.3 Hz), 115.1, 113.9, 109.2 (dd, J_{C-F} = 2.5 Hz, J_{C-F} = 22.7 Hz), 106.0, 56.0, 52.1, 32.9, 30.1, 27.9, 25.0, 21.6 ppm; HRMS (ESI⁺): *m/z* calcd for C₃₃H₃₁F₂N₂O₂⁺ [M]⁺ 525.2348, found 525.2348; HPLC (system A): *t*_R = 5.1 min (purity 99% at 600 nm); LRMS (ESI⁺, recorded during RP-HPLC analysis): *m/z* 525.0 [M]⁺ (100), calcd for C₃₃H₃₁F₂N₂O₂⁺ 525.2; UV-vis (recorded during the HPLC analysis): λ_{\max} = 626 nm (broad peak).



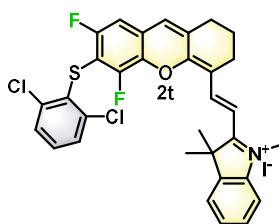
2q: 45% yield; Dark green solid; ¹H NMR (400.0 MHz, CD₃OD): δ = 8.74 (d, *J* = 15.2 Hz, 1H), 7.68 (dd, *J* = 8.1, 8.5 Hz, 2H), 7.56 (d, *J* = 7.9 Hz, 2H), 7.50 (m, 2H), 7.40 (m, 1H), 7.32 (t, *J* = 7.4 Hz, 1H), 7.19 (m, 4H), 6.98 (d, *J*_{H-F} = 8.0 Hz, 1H), 6.60 (d, *J* = 15.1 Hz, 1H), 3.88 (s, 3H), 3.82 (s, 2H), 2.77 (t, *J* = 5.8 Hz, 2H), 2.71 (t, *J* = 5.9 Hz, 2H), 1.94 (m, 2H), 1.73 (s, 6H) ppm; ¹⁹F NMR (376.5 MHz, CD₃OD): δ = -126.7 (m, 1F), -144.9 (s, 1F) ppm; ¹³C NMR (100.0 MHz, CD₃OD): δ = 180.5, 160.8, 153.4 (dd, J_{C-F} = 5.7 Hz, $^1J_{C-F}$ = 244.5 Hz), 147.4, 145.7, 144.8 (d, J_{C-F} = 6.2 Hz), 144.2, 143.7, 143.1, 143.0, 140.4 (d, J_{C-F} = 9.9 Hz), 137.3, 130.5, 130.3, 129.0, 128.0, 127.0, 126.0, 125.3 (dd, J_{C-F} = 11.0 Hz, J_{C-F} = 16.9 Hz), 123.9, 121.1, 120.0, 118.1, 117.1 (d, J_{C-F} = 10.3 Hz), 116.3, 115.7, 114.2, 109.5 (d, J_{C-F} = 22.8 Hz), 106.7, 52.3, 37.8, 33.2, 30.3, 28.0, 25.0, 21.7 ppm; HRMS (ESI⁺): *m/z* calcd for C₃₉H₃₃F₂N₂O⁺ [M]⁺ 583.2555 found 583.2541.



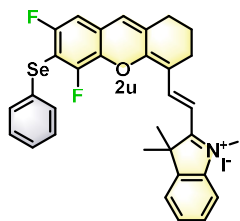
2r: 86% yield; Dark green solid; $^1\text{H NMR}$ (600.0 MHz, CD_3OD): δ = 8.72 (d, J = 15.5 Hz, 1H), 7.72 (d, J = 7.2 Hz, 1H), 7.67 (d, J = 8.0 Hz, 1H), 7.59 (dt, J = 1.0, 7.6 Hz, 1H), 7.54 (dt, J = 0.7, 7.5 Hz, 1H), 7.20 (m, 1H), 7.15 (s, 1H), 7.13 (d, J = 11.7 Hz, 2H), 7.05 (dd, $J_{\text{H-F}}$ = 1.4, 9.1 Hz, 1H), 6.76 (d, J = 15.4 Hz, 1H), 3.96 (s, 3H), 2.77 (t, J = 5.7 Hz, 2H), 2.73 (t, J = 6.0 Hz, 2H), 2.47 (s, 6H), 1.94 (m, 2H), 1.79 (s, 6H) ppm; $^{19}\text{F NMR}$ (376.5 MHz, $\text{DMSO-}d_6$): δ = -112.7 (d, $J_{\text{H-F}}$ = 9.1 Hz, 1F), -131.3 (s, 1F) ppm; $^{13}\text{C NMR}$ (100.0 MHz, $\text{DMSO-}d_6$): δ = 179.4, 156.8 (dd, $J_{\text{C-F}}$ = 3.6 Hz, $^1J_{\text{C-F}}$ = 244.0 Hz), 156.1, 148.1 (dd, $J_{\text{C-F}}$ = 6.5 Hz, $^1J_{\text{C-F}}$ = 248.0 Hz), 145.0, 142.6, 142.1, 142.0, 137.0 (dd, $J_{\text{C-F}}$ = 2.5 Hz, $J_{\text{C-F}}$ = 11.9 Hz), 132.5, 129.6, 129.3, 129.0, 128.6, 128.2, 127.5, 122.8, 122.6 (dd, $J_{\text{C-F}}$ = 1.6 Hz, $J_{\text{C-F}}$ = 10.8 Hz), 115.0, 114.2, 113.7 (dd, $J_{\text{C-F}}$ = 17.4 Hz, $J_{\text{C-F}}$ = 23.3 Hz), 108.6, 108.5 (m), 51.0, 33.5, 28.8, 26.7, 23.4, 21.3, 19.7 ppm; HRMS (ESI⁺): m/z calcd for $\text{C}_{34}\text{H}_{32}\text{F}_2\text{NOS}^+$ $[\text{M}]^+$ 540.2167, found 540.2158.



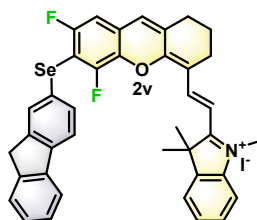
2s: 71% yield; Dark green solid; $^1\text{H NMR}$ (400.0 MHz, $\text{DMSO-}d_6$): δ = 8.51 (d, J = 15.5 Hz, 1H), 7.88 (d, J = 8.5 Hz, 2H), 7.82 (m, 2H), 7.77 (dd, J = 8.1, 8.5 Hz, 2H), 7.58 (t, J = 7.3 Hz, 1H), 7.46 (m, 3H), 7.42 (d, J = 8.5 Hz, 1H), 7.36 (dd, $J_{\text{H-F}}$ = 1.8 Hz, $J_{\text{H-F}}$ = 8.7 Hz, 1H), 7.25 (s, 1H), 6.82 (d, J = 15.6 Hz, 1H), 3.99 (s, 3H), 2.70 (m, 4H), 1.83 (m, 2H), 1.69 (s, 6H) ppm; $^{19}\text{F NMR}$ (376.5 MHz, $\text{DMSO-}d_6$): δ = -110.6 (m, 1F), -128.4 (s, 1F) ppm; $^{13}\text{C NMR}$ (100.0 MHz, $\text{DMSO-}d_6$): δ = 179.5, 157.6 (dd, $J_{\text{C-F}}$ = 2.4 Hz, $^1J_{\text{C-F}}$ = 244.4 Hz), 155.7, 149.4 (dd, $J_{\text{C-F}}$ = 4.7 Hz, $^1J_{\text{C-F}}$ = 248.5 Hz), 144.9, 142.6, 142.0, 137.2 (dd, $J_{\text{C-F}}$ = 2.6 Hz, $J_{\text{C-F}}$ = 12.1 Hz), 133.4, 133.2, 131.6, 131.3, 129.2, 128.9, 128.3, 127.7, 127.1, 127.0, 126.4, 126.2, 125.7, 124.8 (dd, $J_{\text{C-F}}$ = 2.2 Hz, $J_{\text{C-F}}$ = 11.1 Hz), 122.7, 115.2, 114.3, 110.1 (dd, $J_{\text{C-F}}$ = 18.6 Hz, $J_{\text{C-F}}$ = 24.8 Hz), 108.9, 108.6 (m), 51.0, 33.6, 28.8, 26.6, 23.3, 19.6 ppm; HRMS (ESI⁺): m/z calcd for $\text{C}_{36}\text{H}_{30}\text{F}_2\text{NOS}^+$ $[\text{M}]^+$ 562.2011, found 562.1994.



2t: 92% yield; Dark green solid; $^1\text{H NMR}$ (400.0 MHz, $\text{DMSO-}d_6$): δ = 8.50 (d, J = 15.6 Hz, 1H), 7.84 (d, J = 7.1 Hz, 1H), 7.79 (d, J = 7.8 Hz, 1H), 7.60 (m, 3H), 7.54 (dd, J = 7.3, 7.4 Hz, 1H), 7.47 (dd, J = 7.7, 8.5 Hz, 1H), 7.30 (d, $J_{\text{H-F}}$ = 9.0 Hz, 1H), 7.19 (s, 1H), 6.82 (d, J = 15.6 Hz, 1H), 3.98 (s, 3H), 2.71 (m, 4H), 1.82 (m, 2H), 1.73 (s, 6H) ppm; $^{19}\text{F NMR}$ (376.5 MHz, $\text{DMSO-}d_6$): δ = -112.4 (d, $J_{\text{H-F}}$ = 9.3 Hz, 1F), -130.2 (s, 1F) ppm; $^{13}\text{C NMR}$ (100.0 MHz, $\text{DMSO-}d_6$): δ = 179.5, 156.5 (dd, $J_{\text{C-F}}$ = 2.5 Hz, $^1J_{\text{C-F}}$ = 244.9 Hz), 155.9, 148.2 (dd, $J_{\text{C-F}}$ = 5.3 Hz, $^1J_{\text{C-F}}$ = 249.2 Hz), 145.0, 142.6, 142.1, 138.9, 137.0 (dd, $J_{\text{C-F}}$ = 2.0 Hz, $J_{\text{C-F}}$ = 10.8 Hz), 133.0, 131.9, 129.4, 128.9, 128.8, 128.3, 127.1, 123.4 (dd, $J_{\text{C-F}}$ = 2.2 Hz, $J_{\text{C-F}}$ = 11.0 Hz), 122.8, 115.2, 114.2, 111.8 (dd, $J_{\text{C-F}}$ = 16.9 Hz, $J_{\text{C-F}}$ = 22.9 Hz), 108.8, 108.6 (dd, $J_{\text{C-F}}$ = 2.7 Hz, $J_{\text{C-F}}$ = 24.7 Hz), 51.1, 33.5, 28.8, 26.6, 23.4, 19.6 ppm; HRMS (ESI⁺): m/z calcd for $\text{C}_{32}\text{H}_{26}\text{Cl}_2\text{F}_2\text{NOS}^+$ $[\text{M}]^+$ 580.1075, found 580.1072.



2u: 95% yield; Dark green solid; ^1H NMR (400.0 MHz, $\text{DMSO-}d_6$): δ = 8.52 (d, J = 15.5 Hz, 1H), 7.81 (dd, J = 6.1, 6.8 Hz, 2H), 7.58 (dd, J = 7.3, 7.8 Hz, 1H), 7.53 (dd, J = 7.2, 7.4 Hz, 1H), 7.40 (m, 3H), 7.30 (m, 3H), 7.25 (s, 1H), 6.83 (d, J = 15.6 Hz, 1H), 4.00 (s, 3H), 2.70 (m, 4H), 1.82 (brs, 2H), 1.72 (s, 6H) ppm; ^{19}F NMR (376.5 MHz, $\text{DMSO-}d_6$): δ = -105.1 (d, $J_{\text{H-F}}$ = 7.8 Hz, 1F), -122.6 (s, 1F) ppm; ^{13}C NMR (100.0 MHz, $\text{DMSO-}d_6$): δ = 179.5, 157.4 (dd, $J_{\text{C-F}}$ = 4.3 Hz, $^1J_{\text{C-F}}$ = 241.5 Hz), 155.9, 149.2 (dd, $J_{\text{C-F}}$ = 6.6 Hz, $^1J_{\text{C-F}}$ = 245.5 Hz), 144.9, 142.6, 142.0, 136.8 (dd, $J_{\text{C-F}}$ = 2.9 Hz, $J_{\text{C-F}}$ = 13.1 Hz), 133.1, 130.7, 129.7, 129.6, 128.9, 128.3, 127.5, 127.3, 124.8 (dd, $J_{\text{C-F}}$ = 2.2 Hz, $J_{\text{C-F}}$ = 10.9 Hz), 122.8, 115.1, 114.3, 108.8, 108.4 (dd, $J_{\text{C-F}}$ = 2.9 Hz, $J_{\text{C-F}}$ = 27.3 Hz), 106.8 (dd, $J_{\text{C-F}}$ = 23.01 Hz, $J_{\text{C-F}}$ = 29.5 Hz), 51.0, 33.5, 28.8, 26.7, 23.3, 19.6 ppm; HRMS (ESI+): m/z calcd for $\text{C}_{32}\text{H}_{28}\text{F}_2\text{NOSe}^+ [\text{M}]^+$ 560.1301, found 560.1290; HPLC (system A): t_{R} = 5.3 min (purity 97% at 600 nm); LRMS (ESI+, recorded during RP-HPLC analysis): m/z 558.1 (60) and 560.1 (100) $[\text{M}]^+$ (two major Se isotopes), calcd for $\text{C}_{32}\text{H}_{28}\text{F}_2\text{NOSe}^+$ 560.1; UV-vis (recorded during the HPLC analysis): λ_{max} = 553 nm (broad peak).

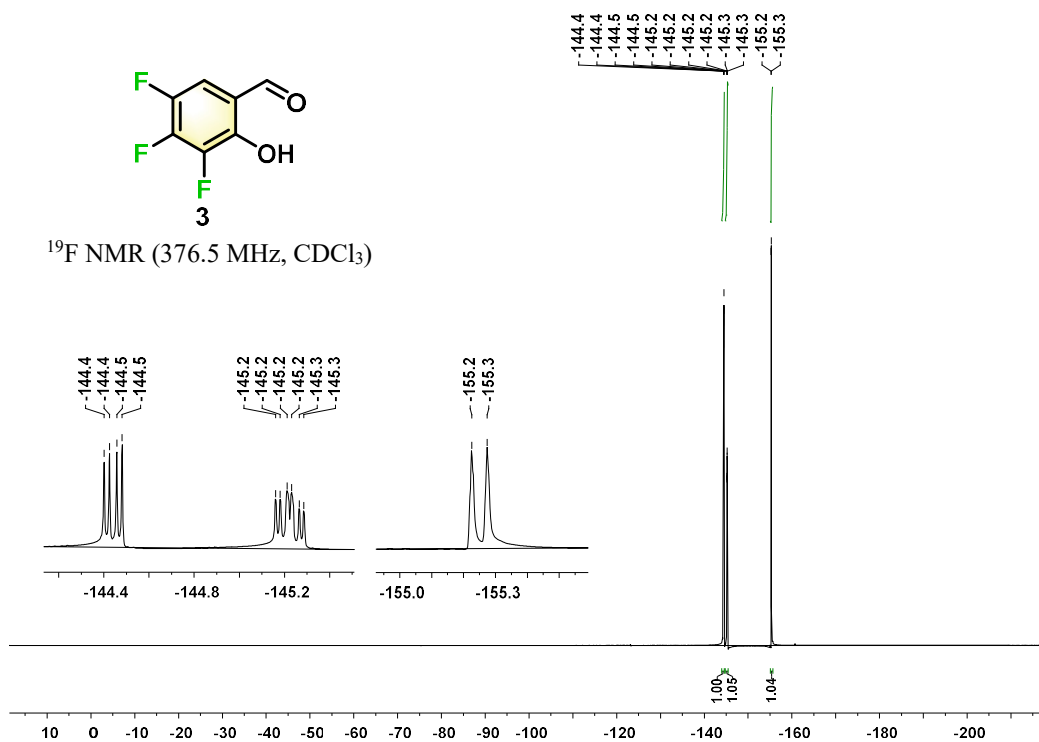
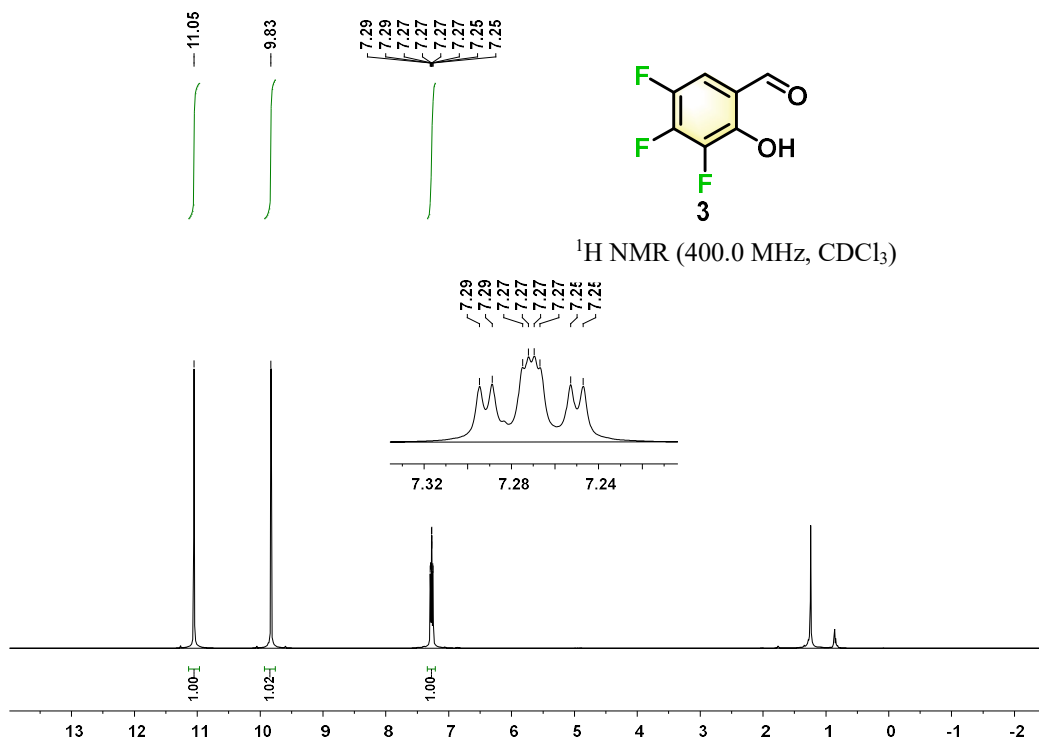


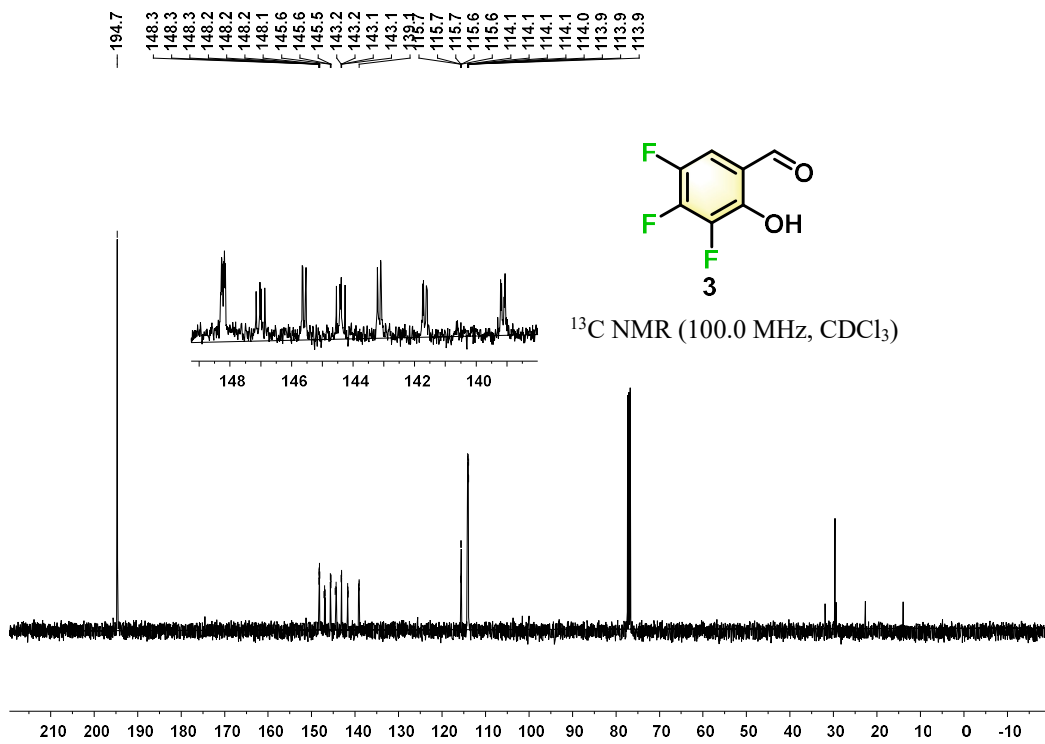
2v: 66% yield; Dark green solid; ^1H NMR (400.0 MHz, CDCl_3): δ = 8.35 (d, J = 15.5 Hz, 1H), 7.76 (d, J = 7.5 Hz, 1H), 7.73 (s, 1H), 7.70 (d, J = 8.0 Hz, 1H), 7.58 (d, J = 7.9 Hz, 1H), 7.52 (m, 2H), 7.46 (m, 2H), 7.39 (m, 2H), 7.32 (dt, J = 1.0, 7.5 Hz, 1H), 7.04 (d, J = 15.4 Hz, 1H), 6.87 (m, 2H), 4.25 (s, 3H), 3.88 (s, 2H), 2.95 (t, J = 6.0 Hz, 2H), 2.72 (t, J = 5.7 Hz, 2H), 1.94 (m, 2H), 1.76 (s, 6H) ppm; ^{19}F NMR (376.5 MHz, $\text{DMSO-}d_6$): δ = -105.1 (s, 1F), -122.7 (s, 1F) ppm; ^{13}C NMR (100.0 MHz, $\text{DMSO-}d_6$): δ = 179.3, 157.3 (dd, $J_{\text{C-F}}$ = 3.8 Hz, $^1J_{\text{C-F}}$ = 241.8 Hz), 155.8, 149.0 (dd, $J_{\text{C-F}}$ = 6.3 Hz, $^1J_{\text{C-F}}$ = 245.7 Hz), 144.8, 144.4, 142.8, 142.5, 142.0, 140.8, 140.0, 136.7 (dd, $J_{\text{C-F}}$ = 2.5 Hz, $J_{\text{C-F}}$ = 12.9 Hz), 132.8, 130.0, 128.9, 128.2, 128.1, 127.3, 127.2, 126.8, 125.0, 124.4 (d, $J_{\text{C-F}}$ = 10.8 Hz), 122.7, 120.9, 120.1, 115.0, 114.2, 108.7, 108.3 (d, $J_{\text{C-F}}$ = 27.5 Hz), 107.3 (dd, $J_{\text{C-F}}$ = 22.9 Hz, $J_{\text{C-F}}$ = 29.5 Hz), 50.9, 36.3, 33.6, 28.7, 26.7, 23.3, 19.5 ppm; HRMS (ESI+): m/z calcd for $\text{C}_{39}\text{H}_{32}\text{F}_2\text{NOSe}^+ [\text{M}]^+$ 648.1615, found 648.1643.

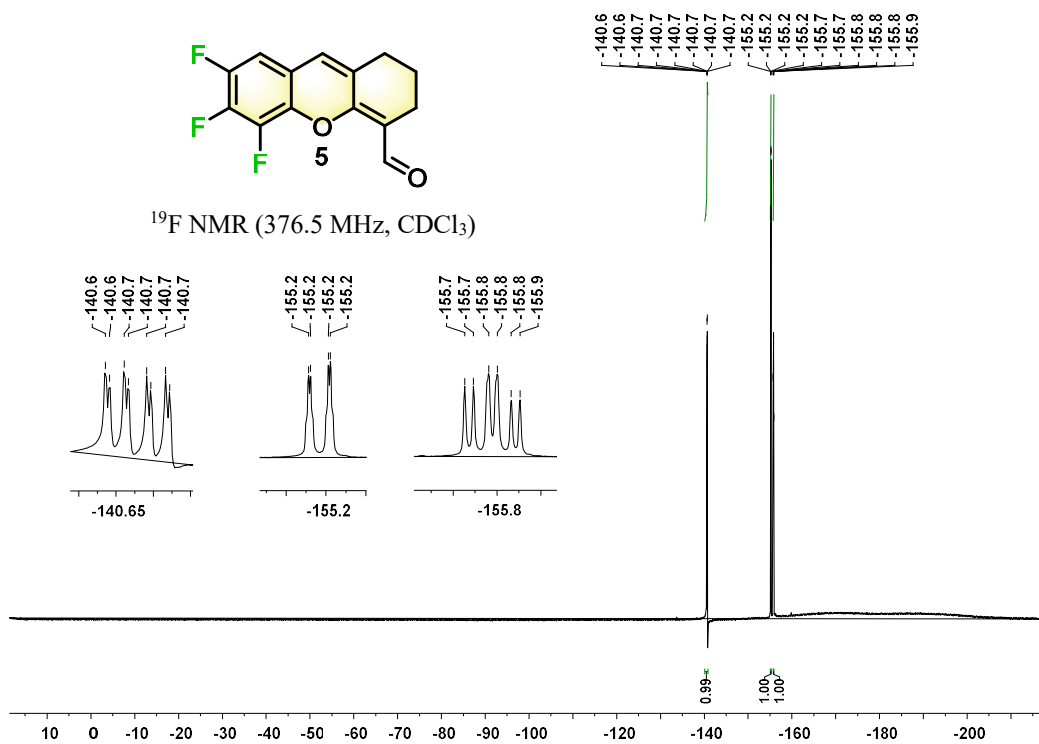
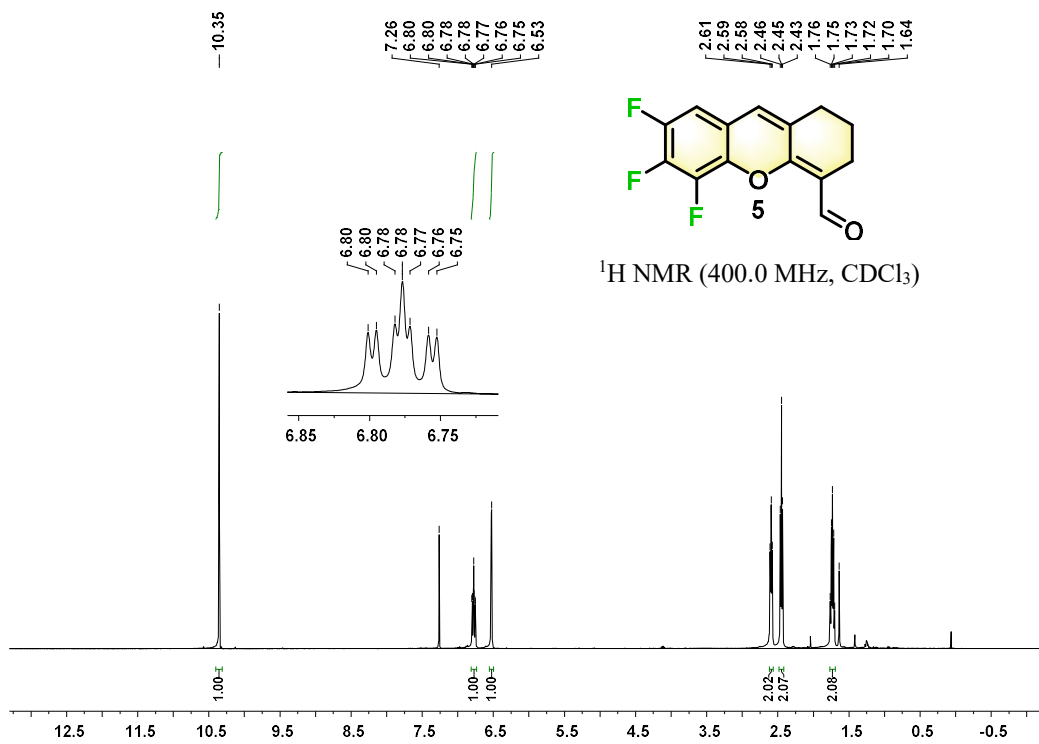
4. References

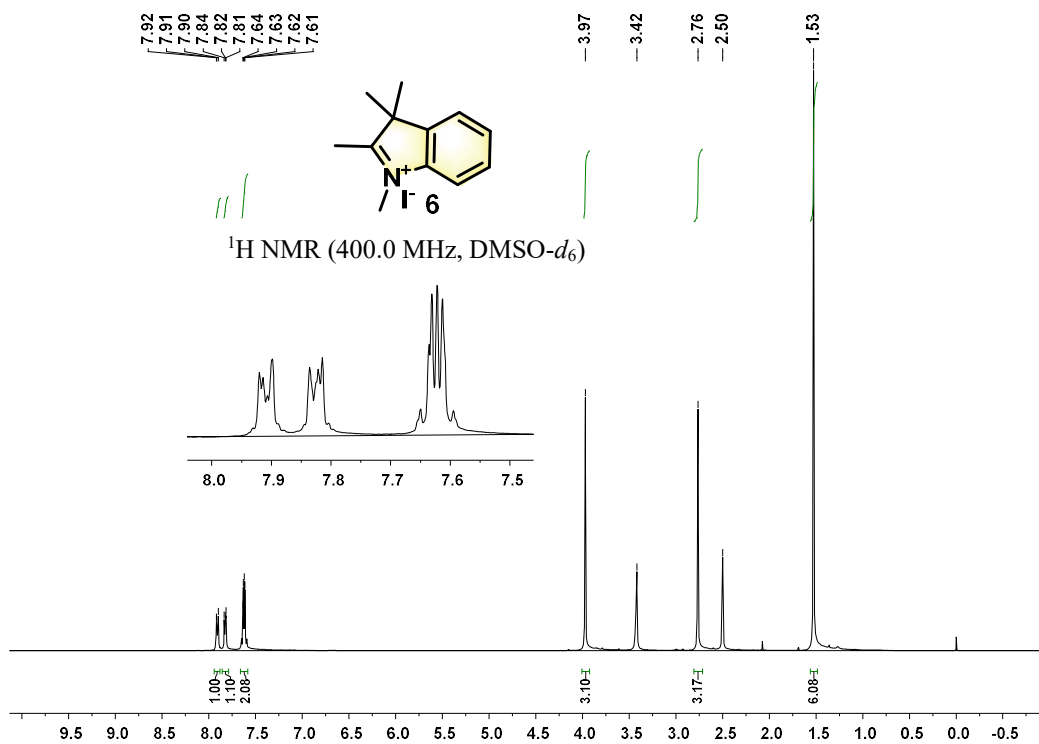
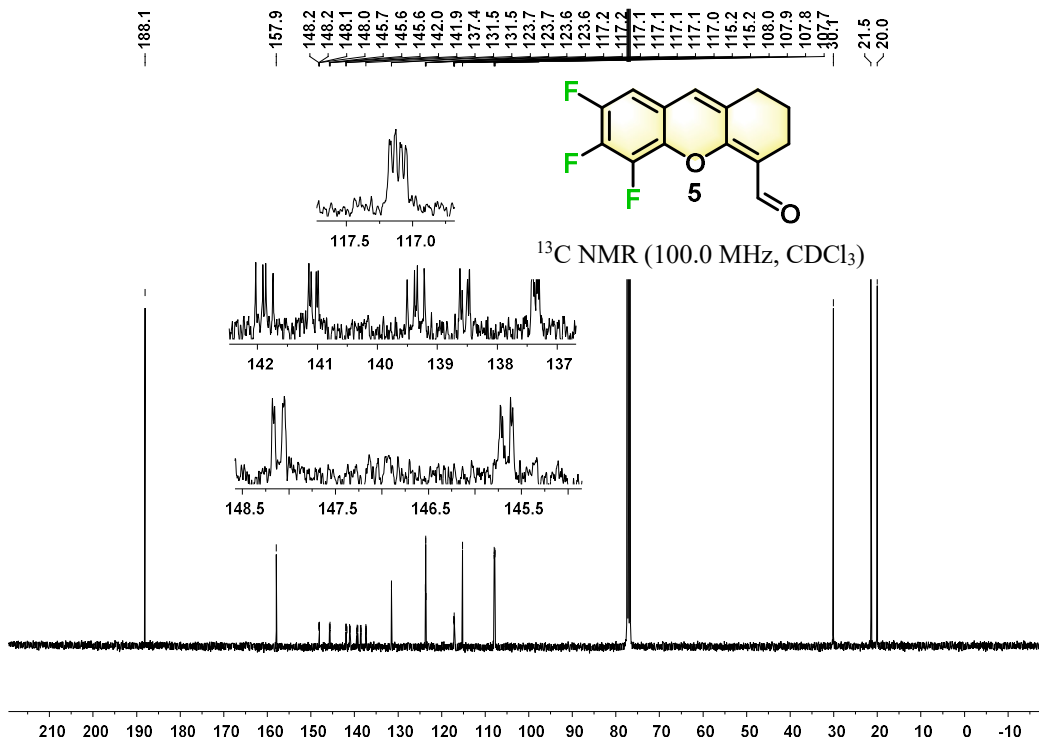
1. X. Zou, L. Yang, X. Liu, H. Sun, H. Lu, *Adv. Synth. Catal.* **2015**, 357, 3040 - 3046.
2. M. J. H. Ong, R. Srinivasan, A. Romieu, J. A. Richard, *Org. Lett.* **2016**, 18, 5122-5125.
3. N. B. Yapici, S. Mandalapu, L. Bi, *Bioorg. Med. Chem. Lett.* **2015**, 25, 3476-3480.

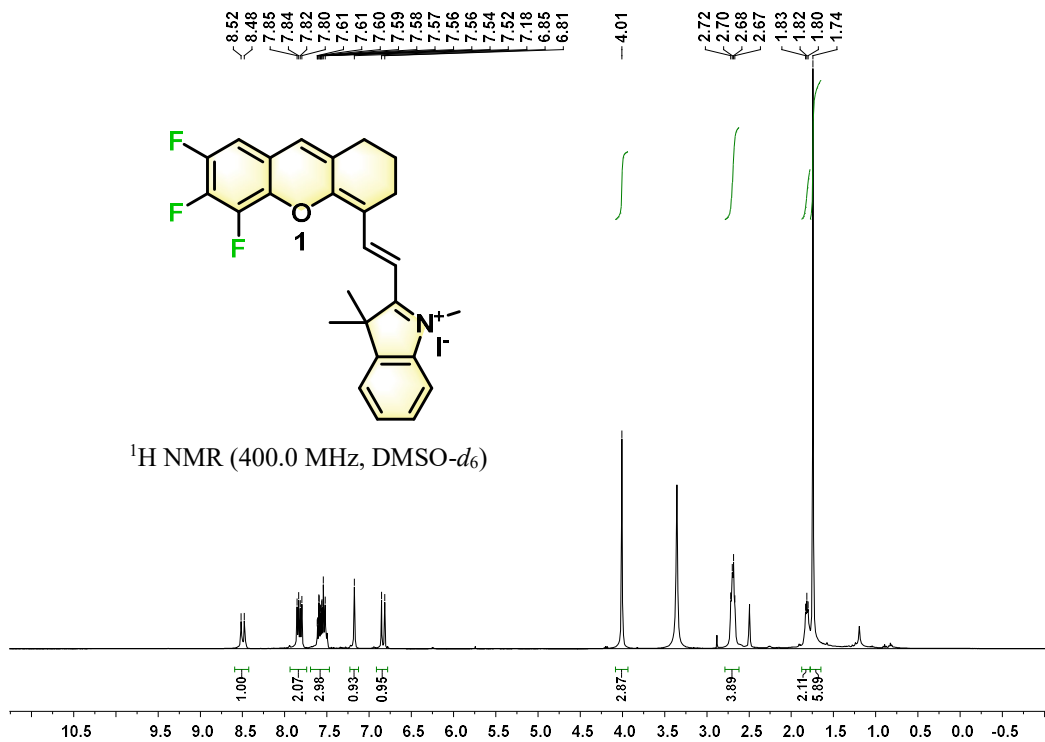
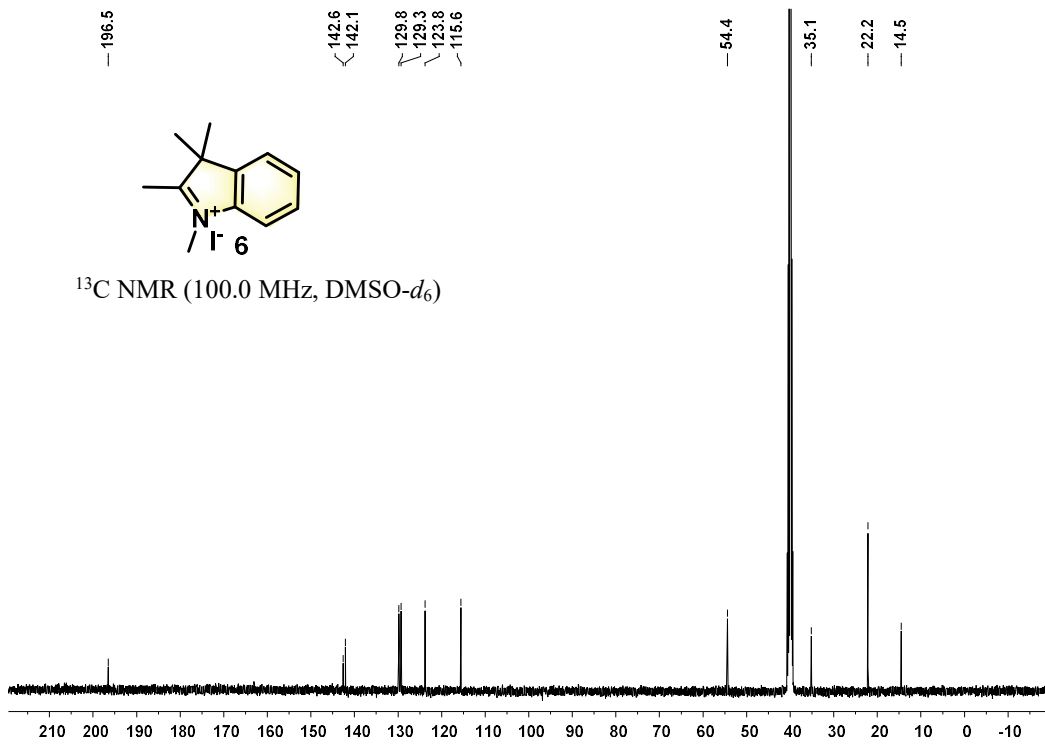
5. ^1H , ^{19}F and ^{13}C NMR spectra of synthesized compounds

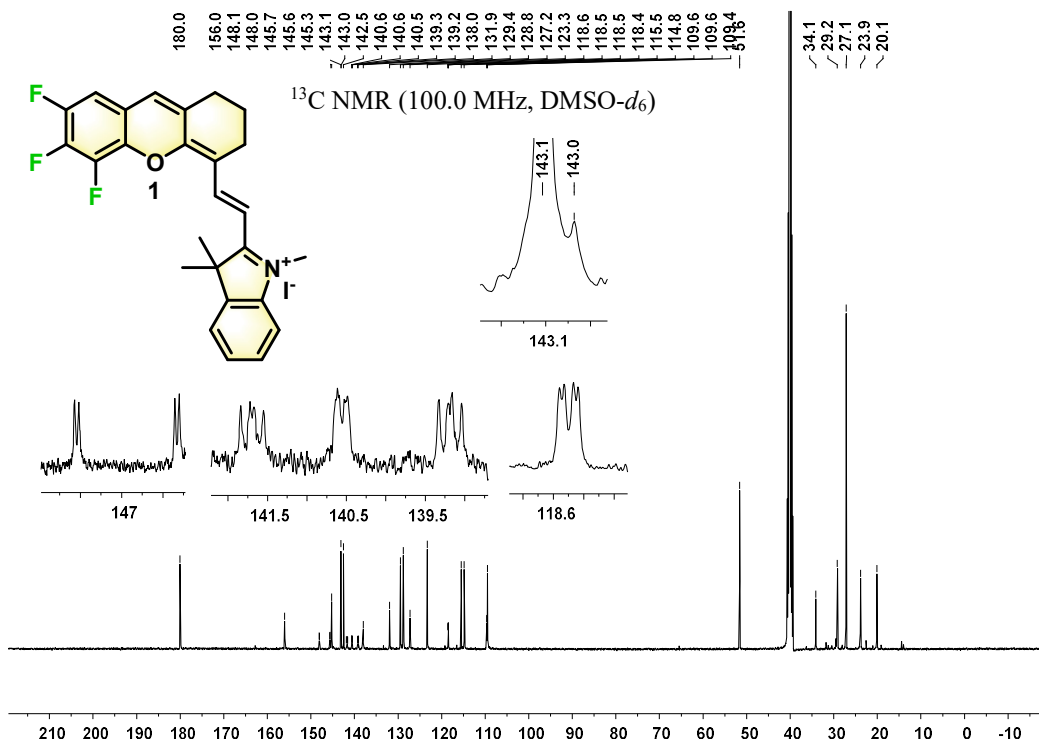
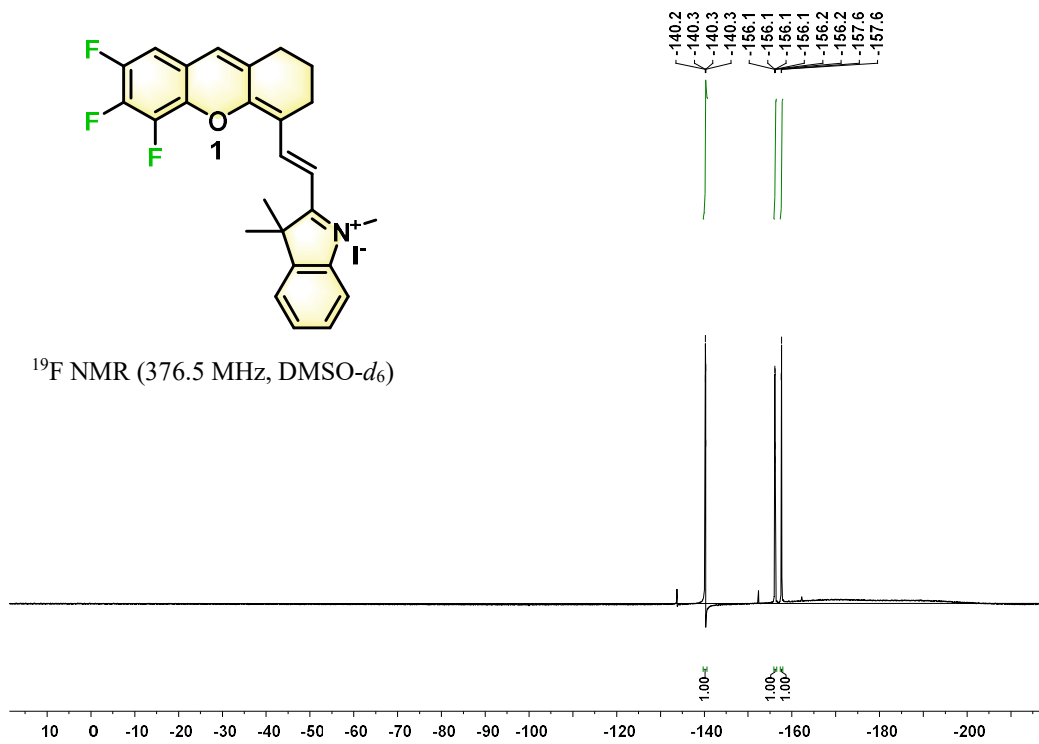


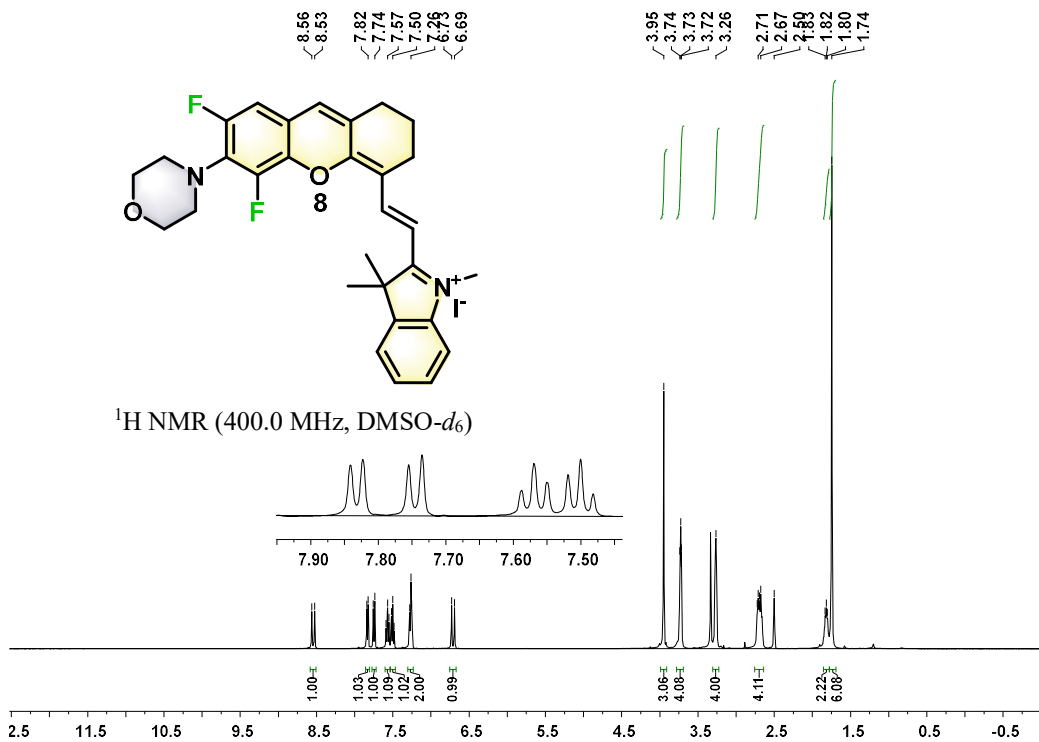
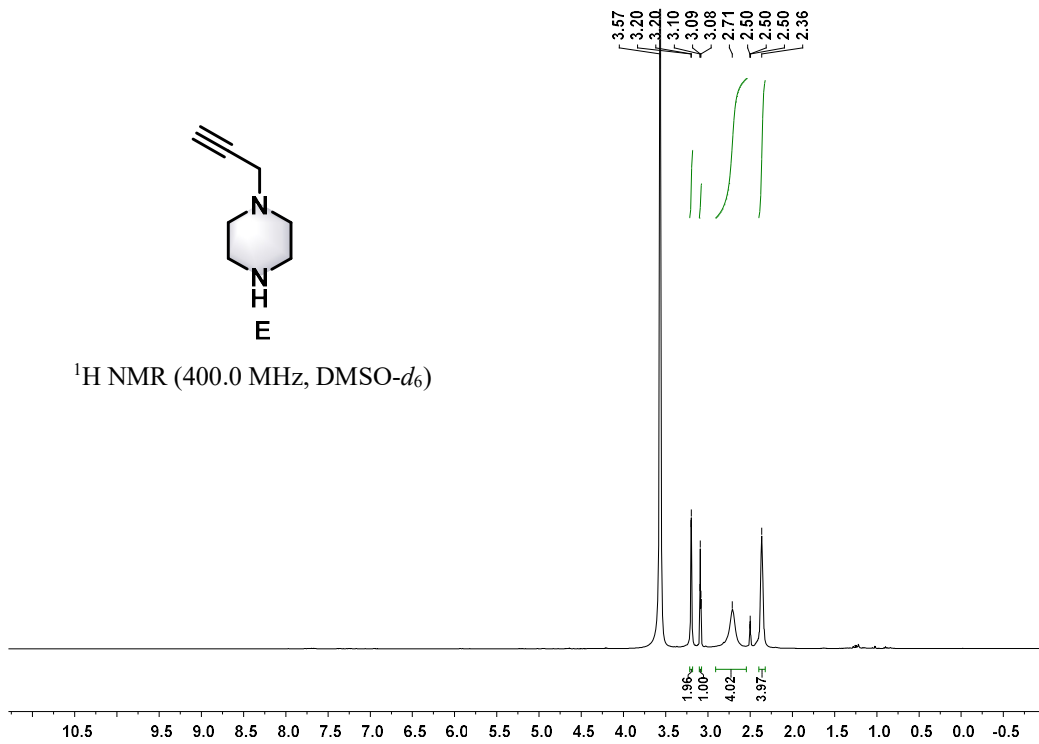


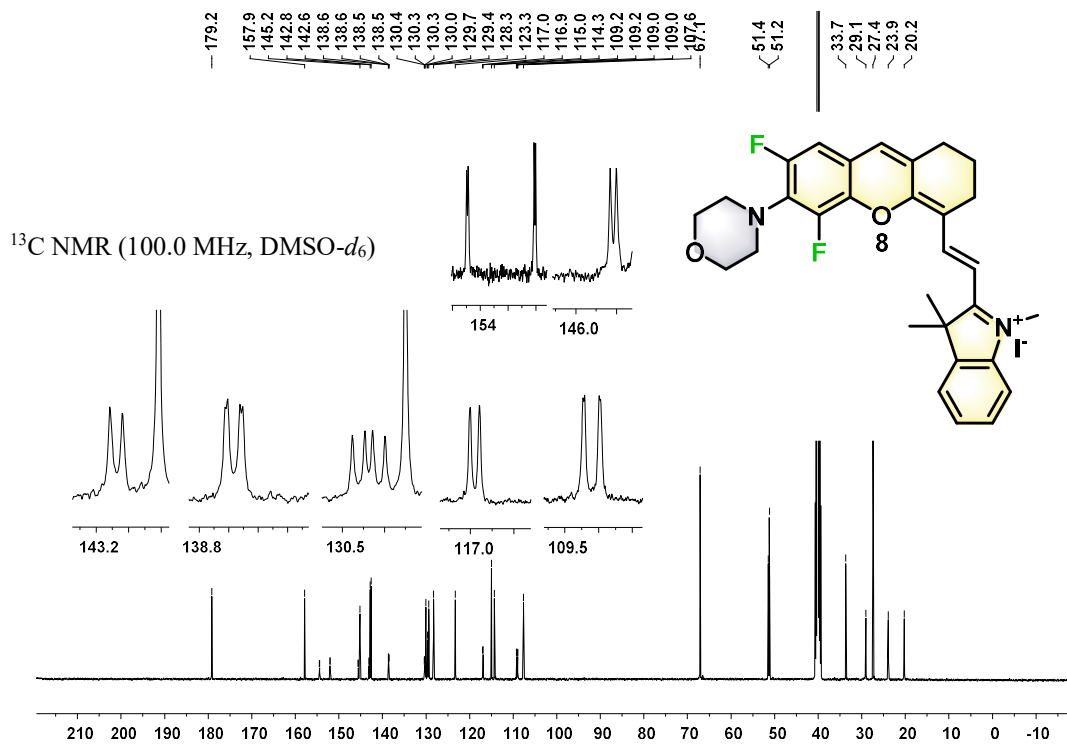
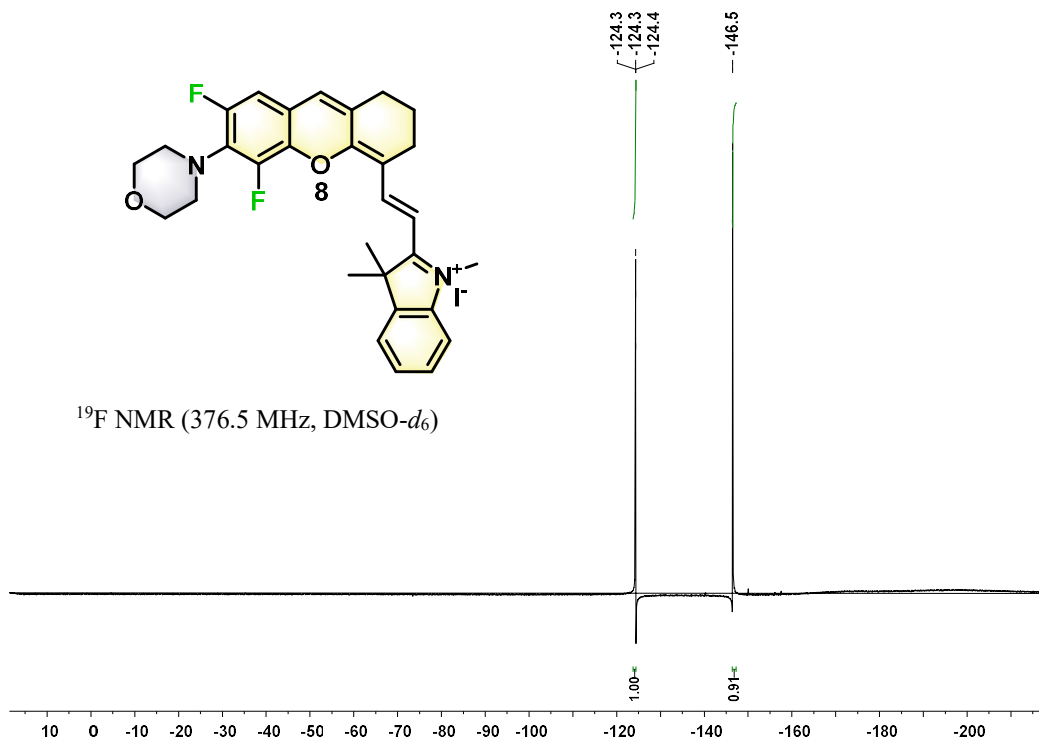


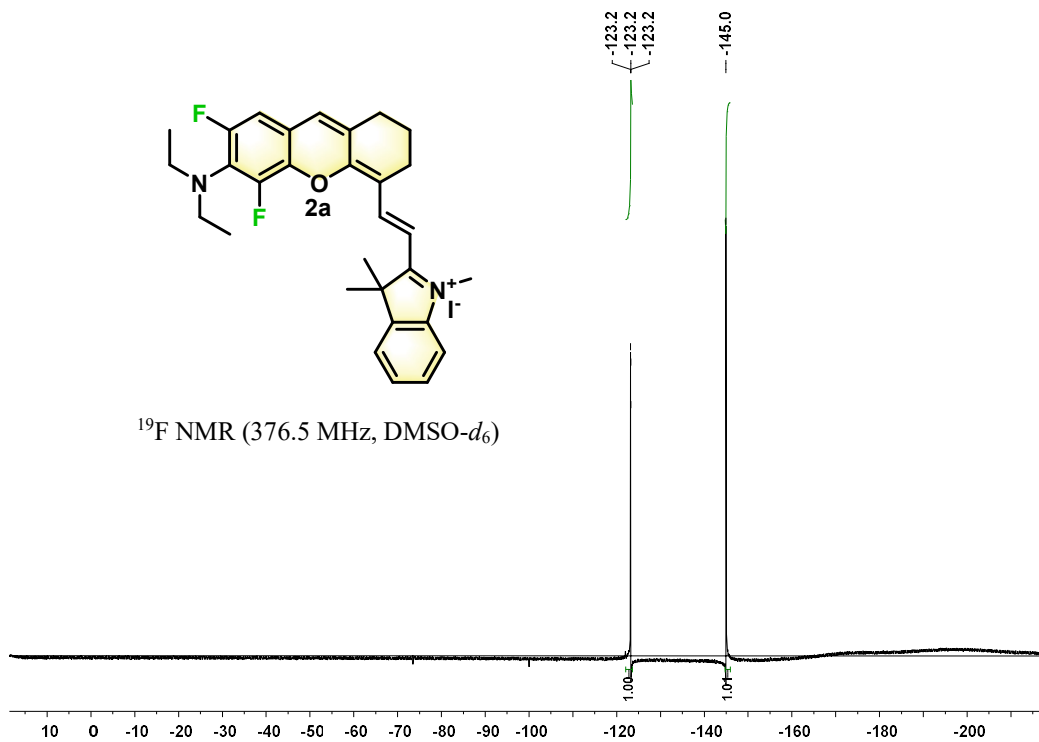
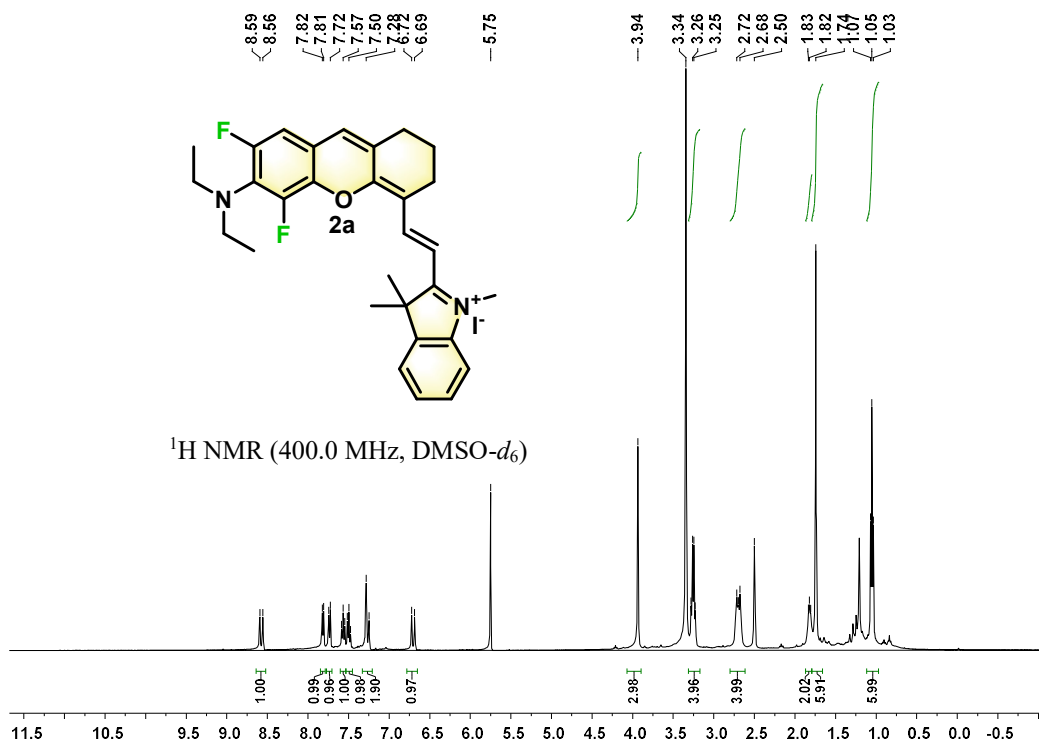


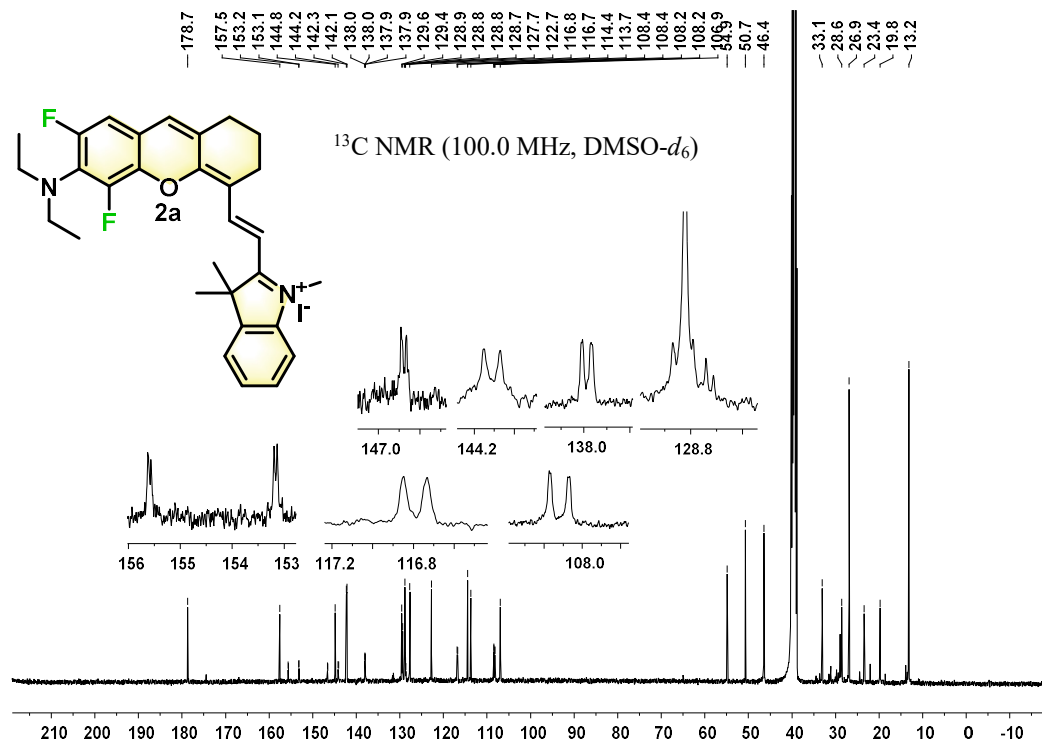


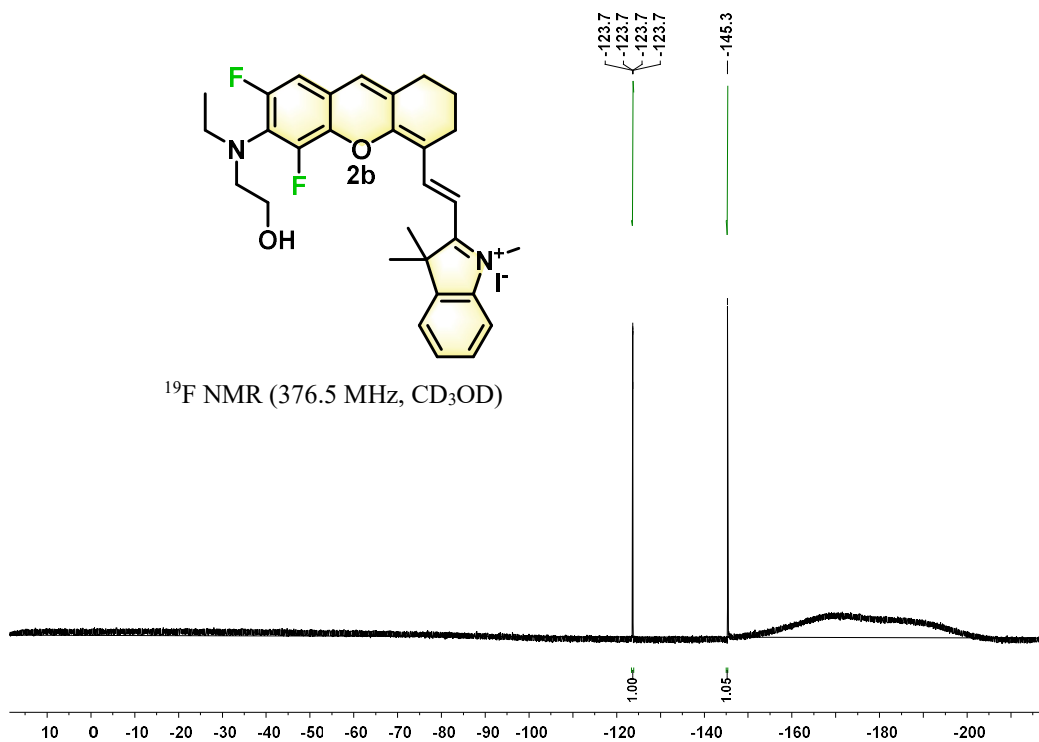
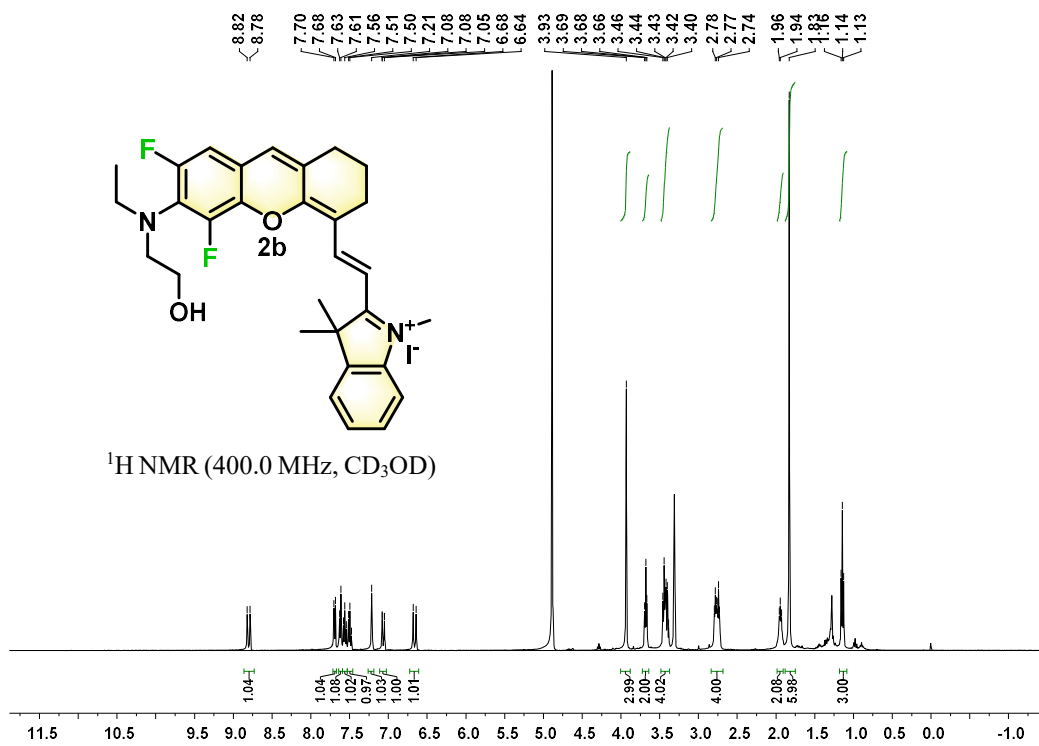


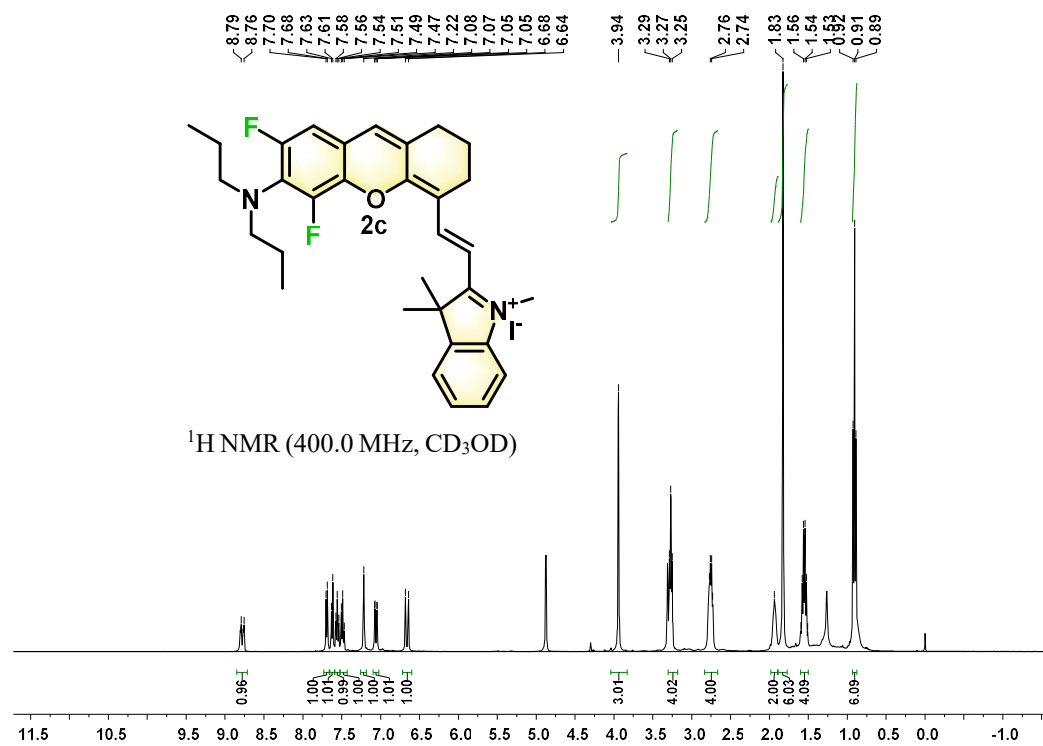
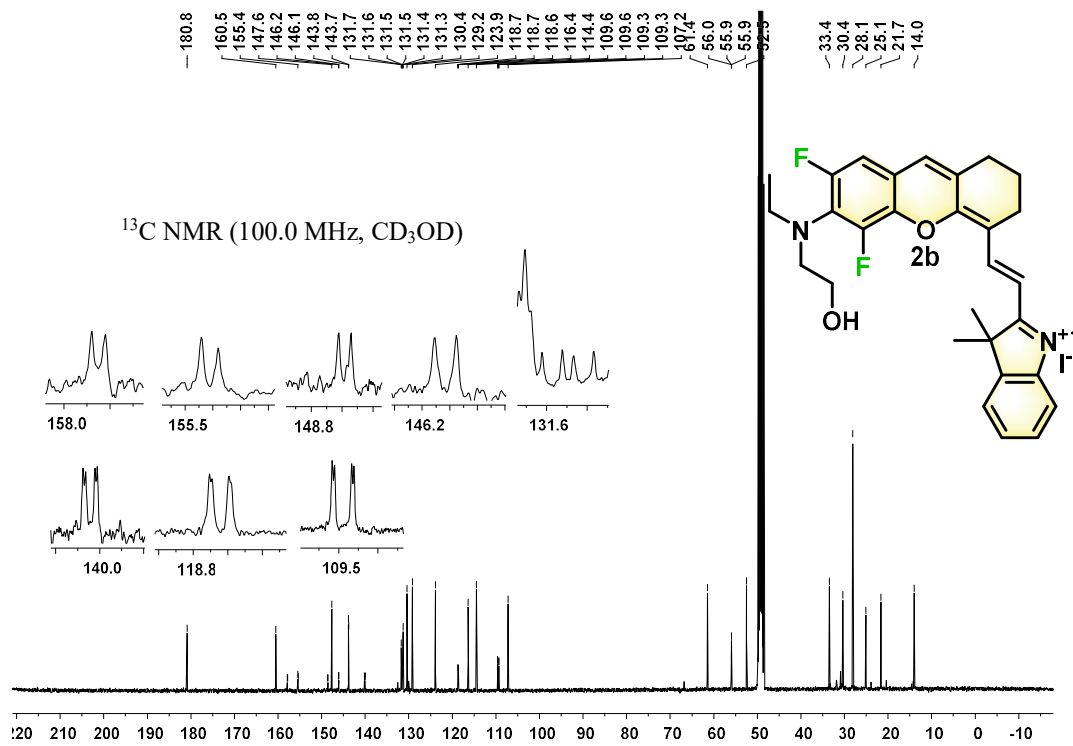


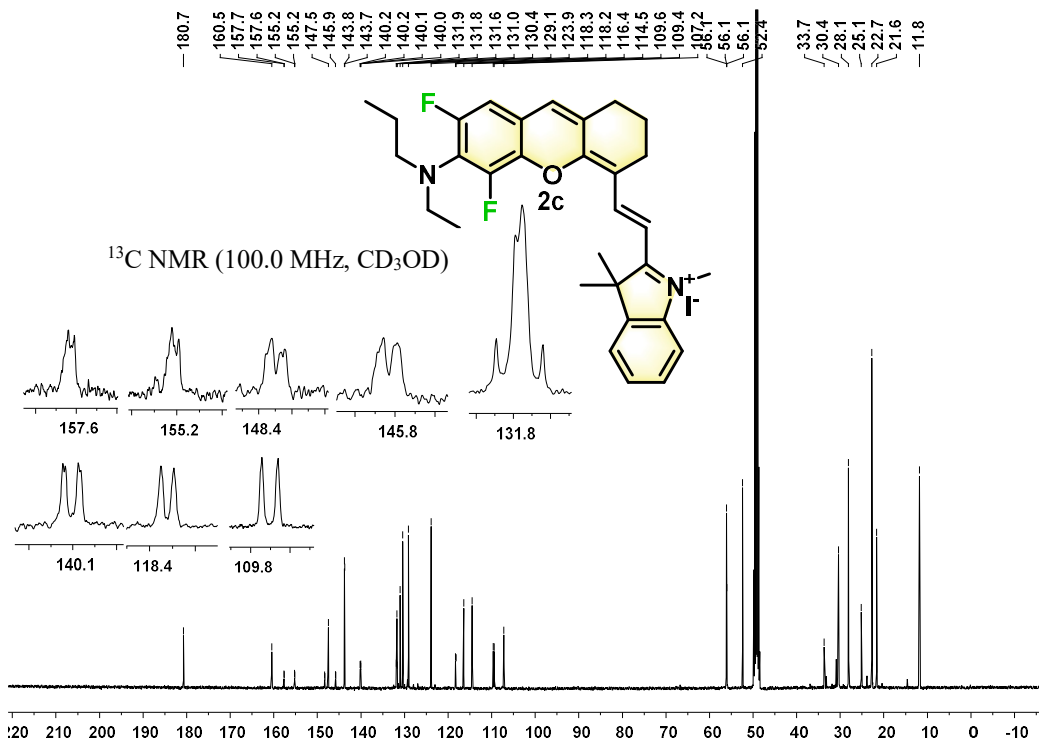
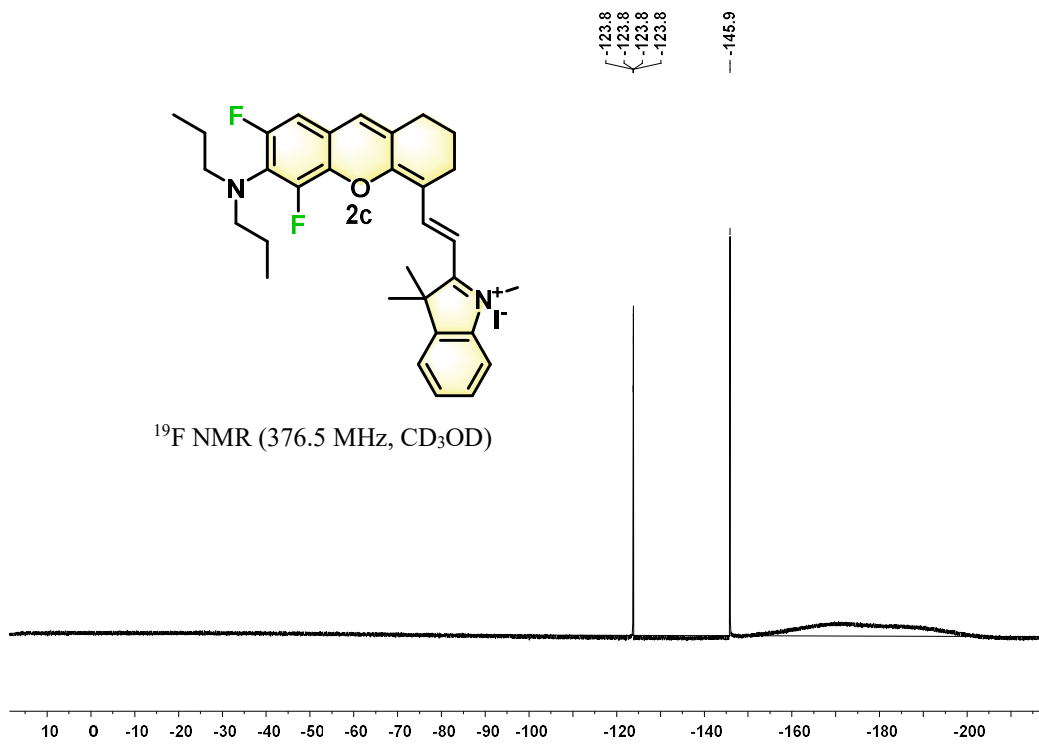


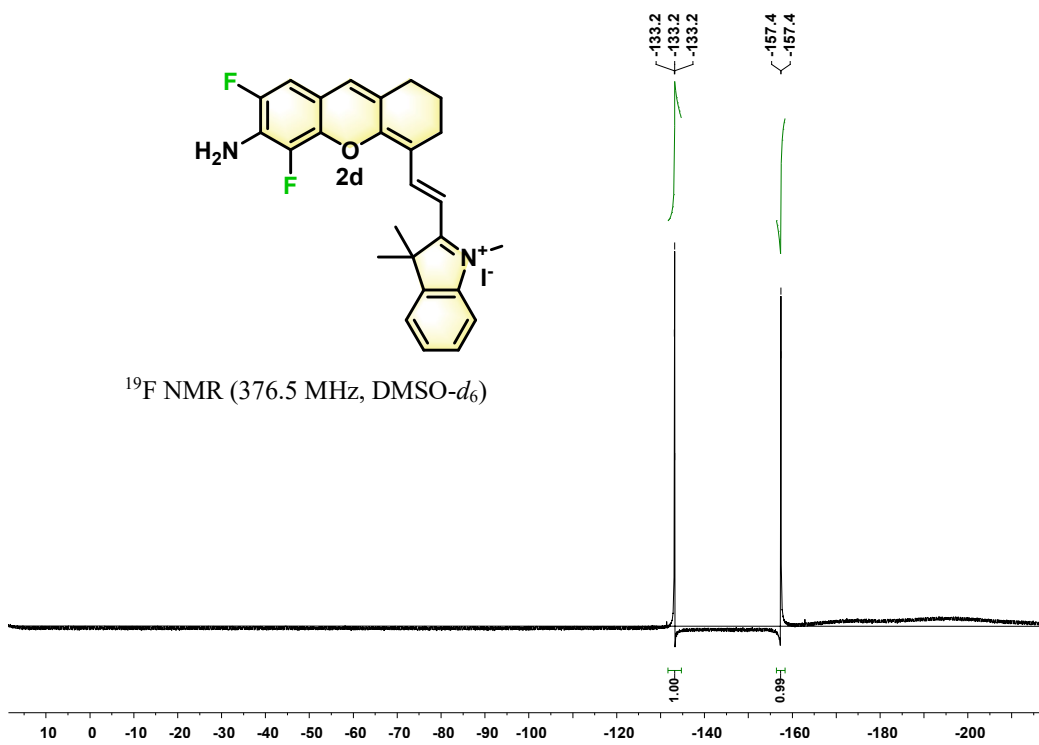
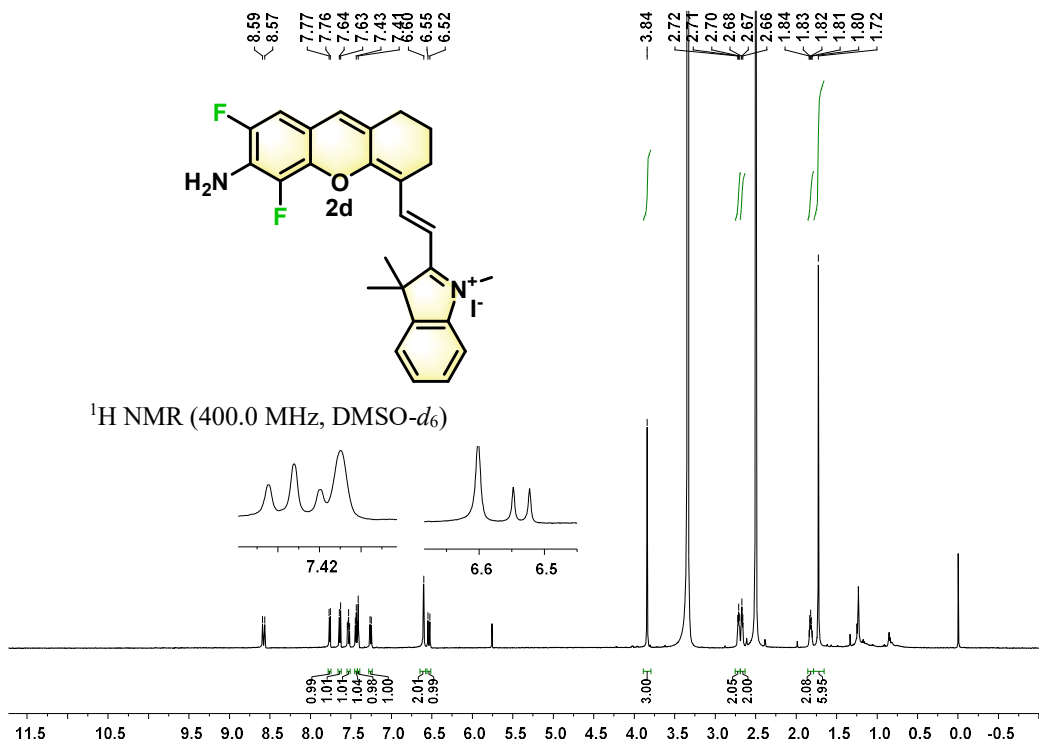


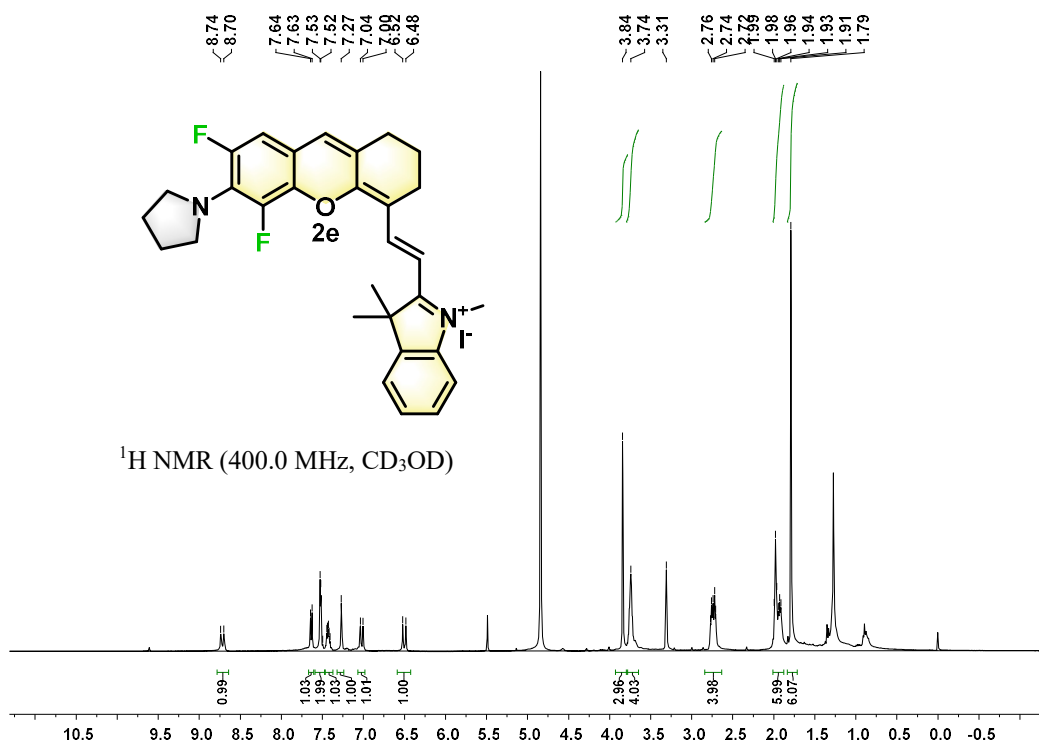
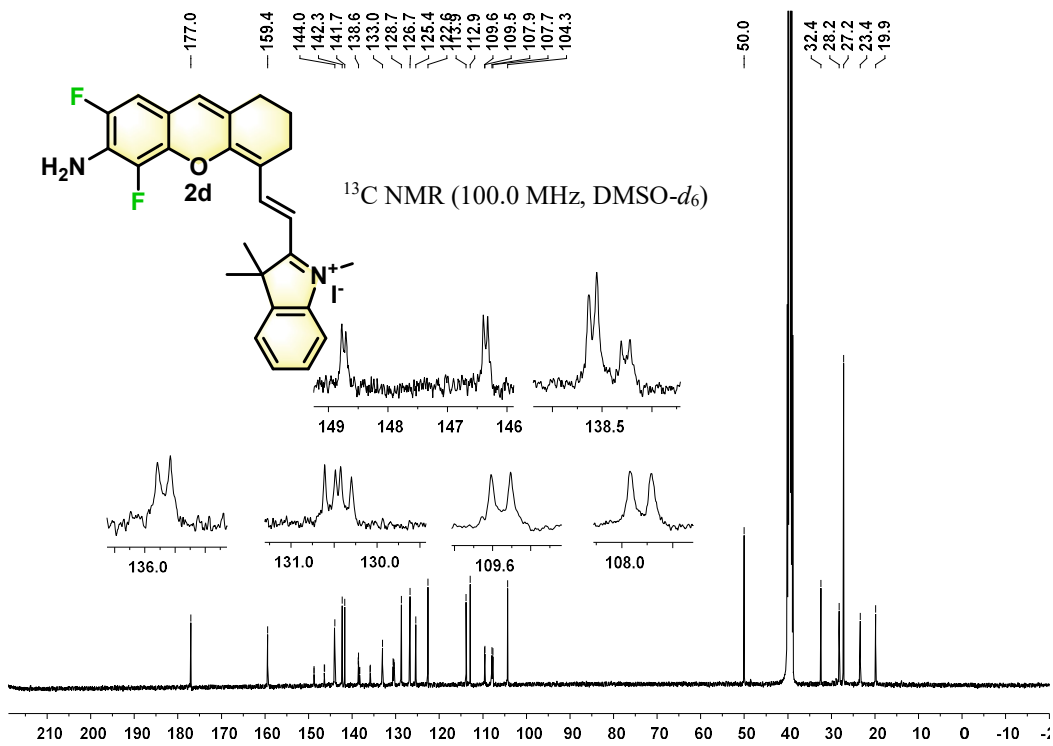


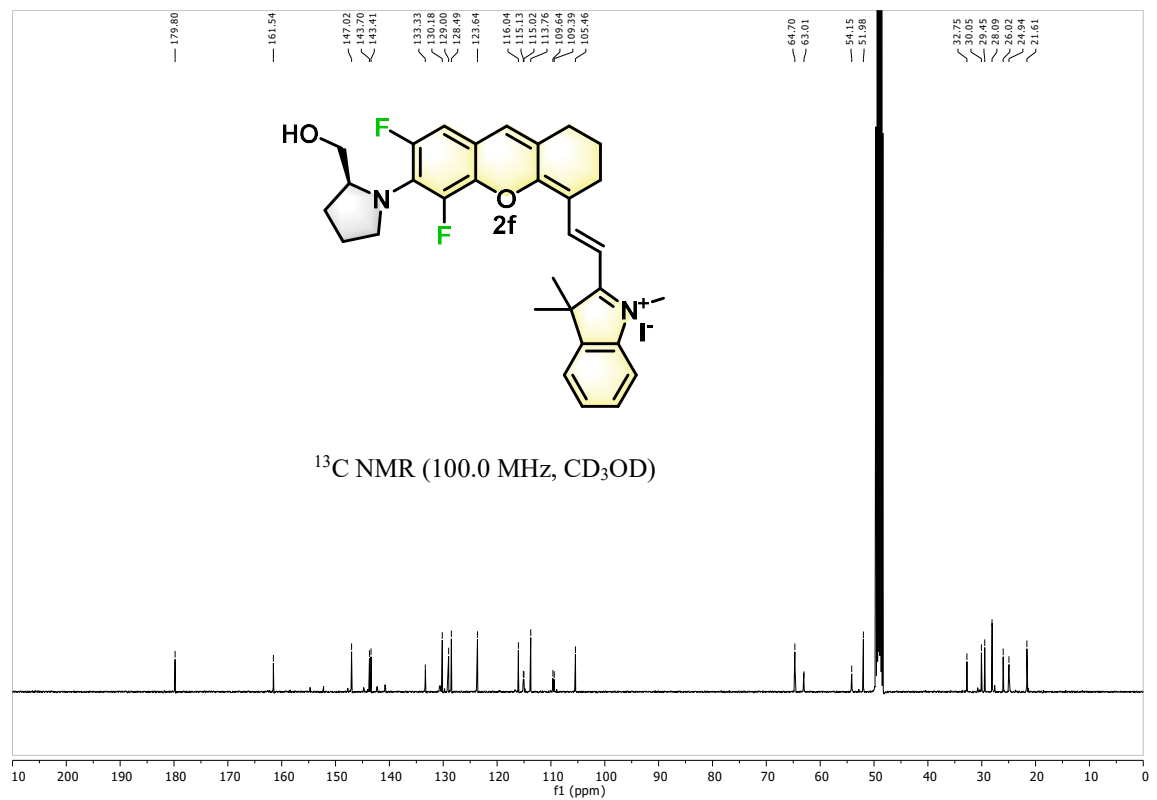
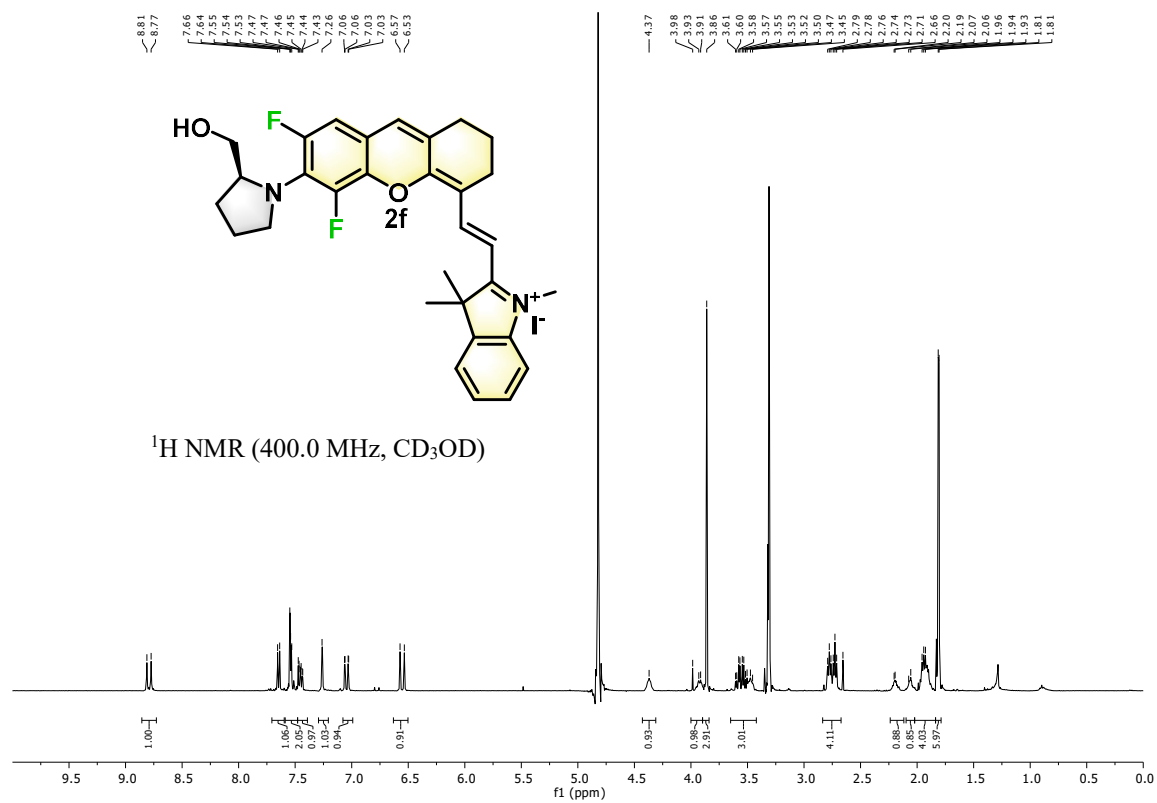


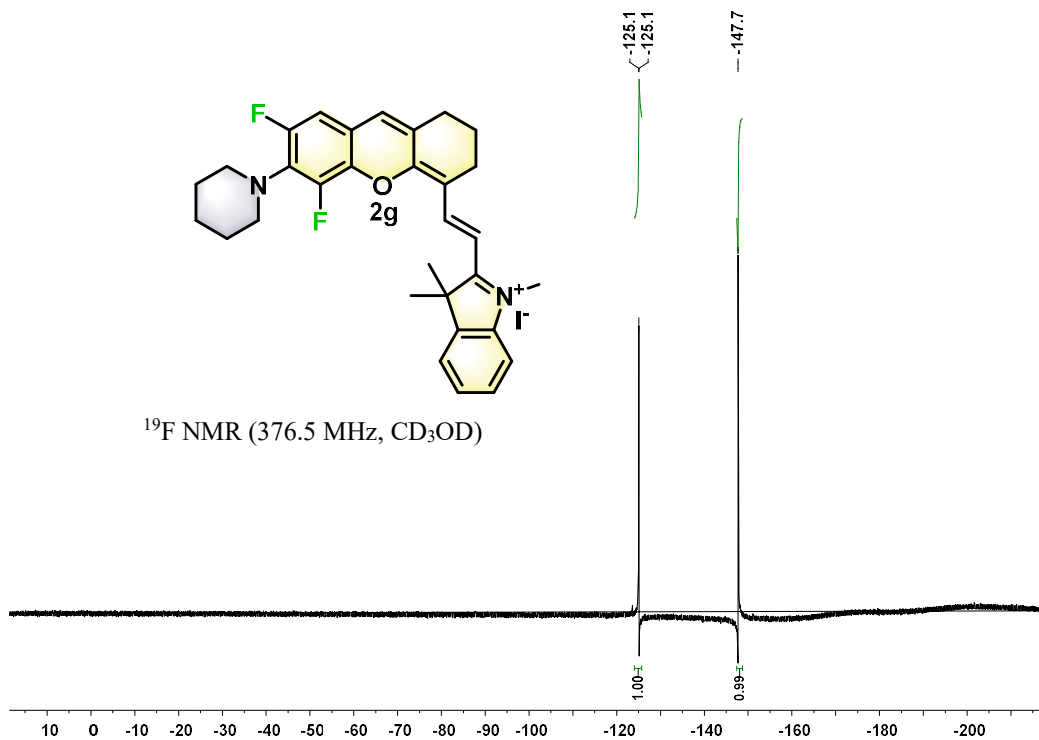
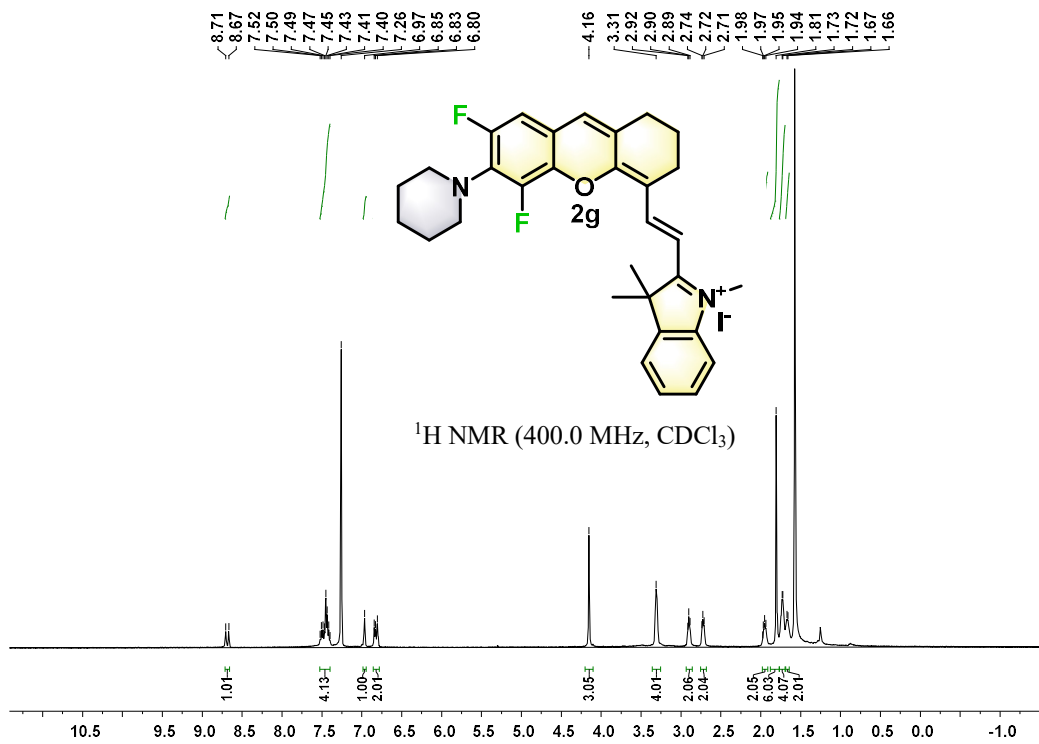


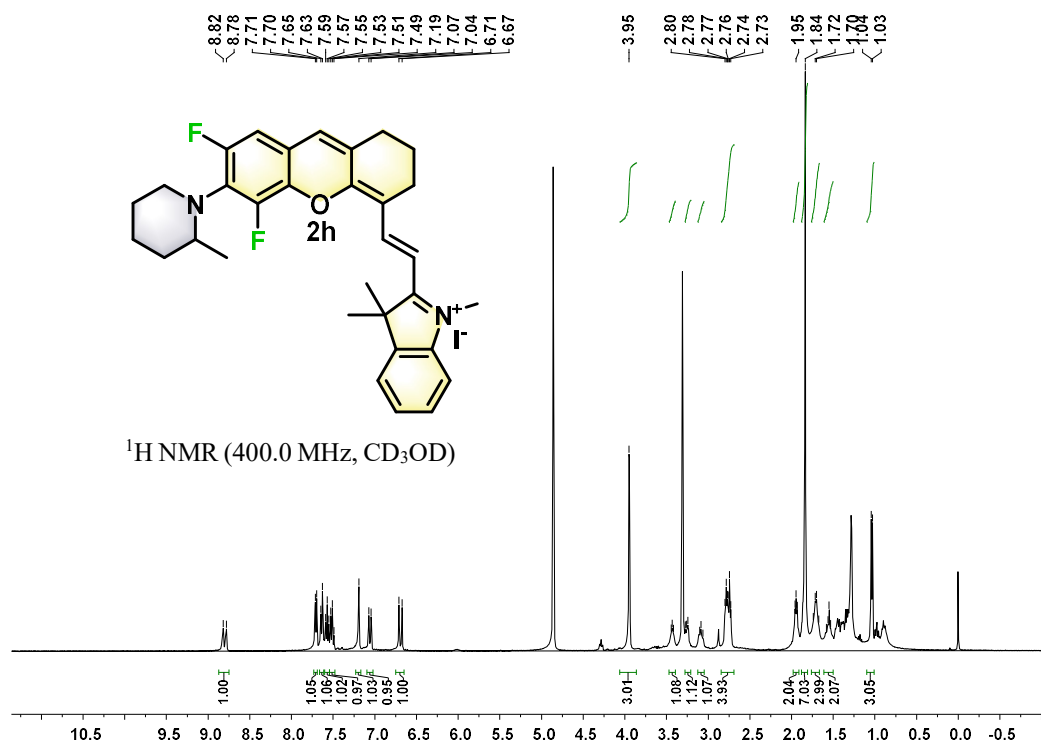
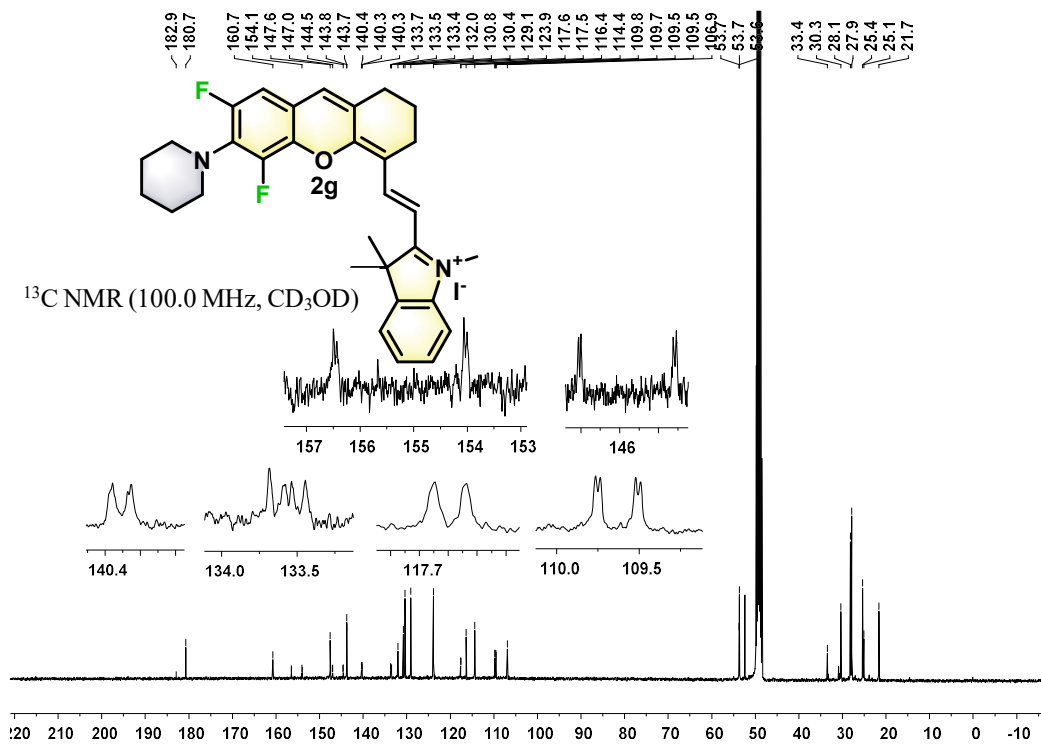


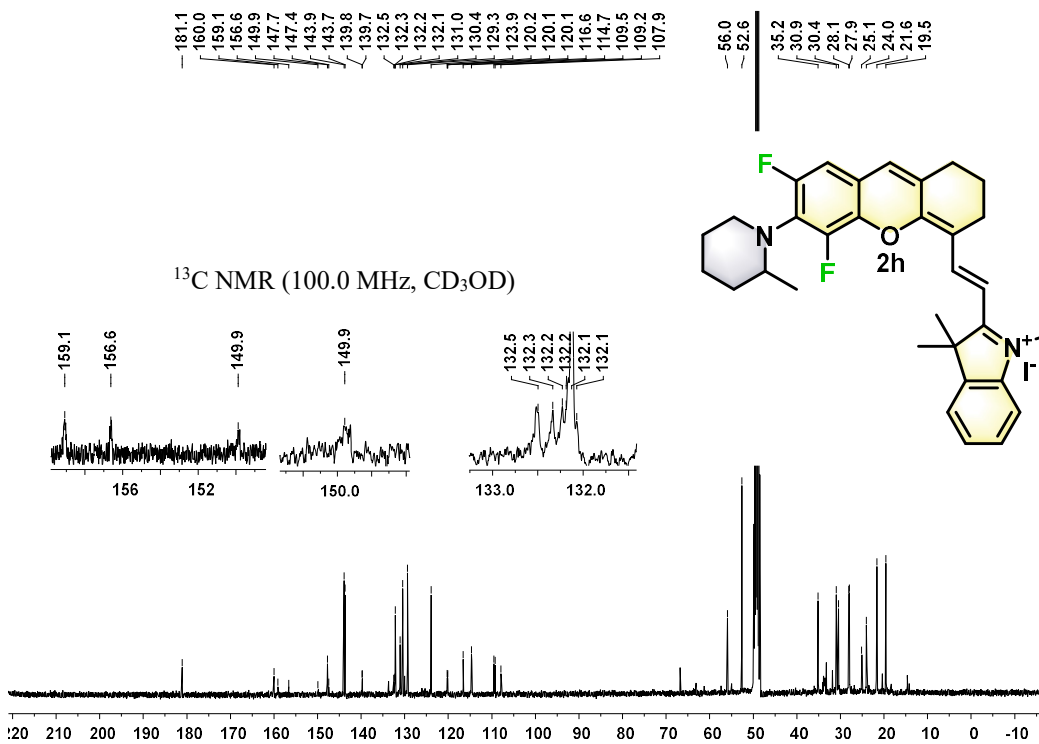
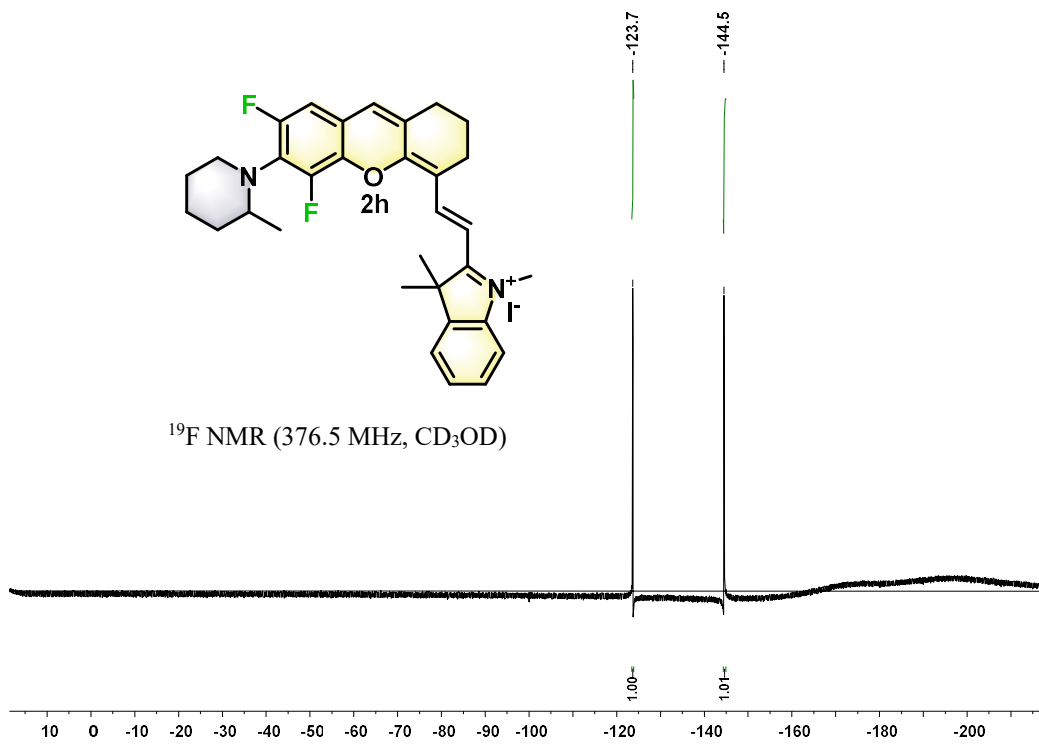


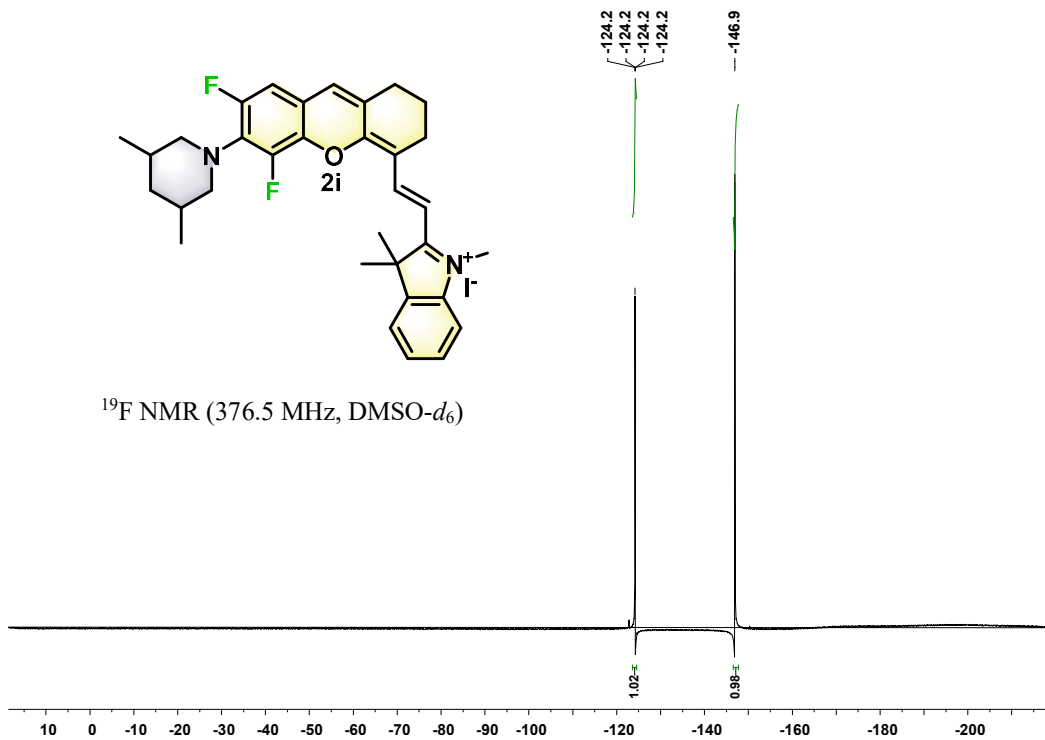
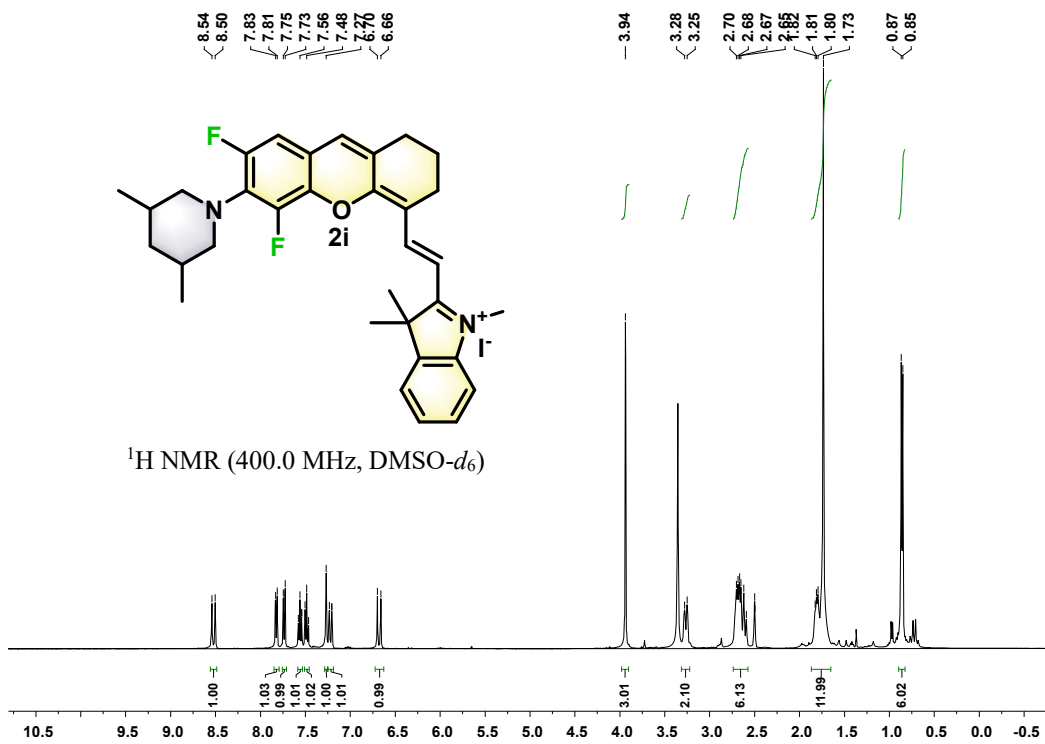


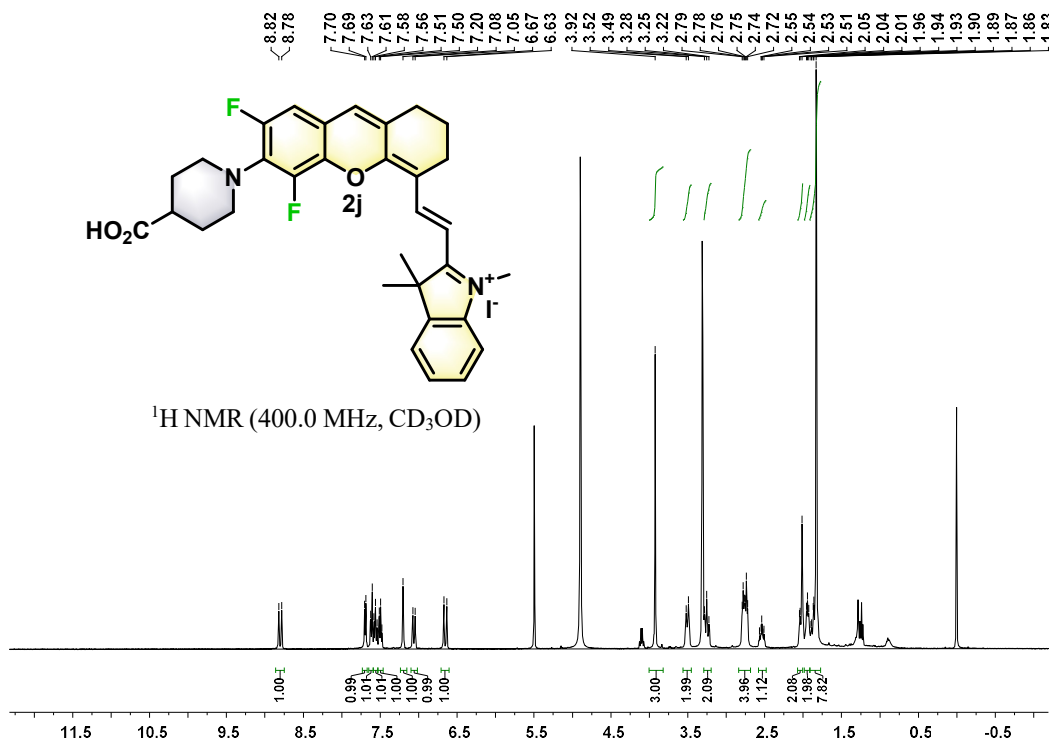
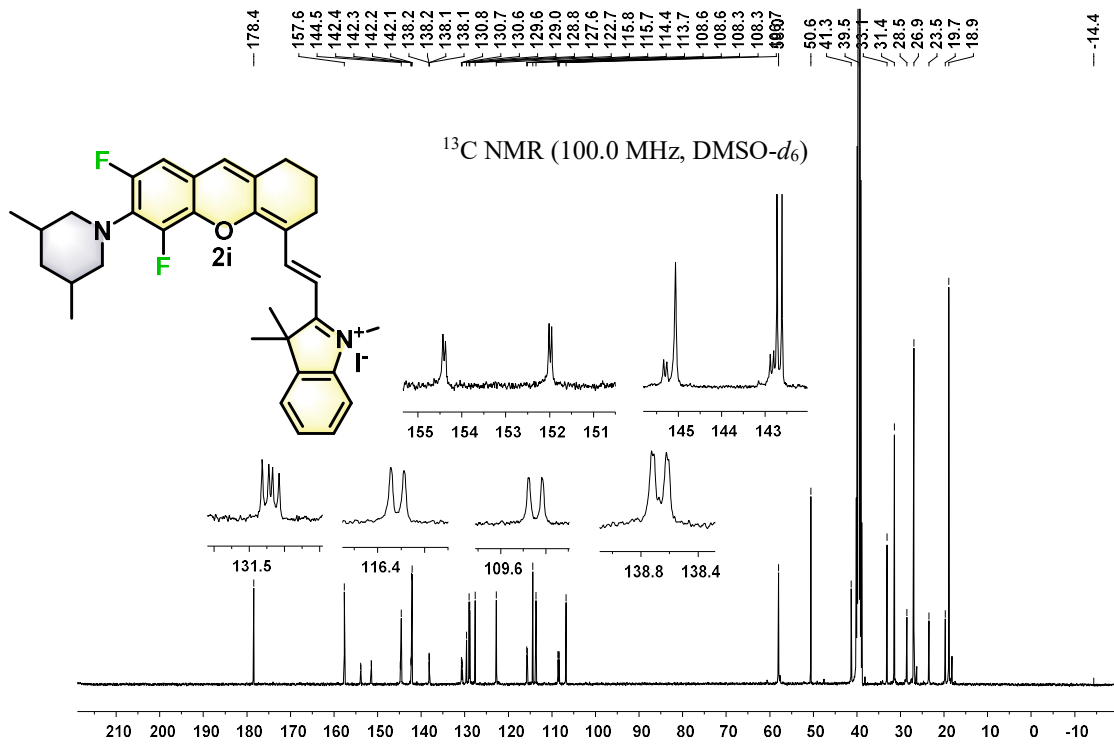


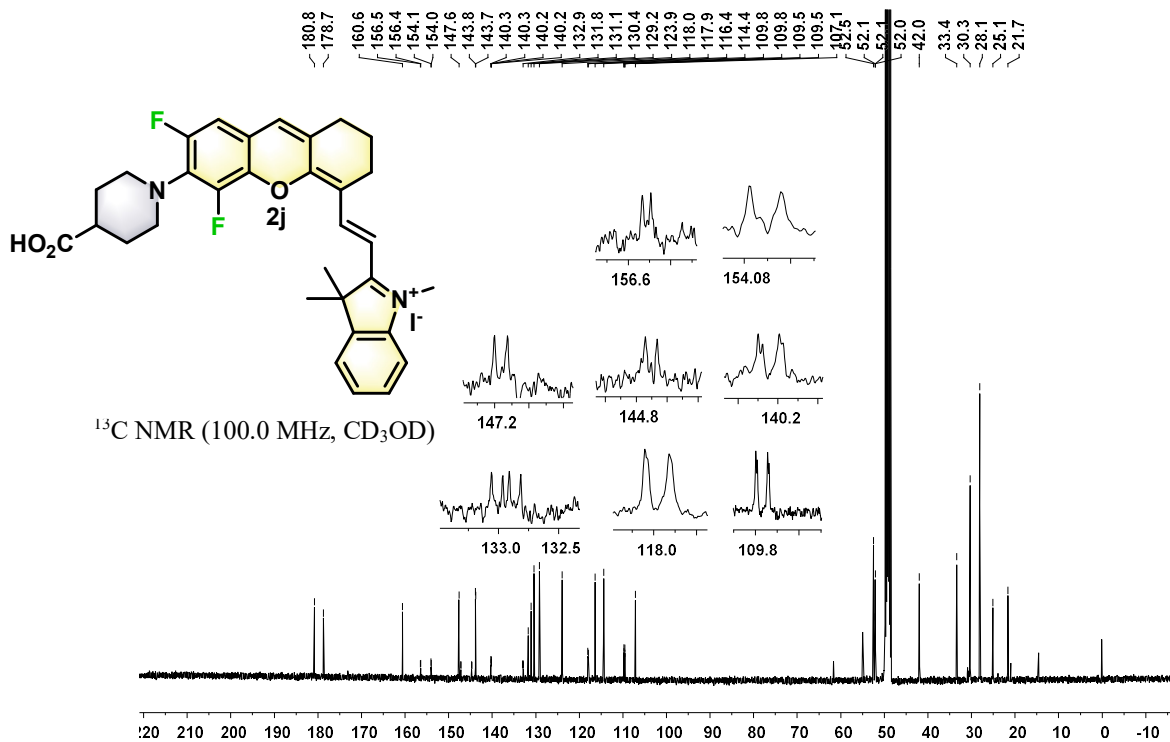
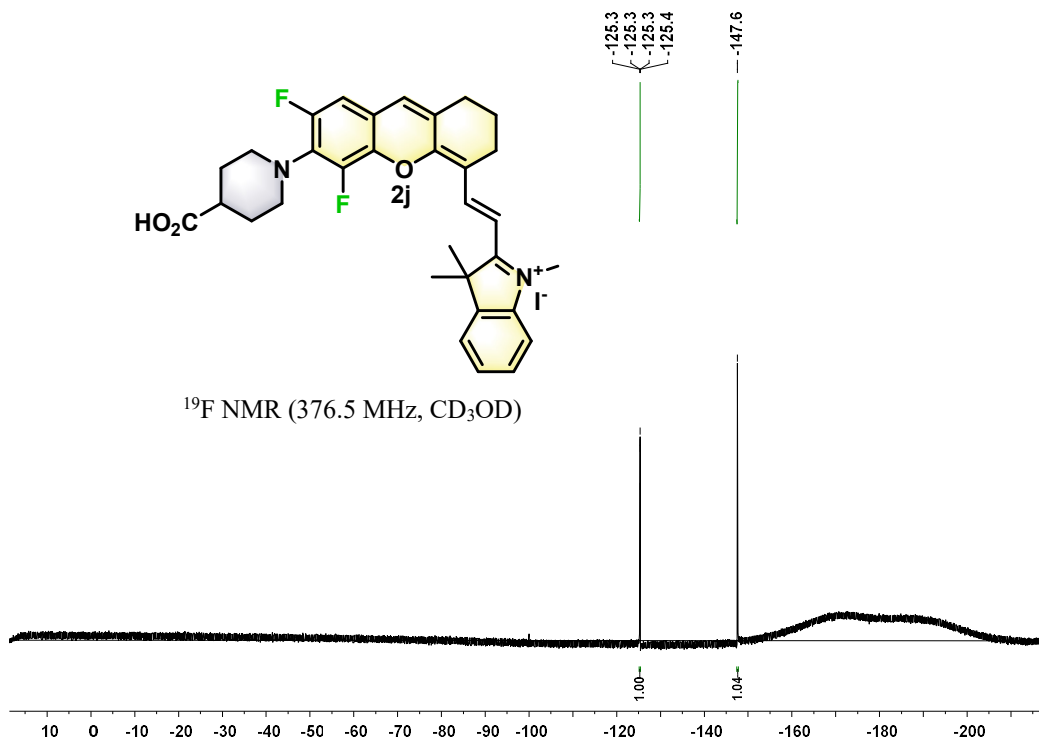


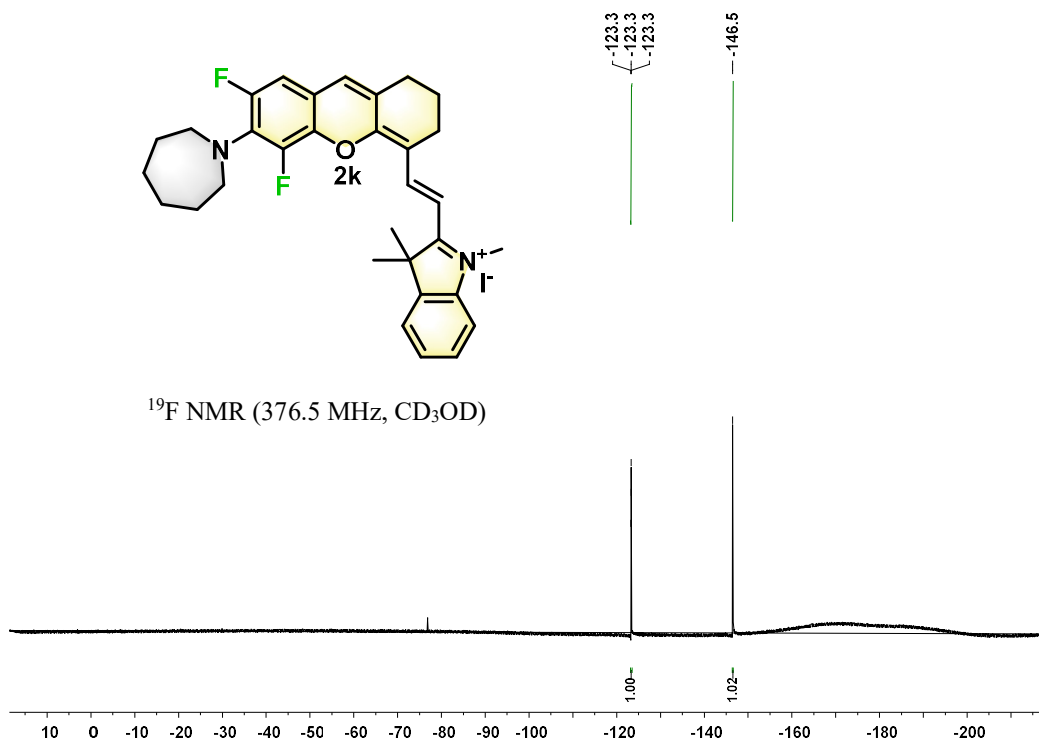
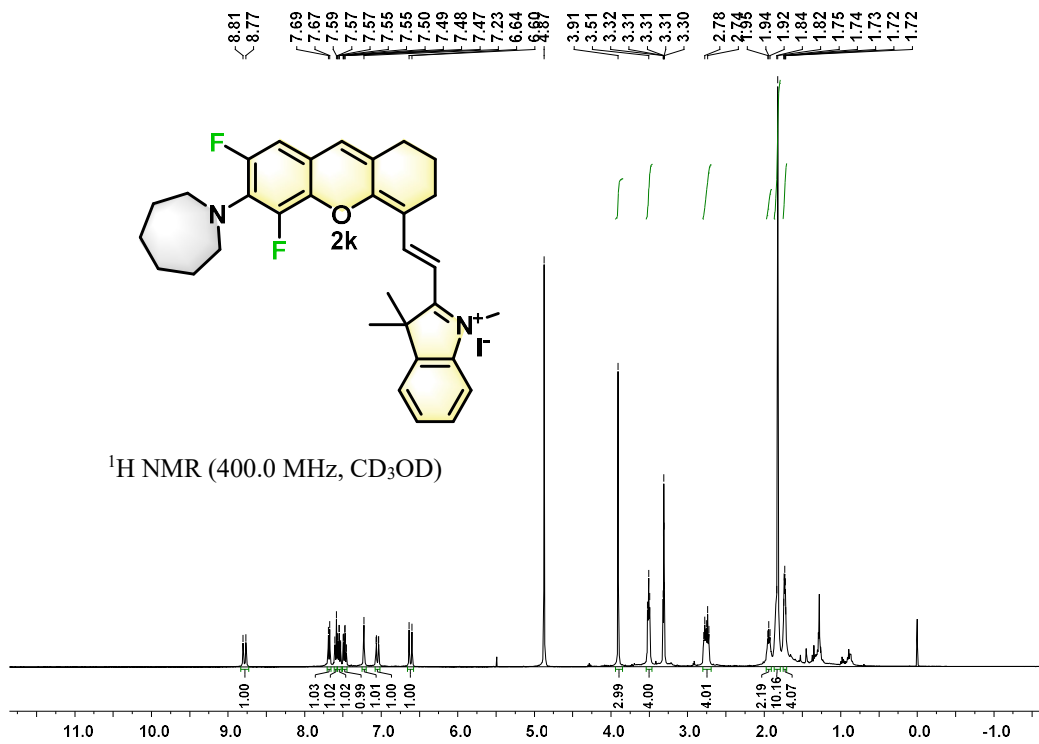


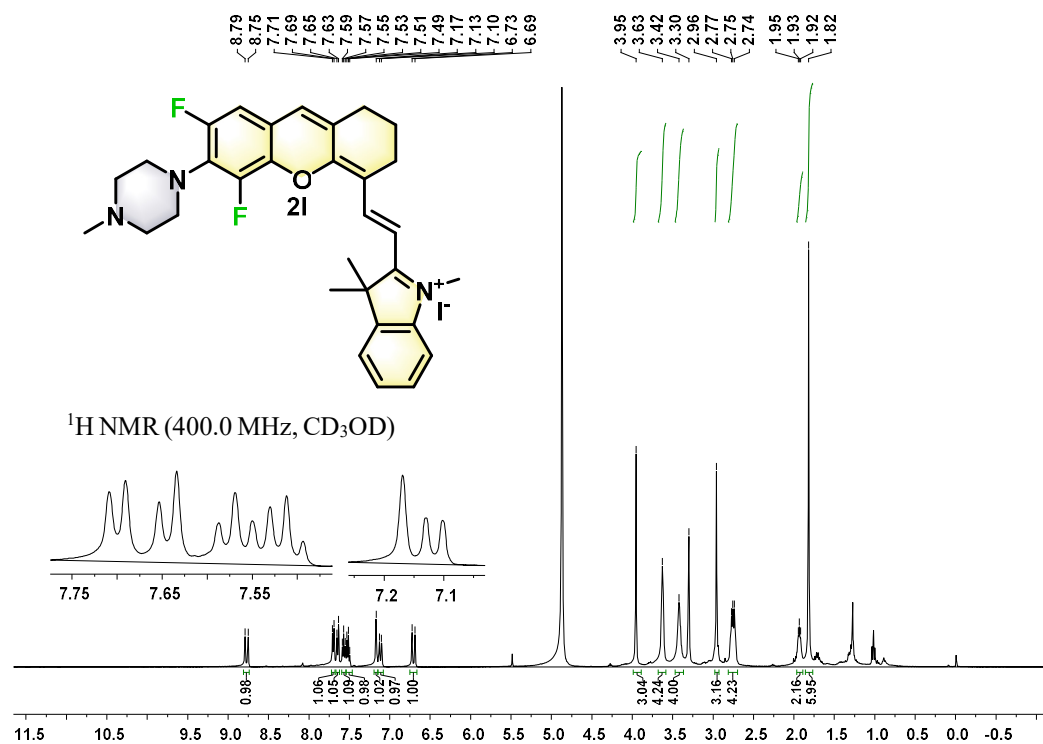
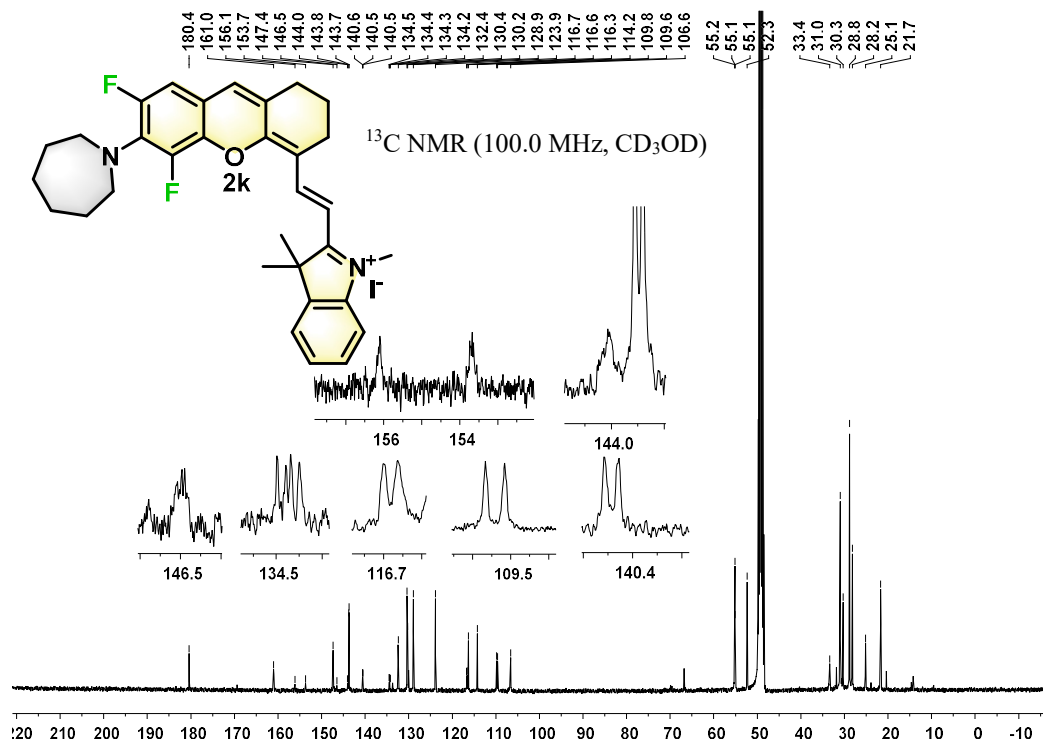


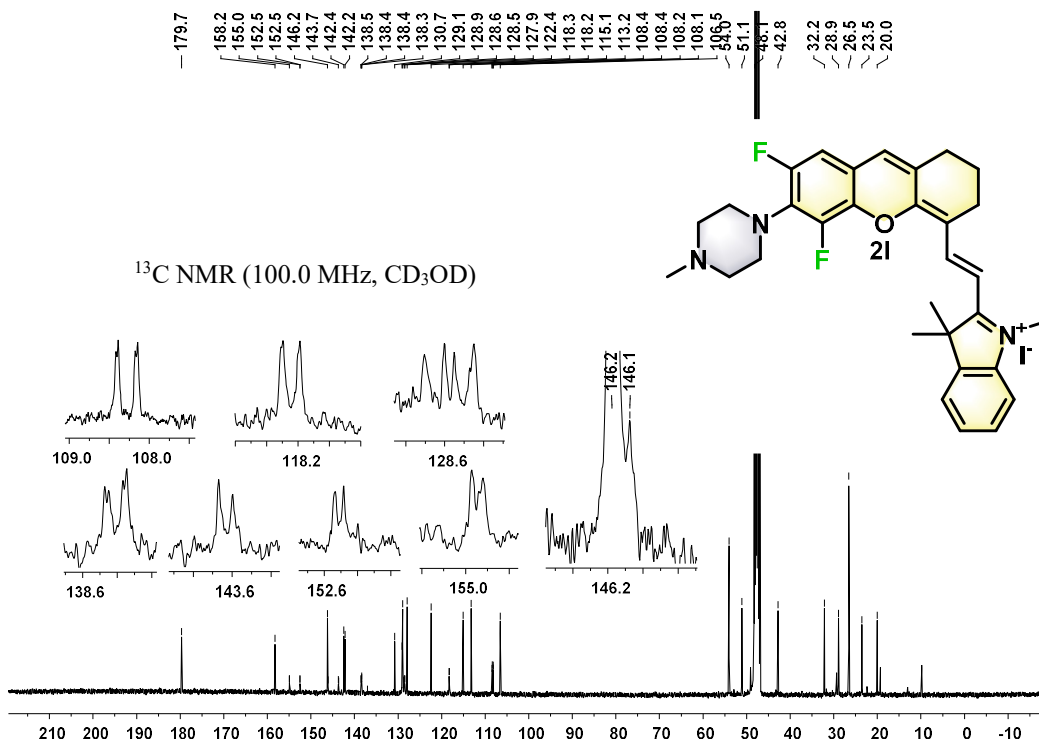
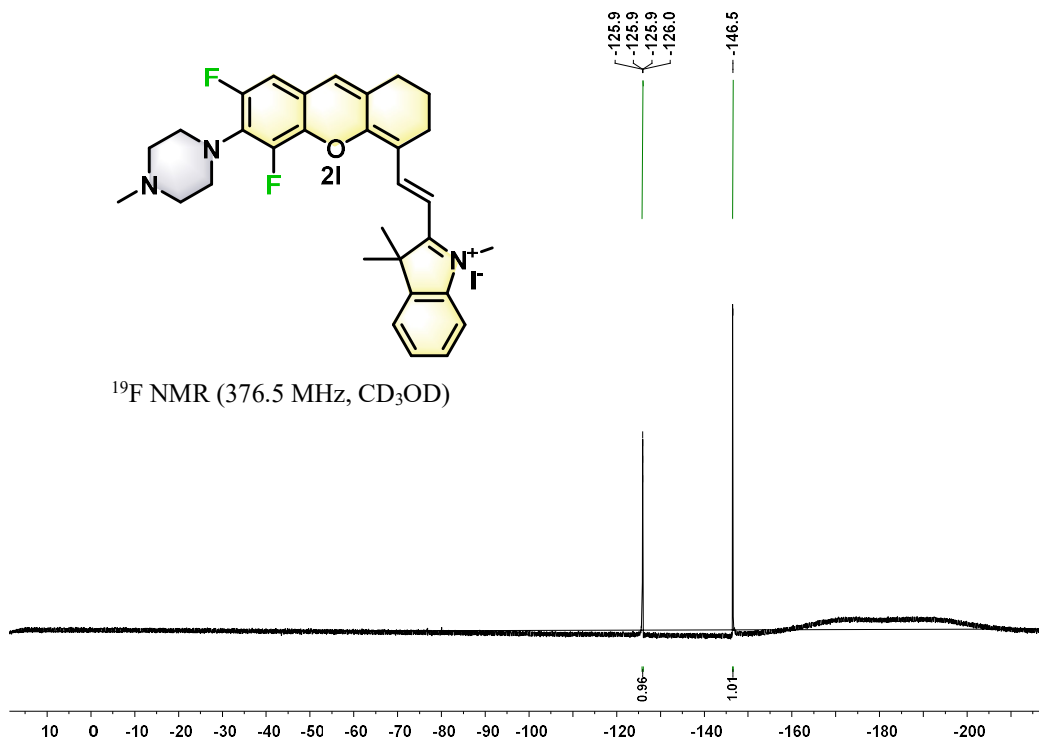


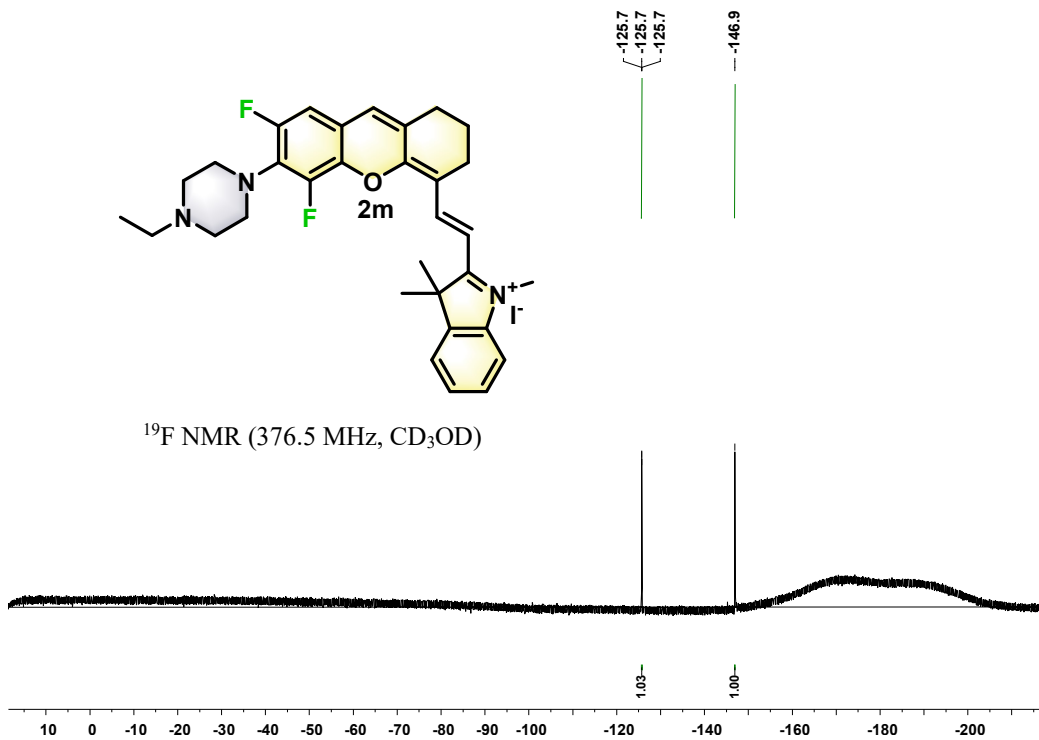
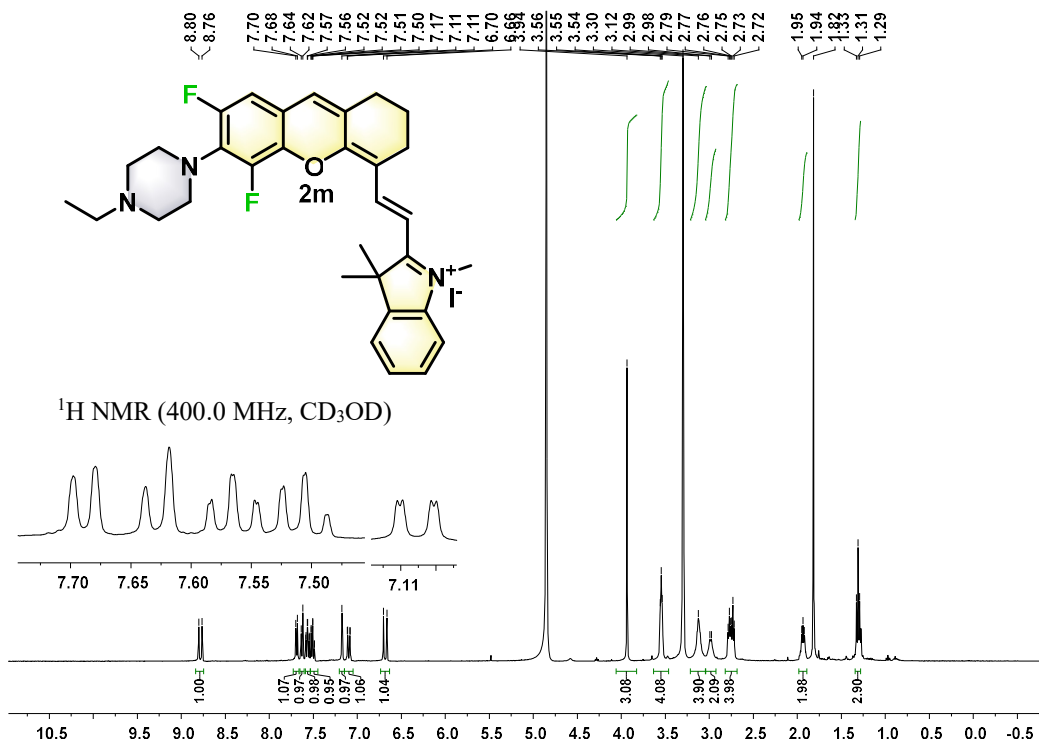


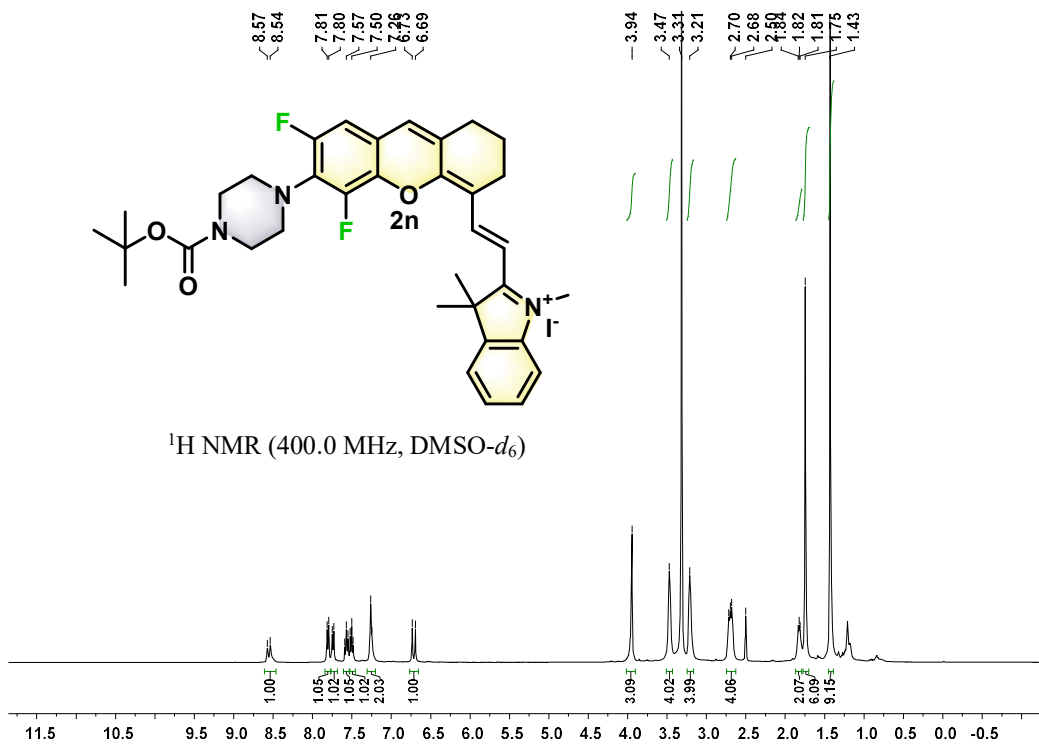
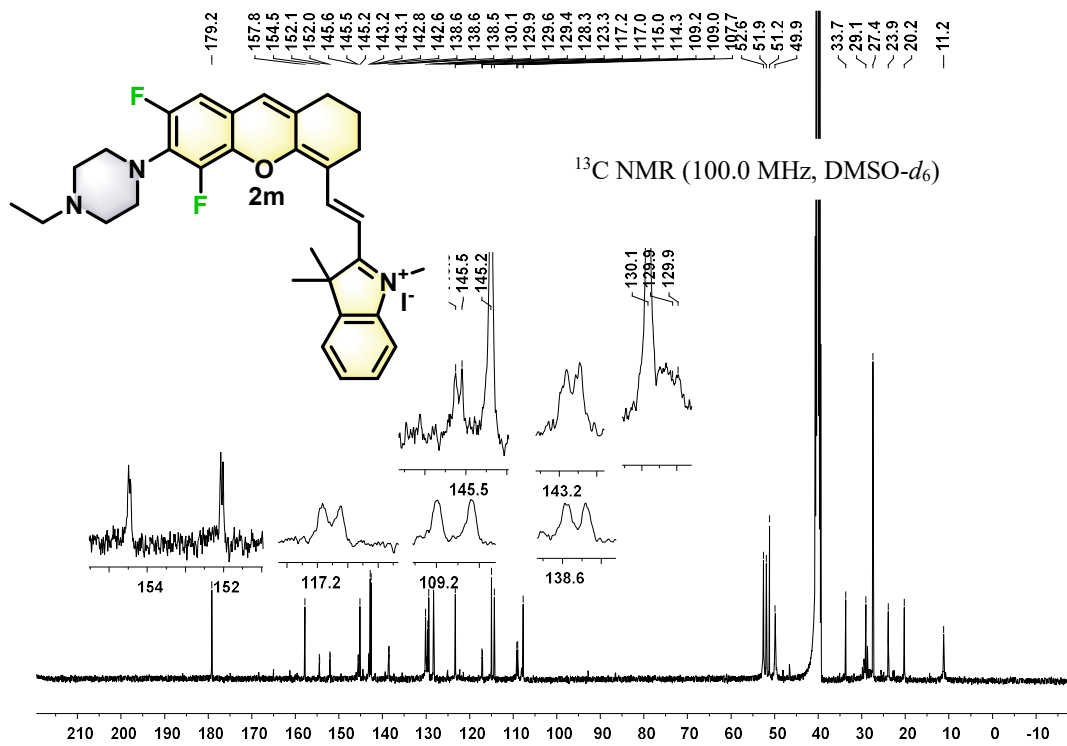


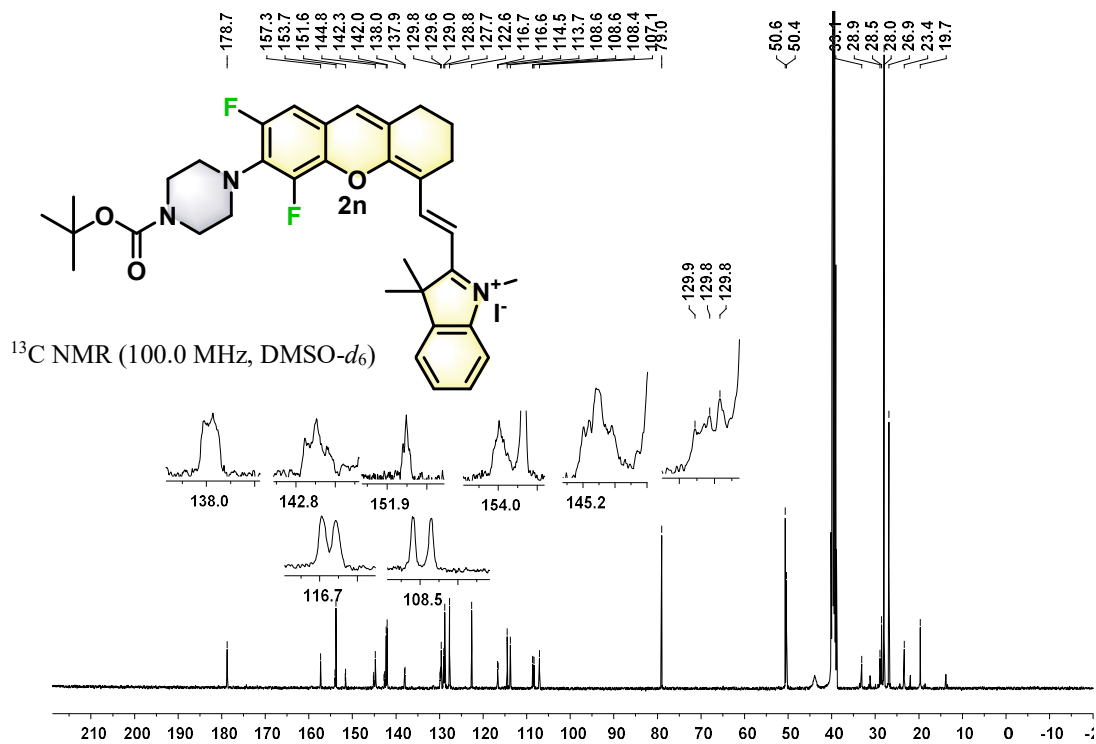
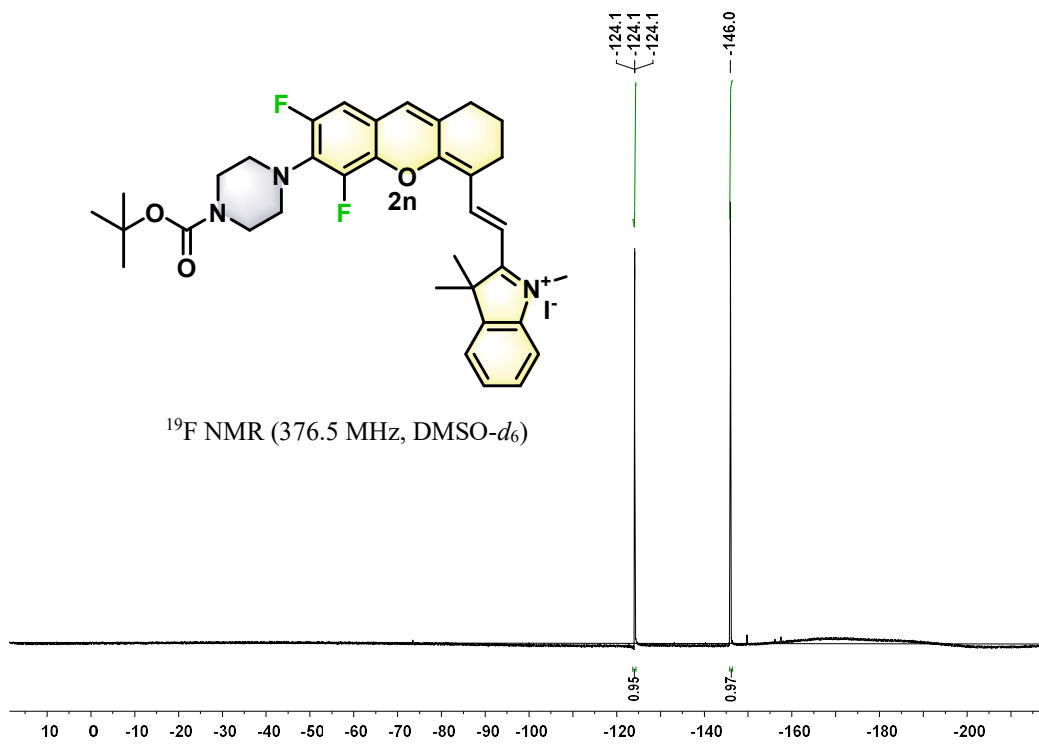


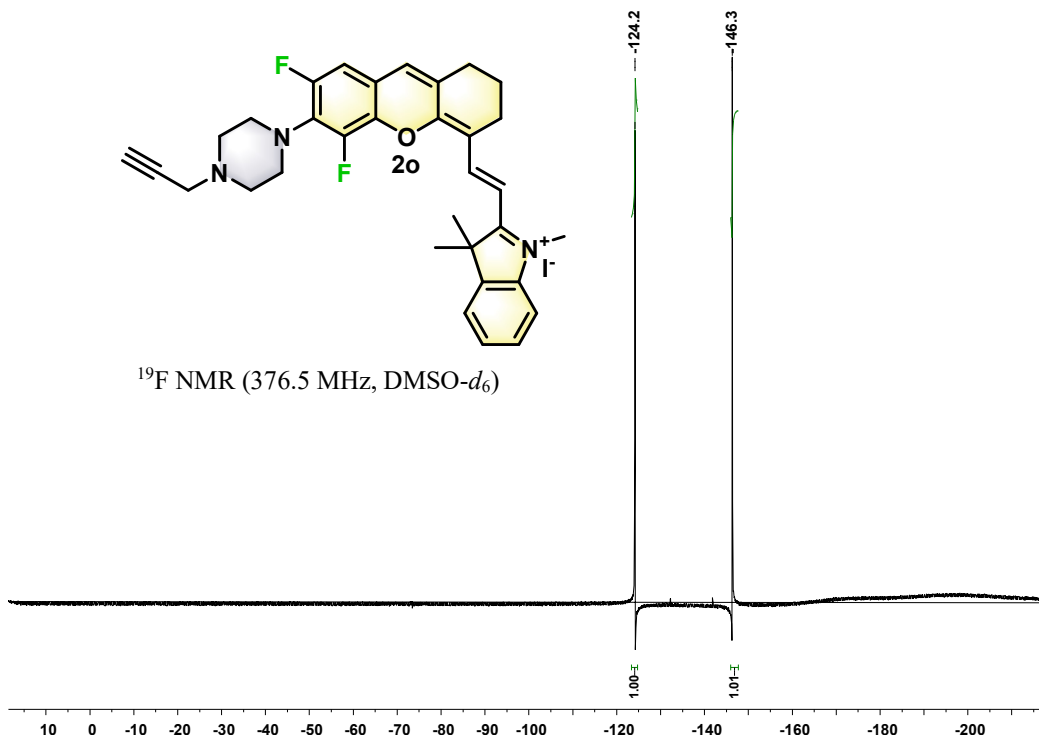
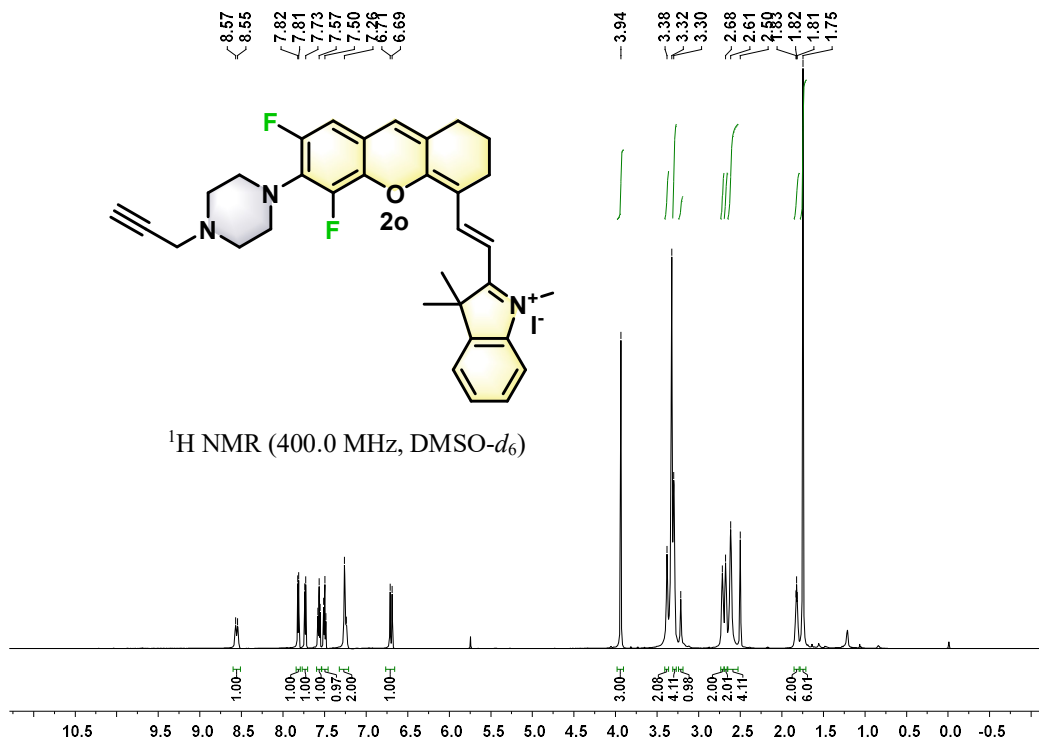


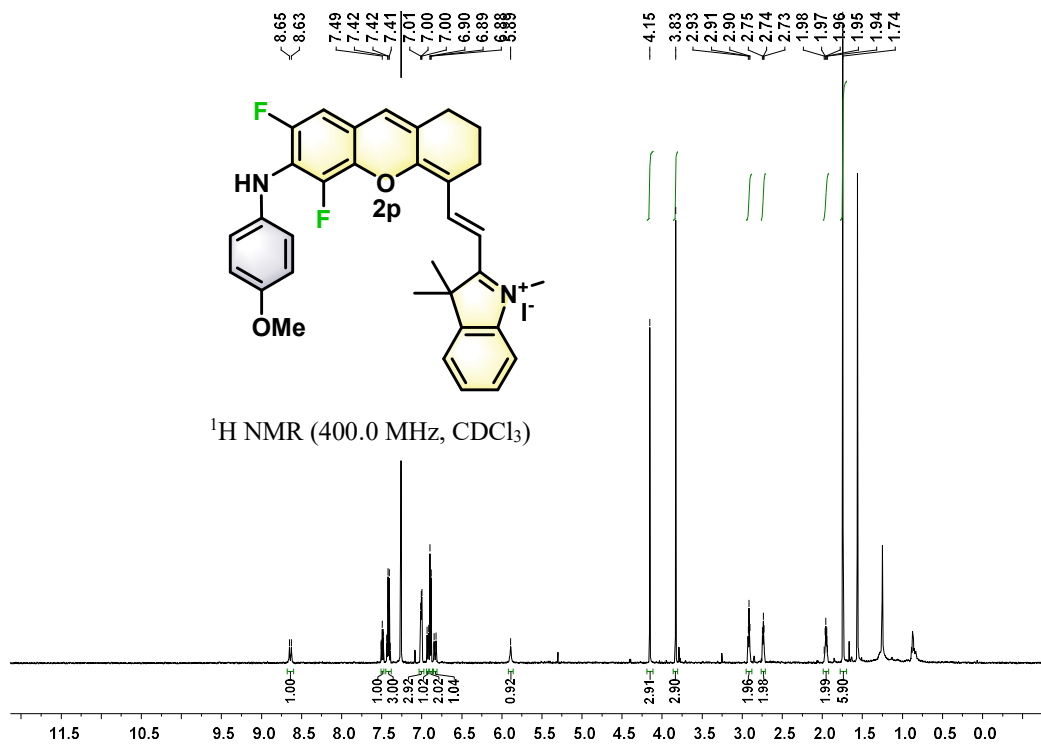
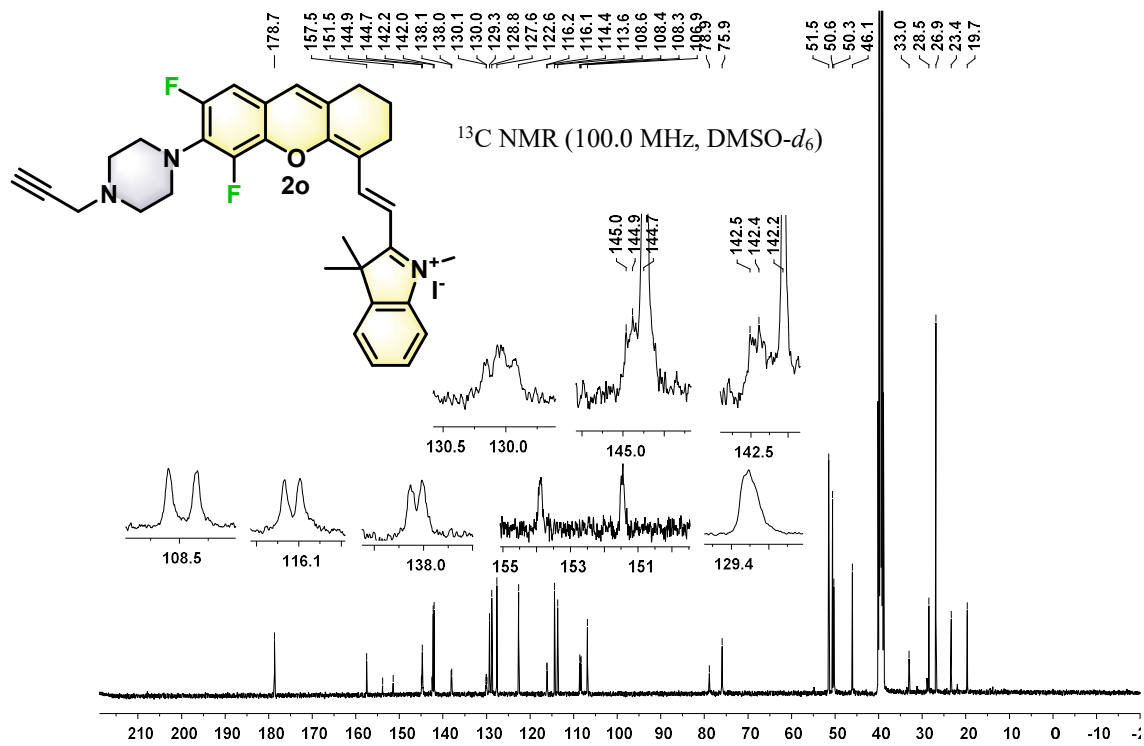


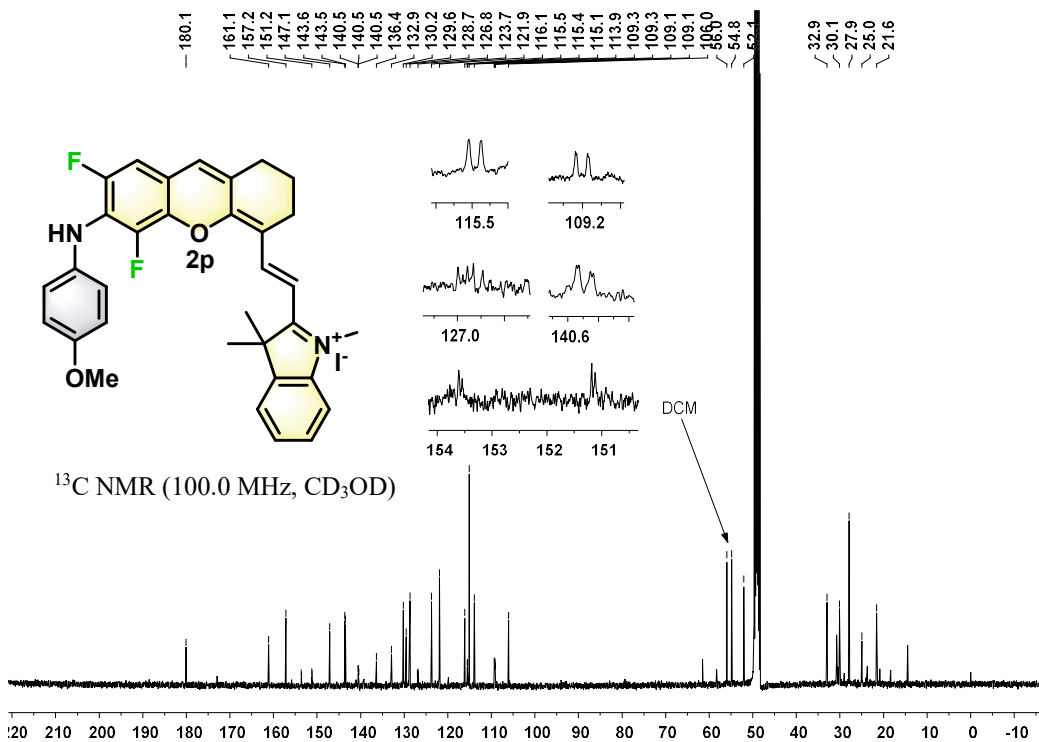
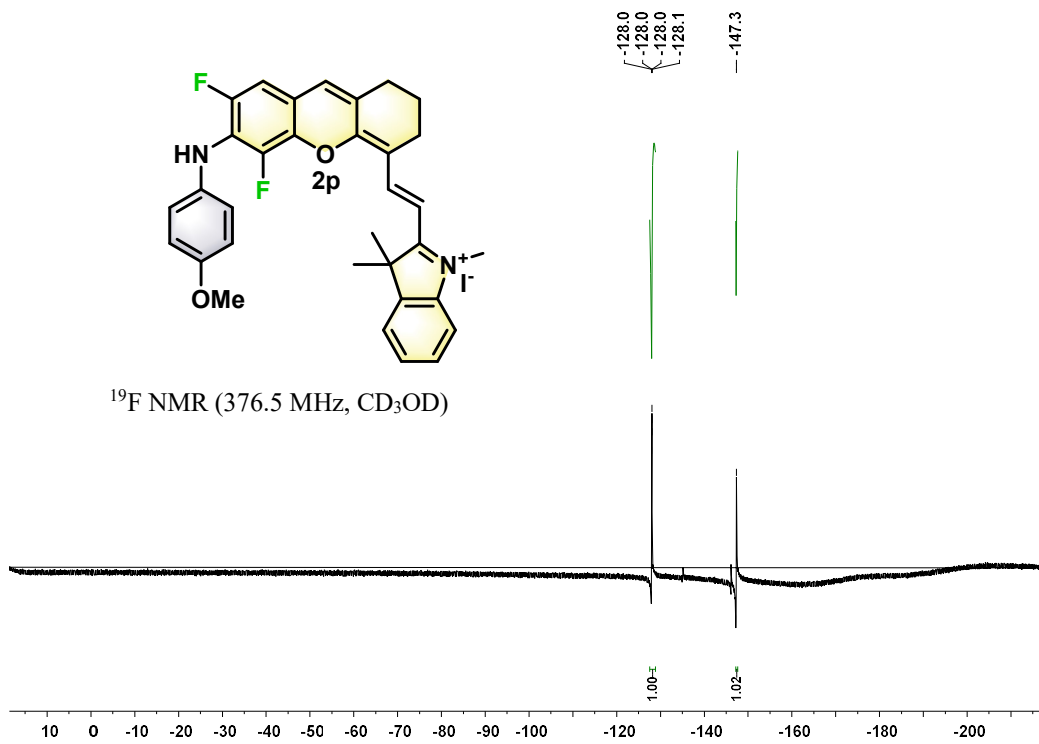


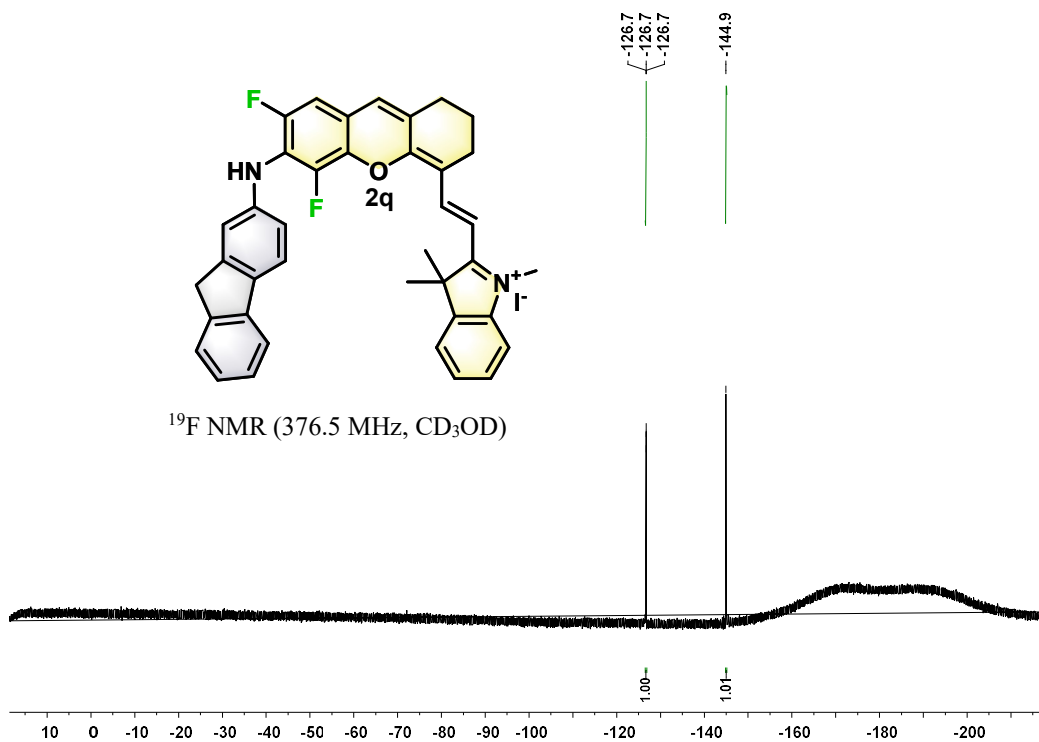
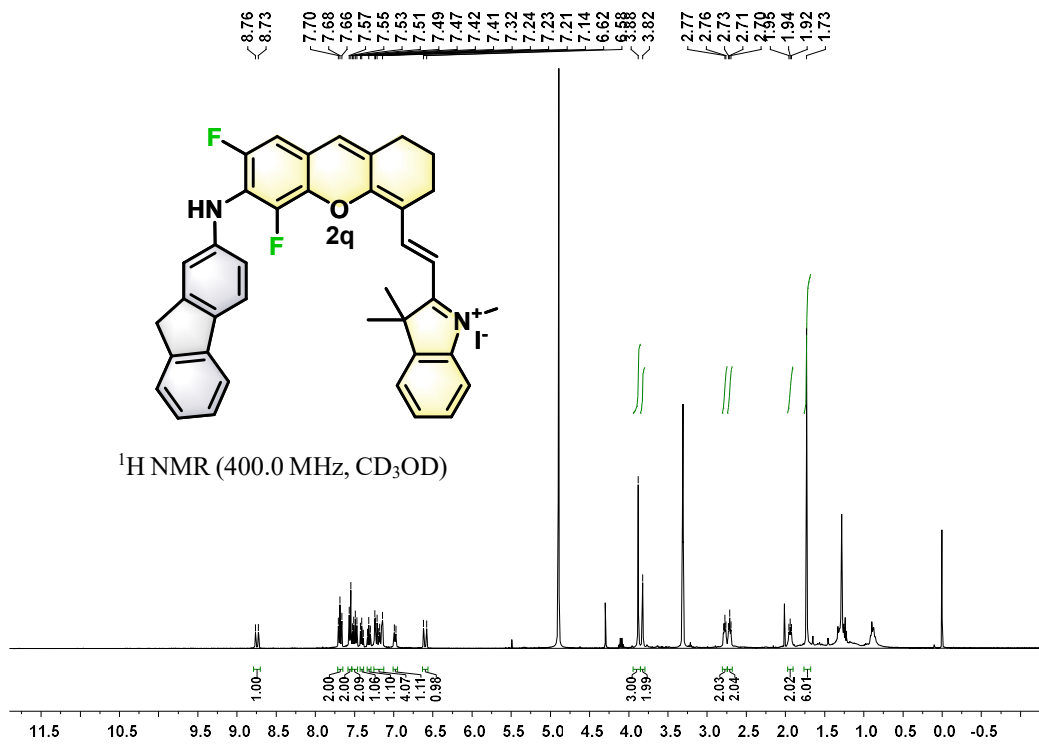


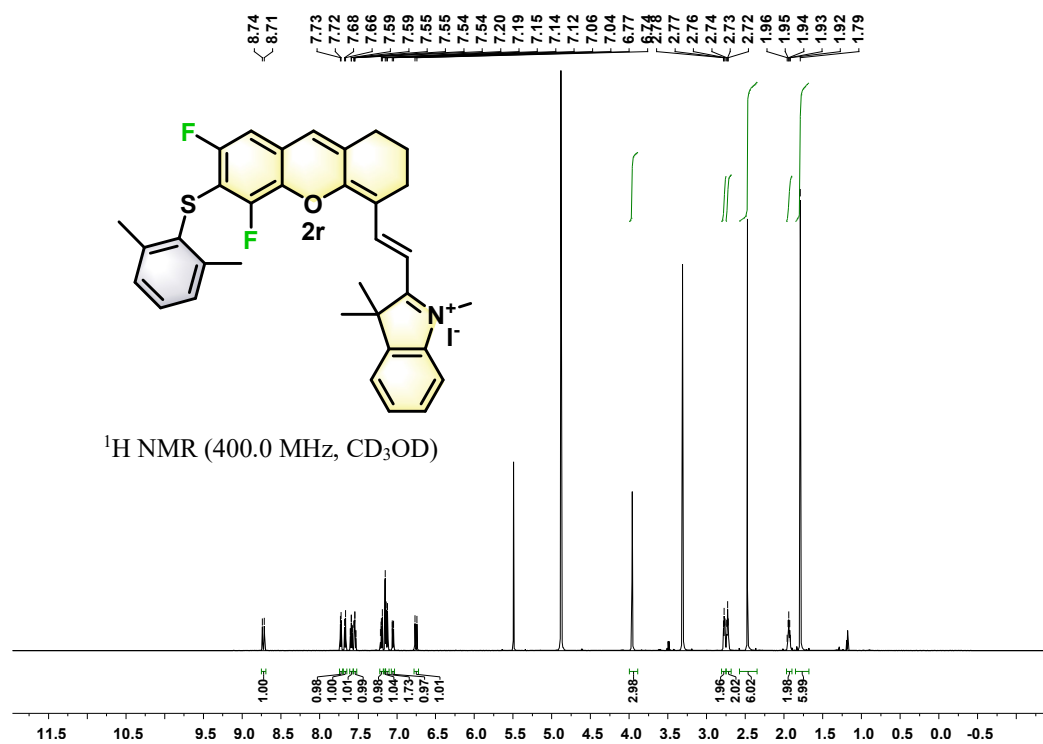
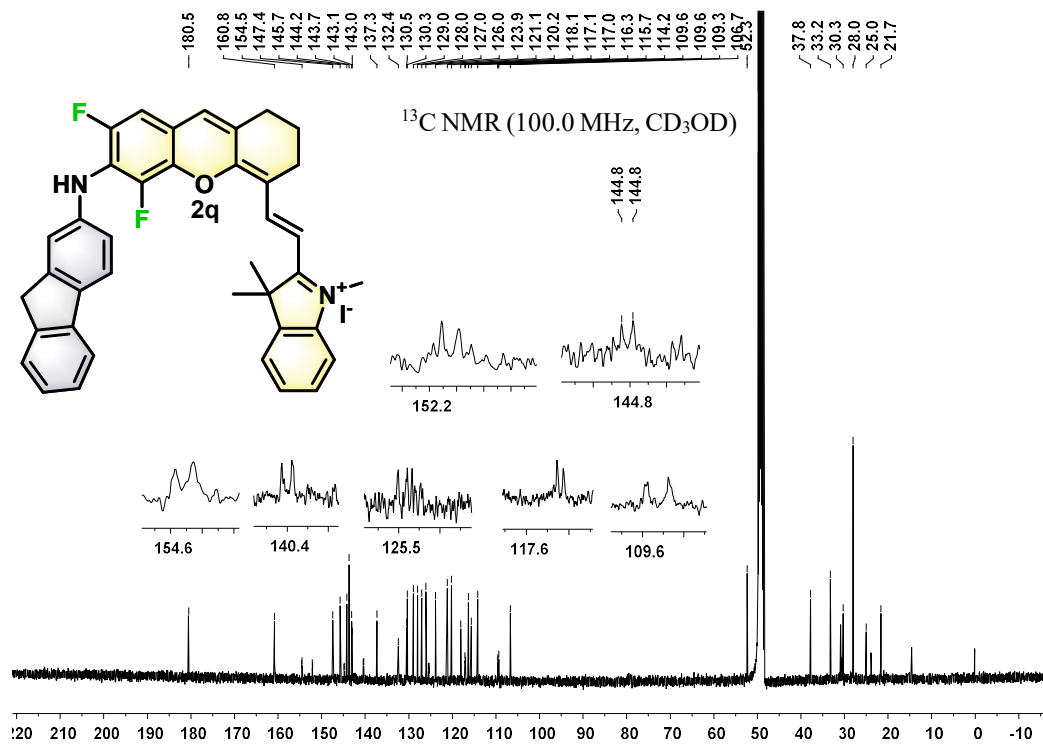


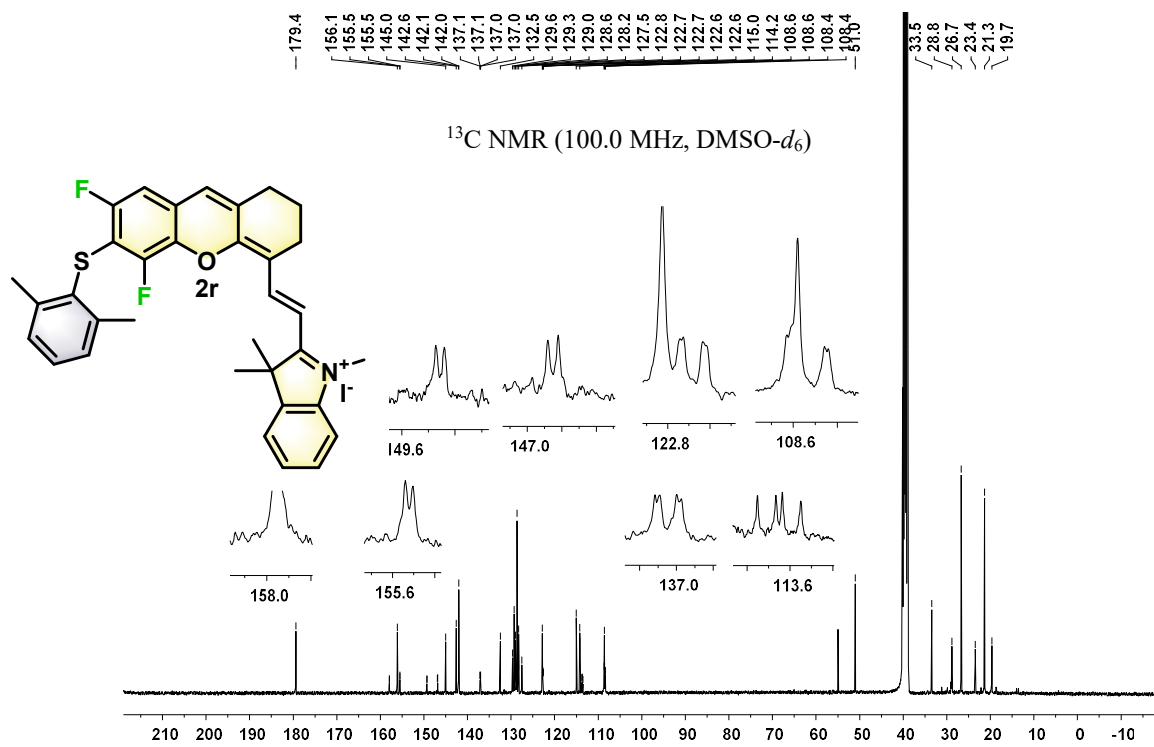
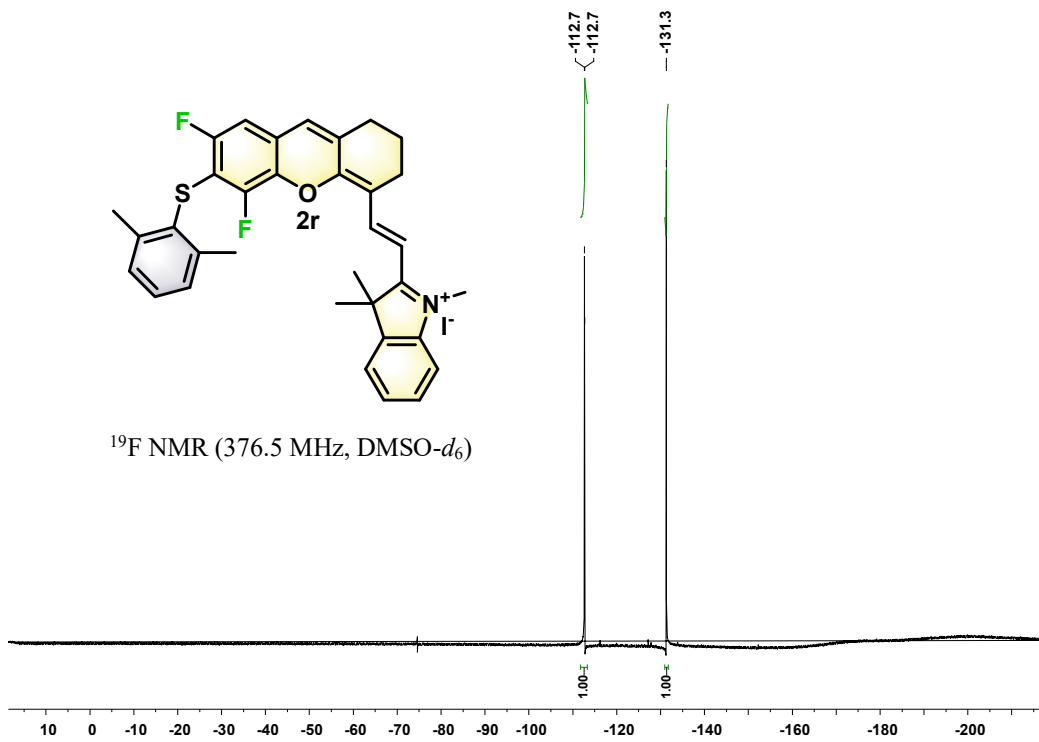


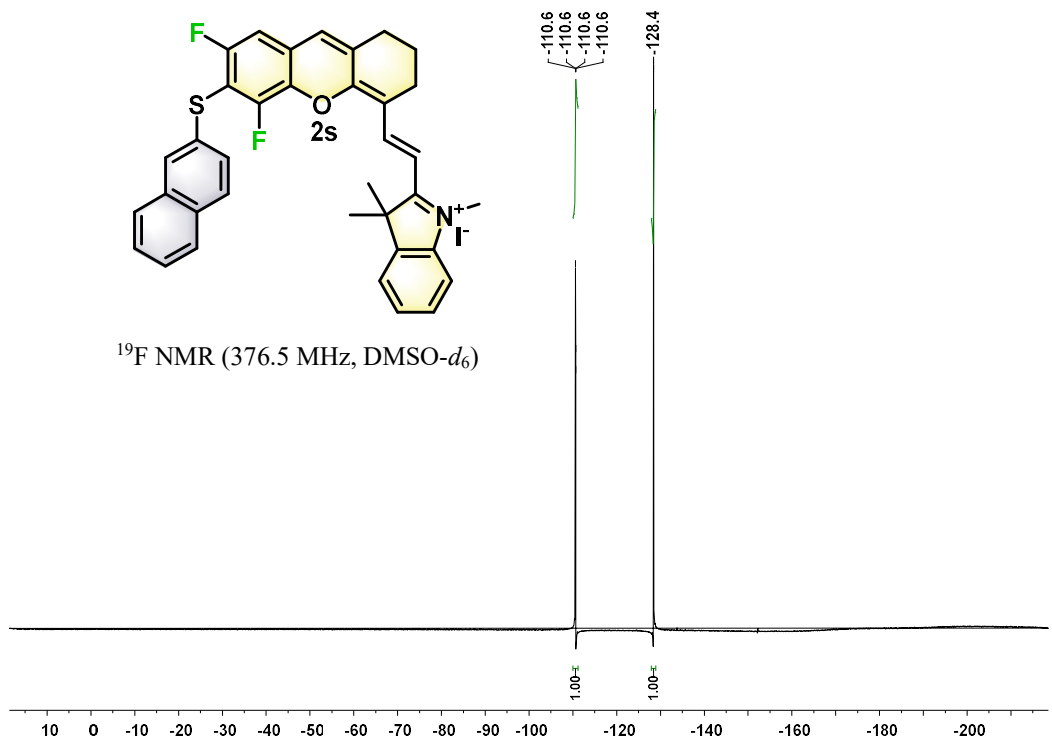
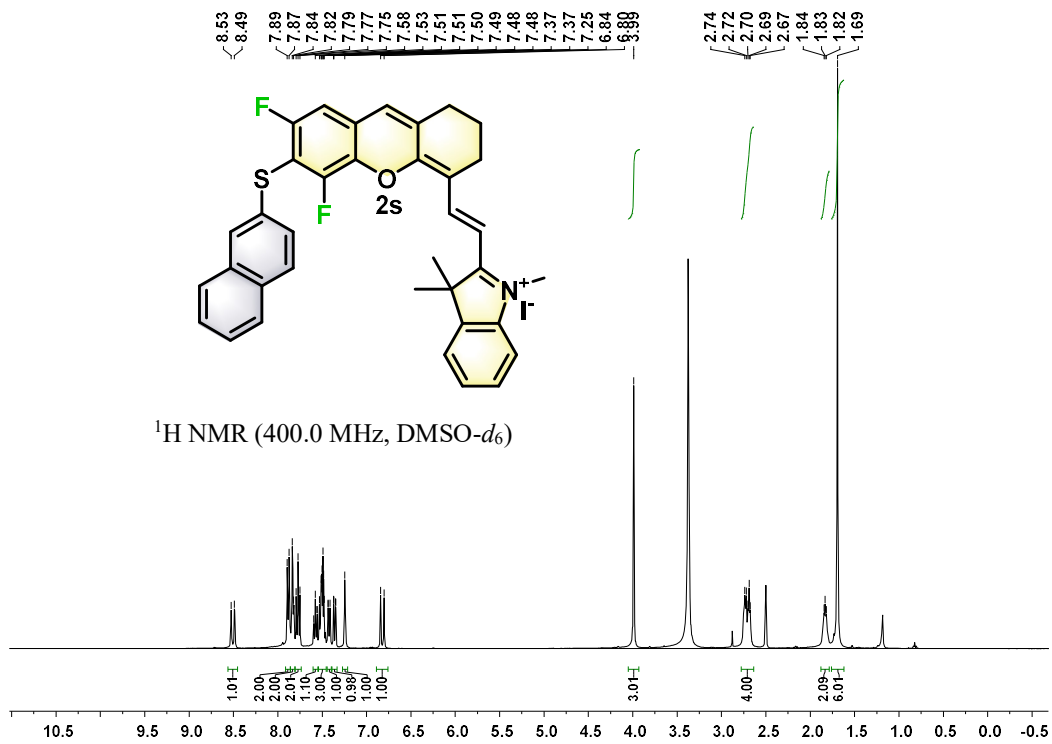


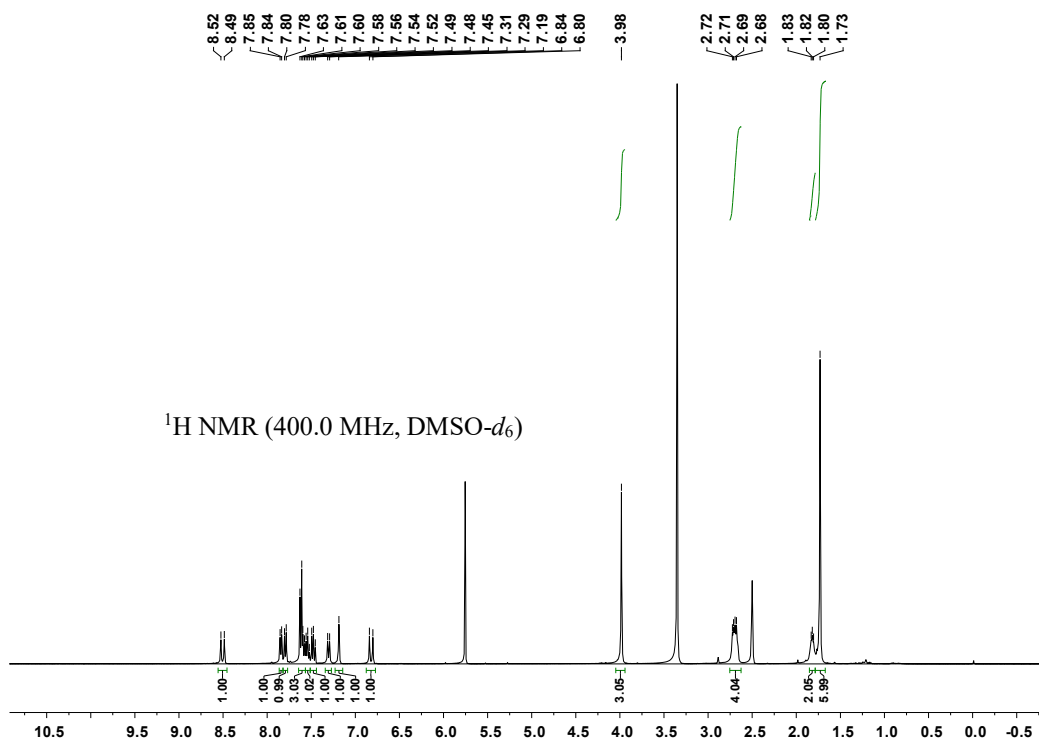
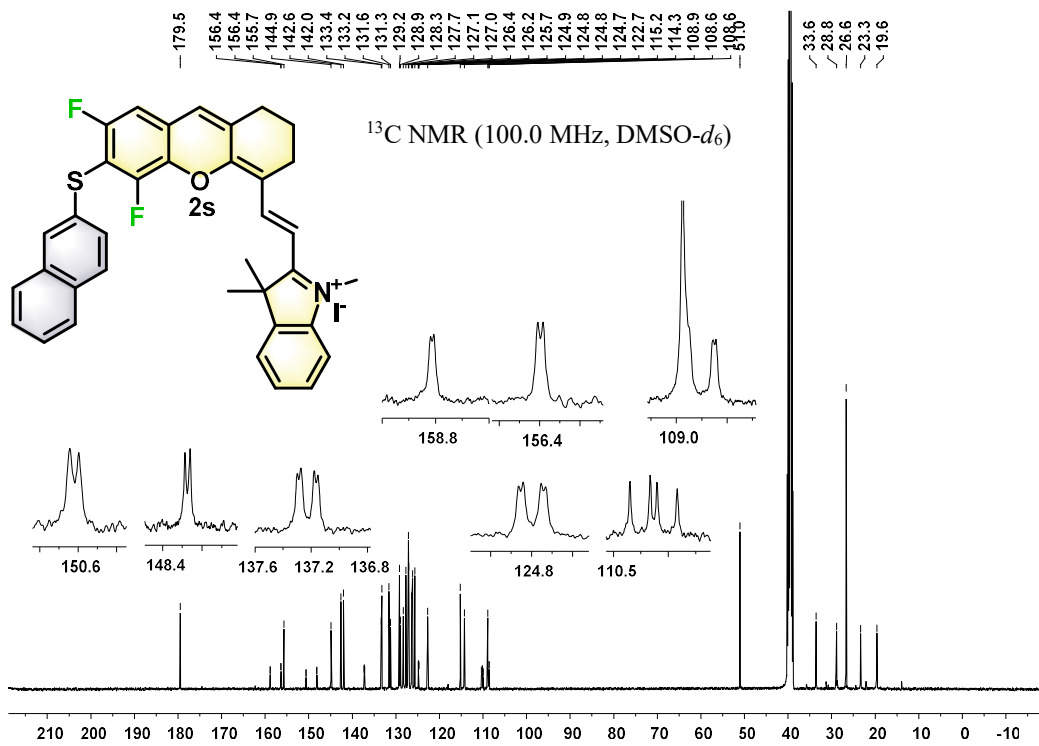


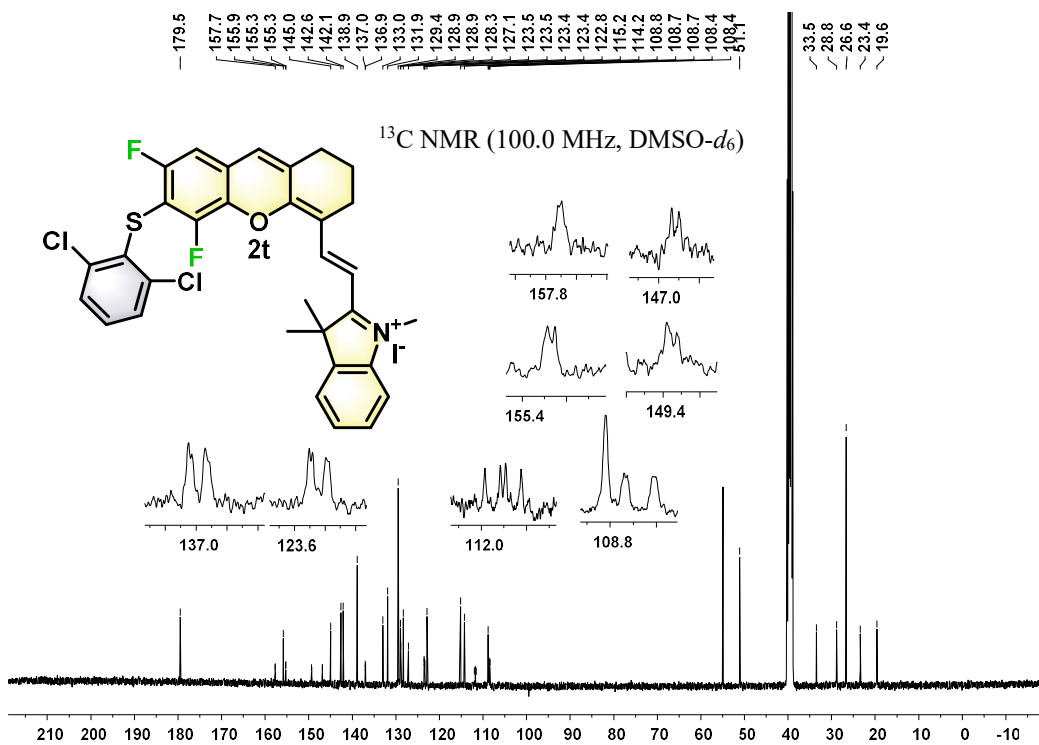
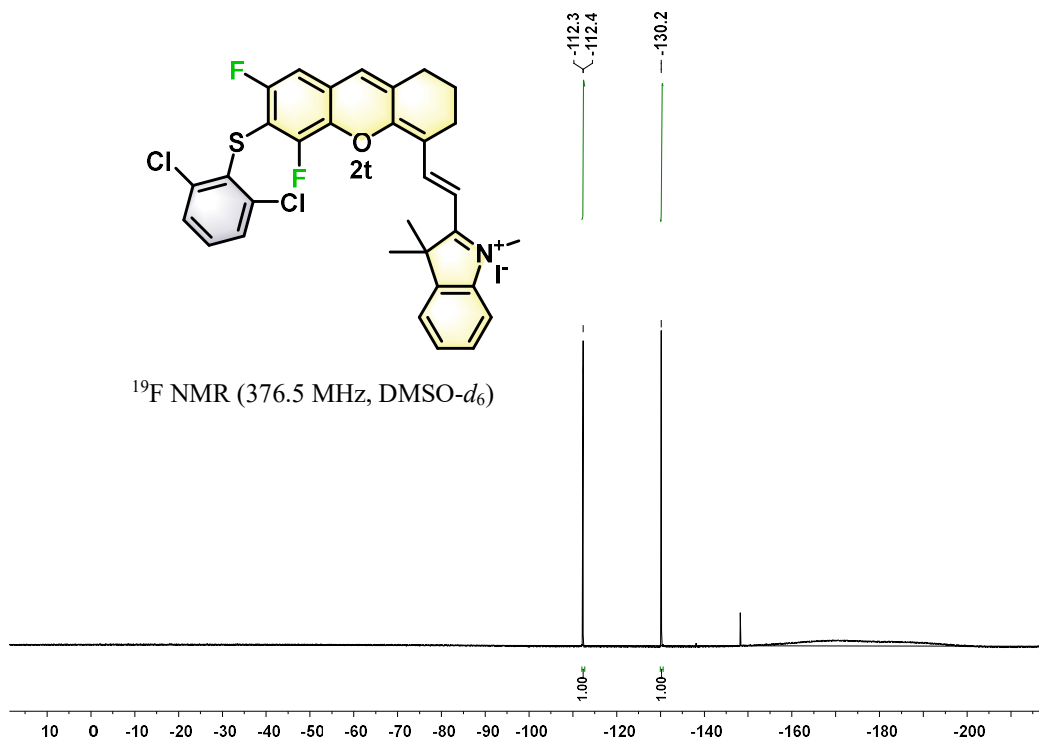


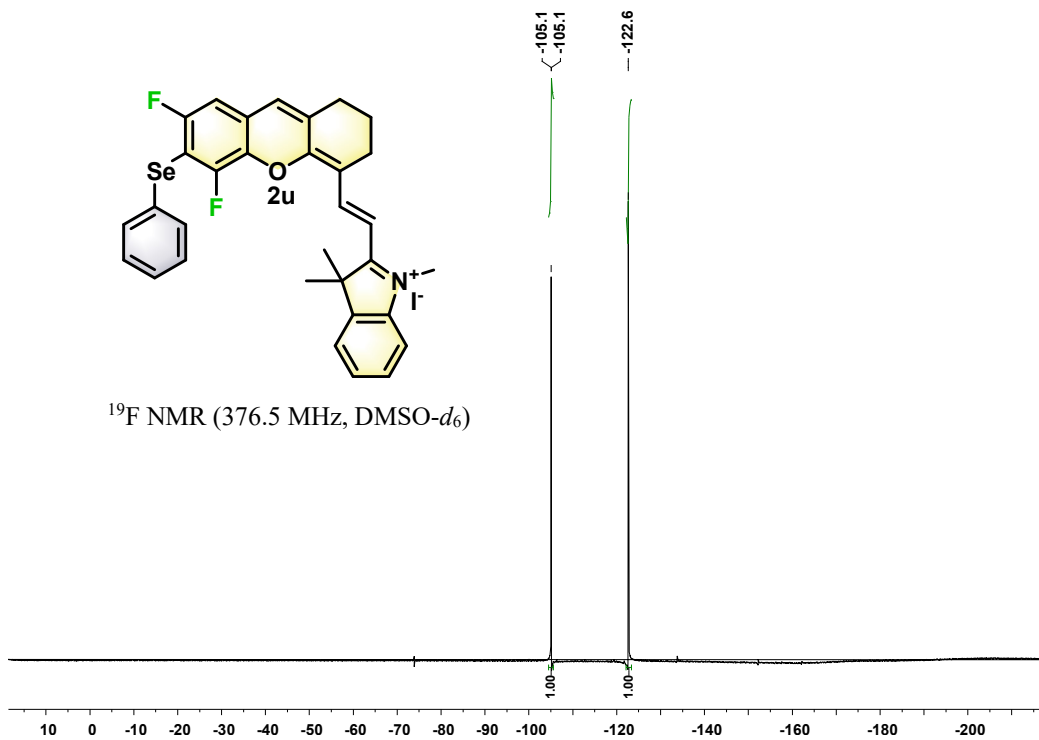
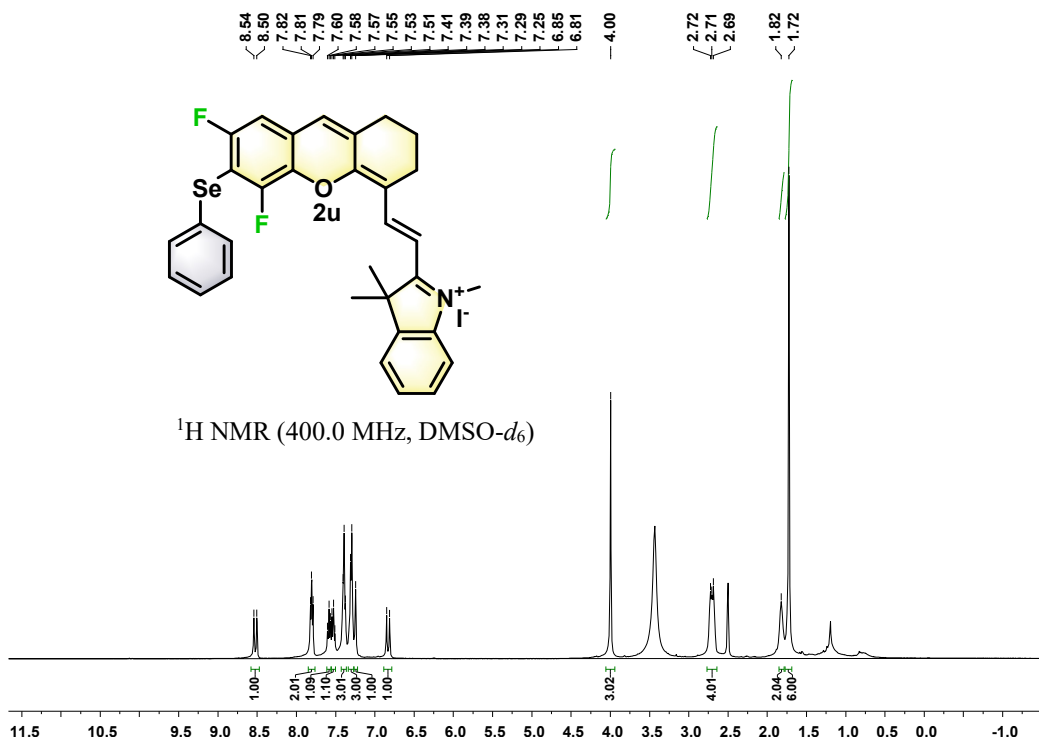


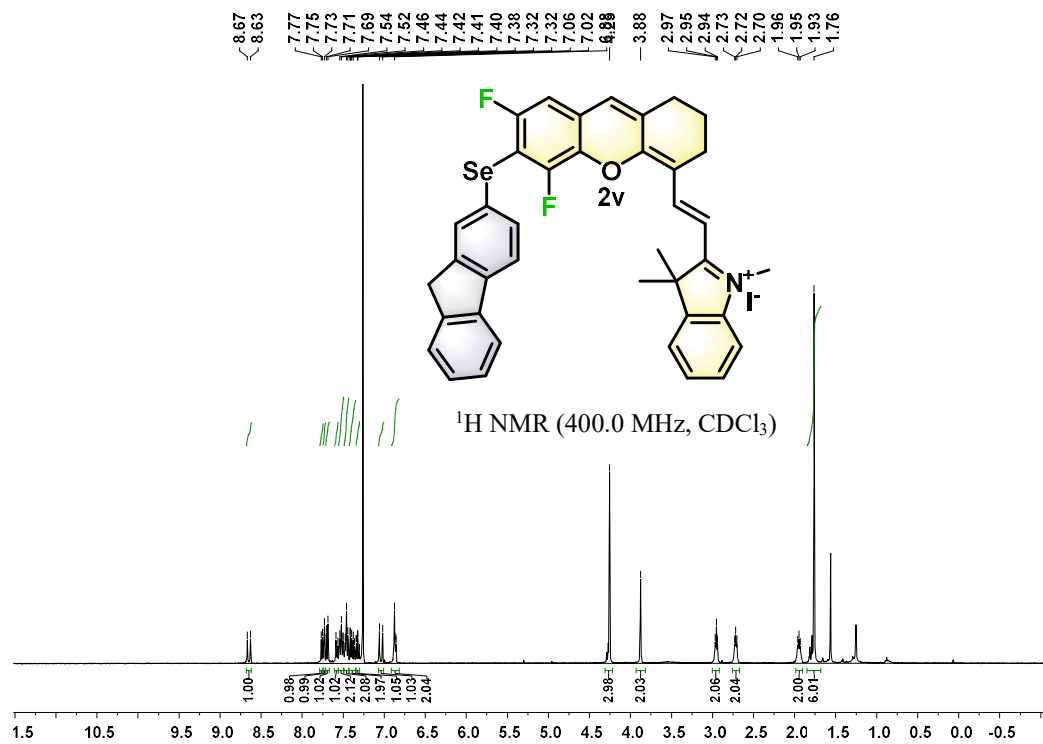
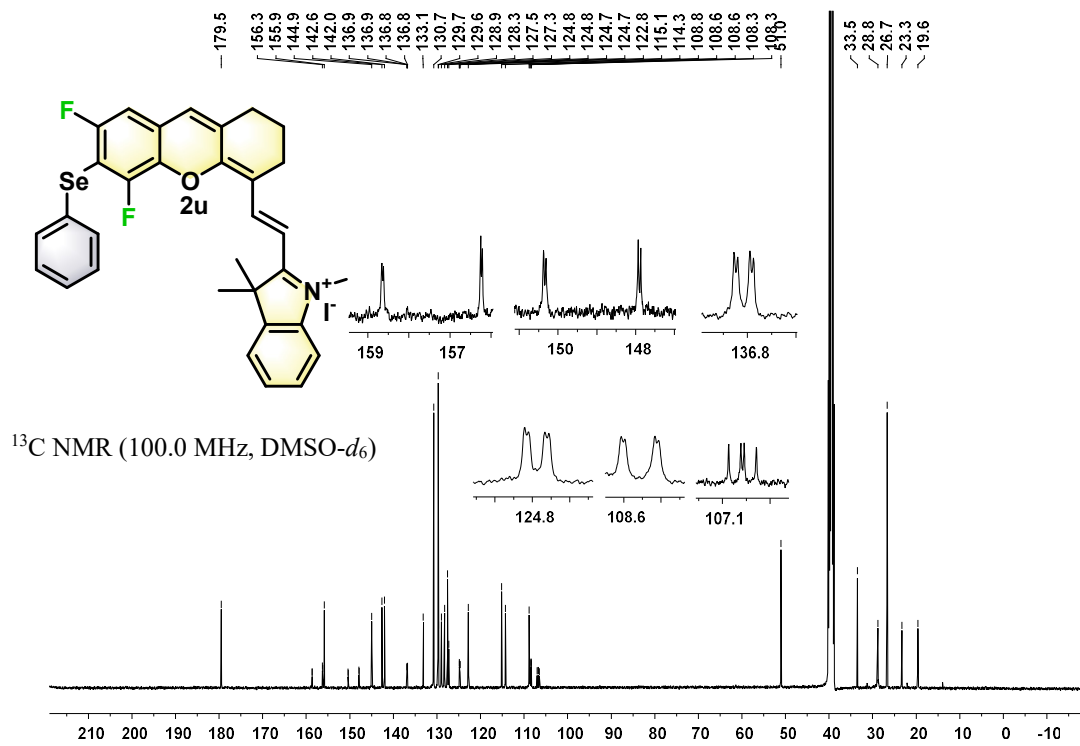


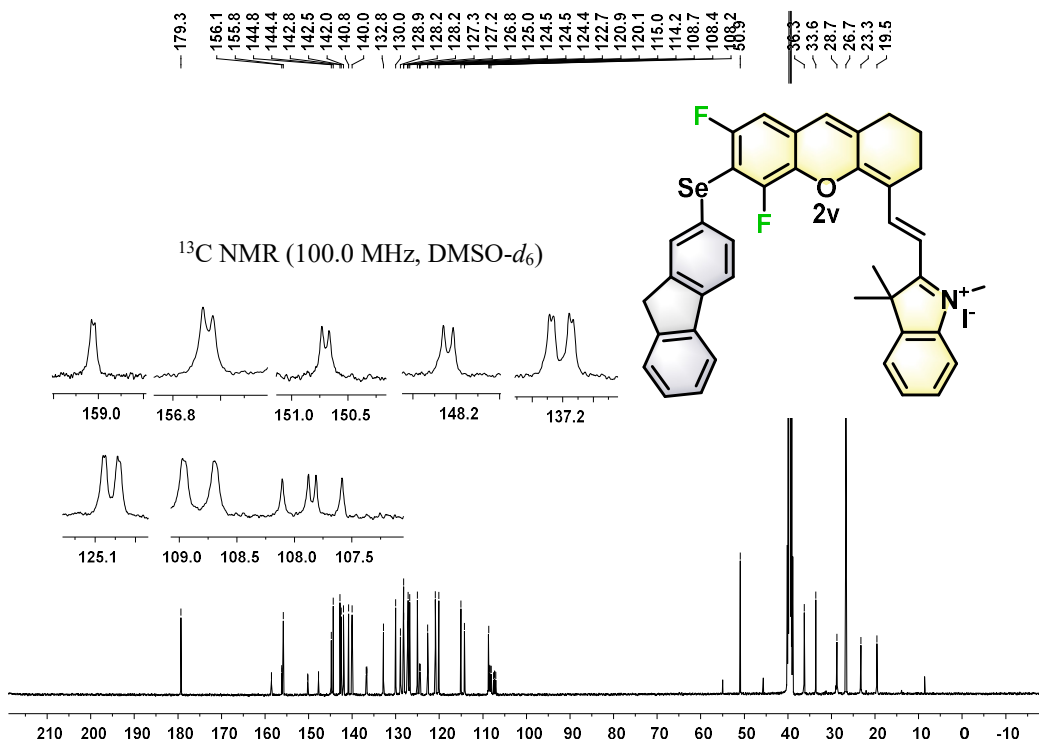
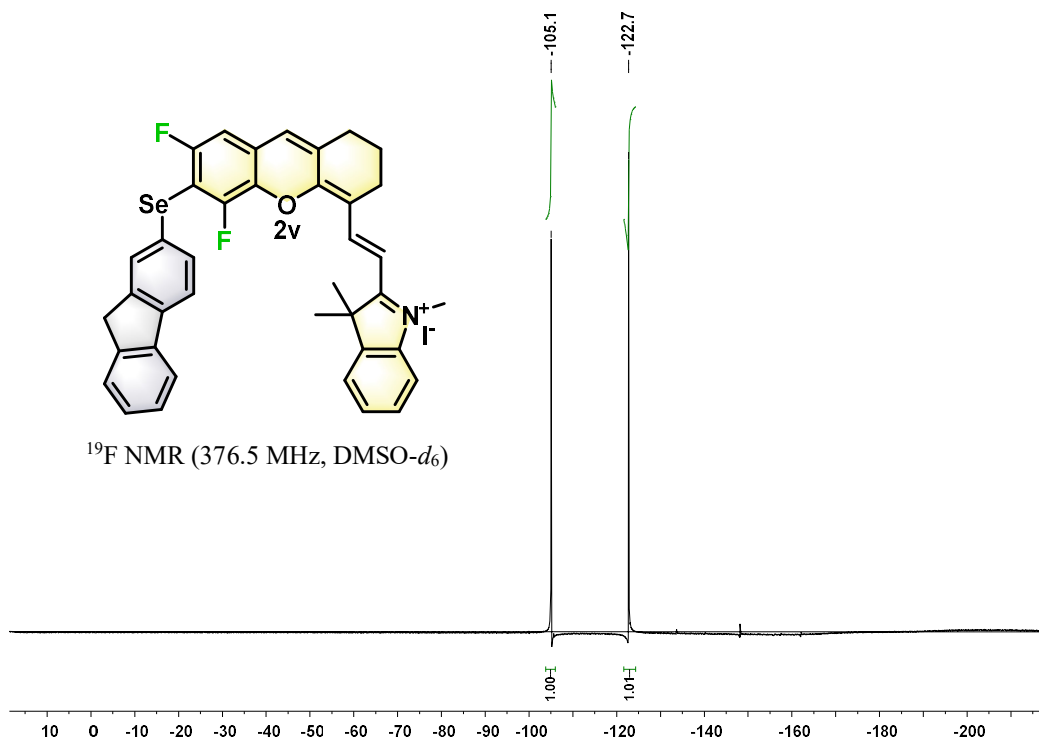








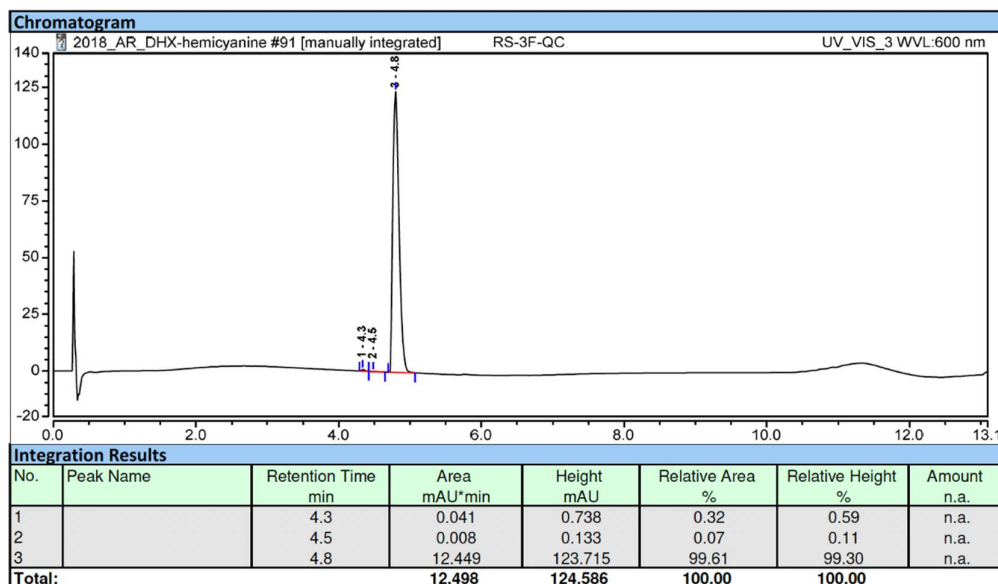




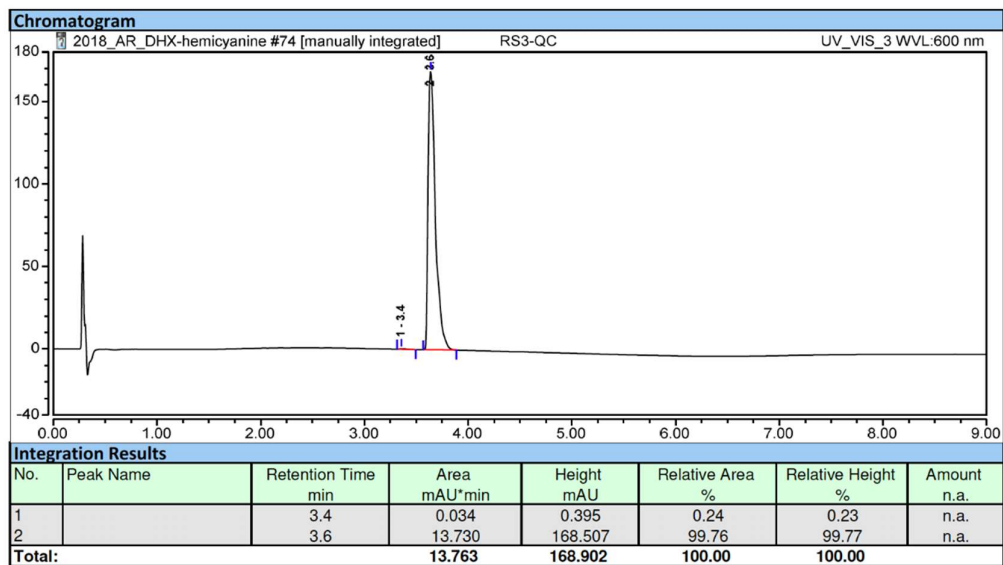
6. High-performance liquid chromatography (HPLC) separations

The following chromatographic system was used for the analytical experiments: *System A*: RP-HPLC (Phenomenex Kinetex C₁₈ column, 2.6 μm, 2.1 × 50 mm) with CH₃CN (+ 0.1% FA) and 0.1% aq. formic acid (aq. FA, pH 2.5) as eluents [5% CH₃CN (0.1 min) followed by linear gradient from 5% to 100% CH₃CN (5 min), then 100% CH₃CN (4 min)] at a flow rate of 0.5 mL/min. UV-visible detection was achieved at 220, 260, 600 and 700 nm (+ diode array detection in the range 220-800 nm). Low resolution ESI-MS detection in the positive mode (full scan, 100-1500 a.m.u., data type: centroid, needle voltage: 3.0 kV, probe temperature: 350 °C, cone voltage: 75 V and scan time: 1 s).

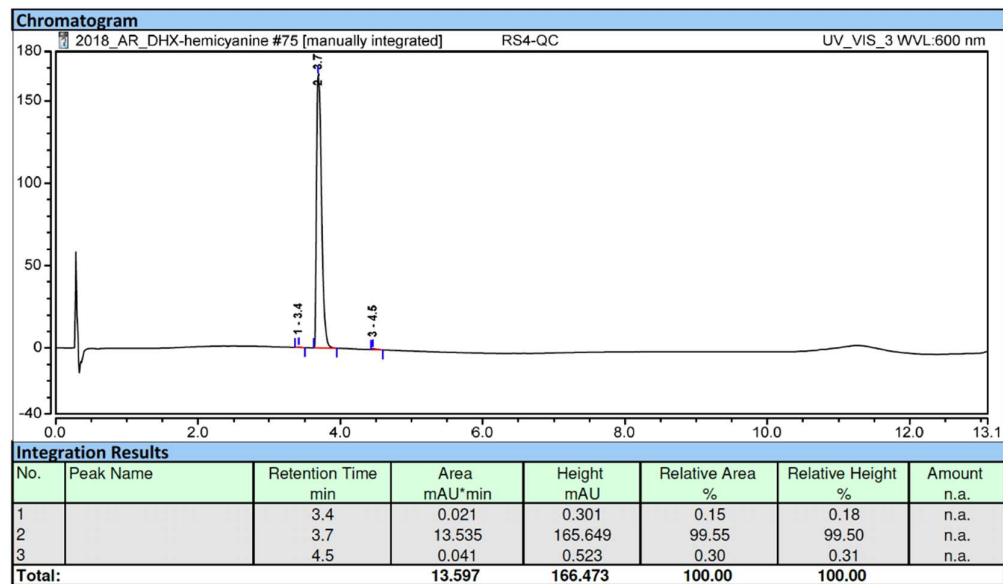
RP-HPLC elution profile of 1 (system A, detection at 600 nm)



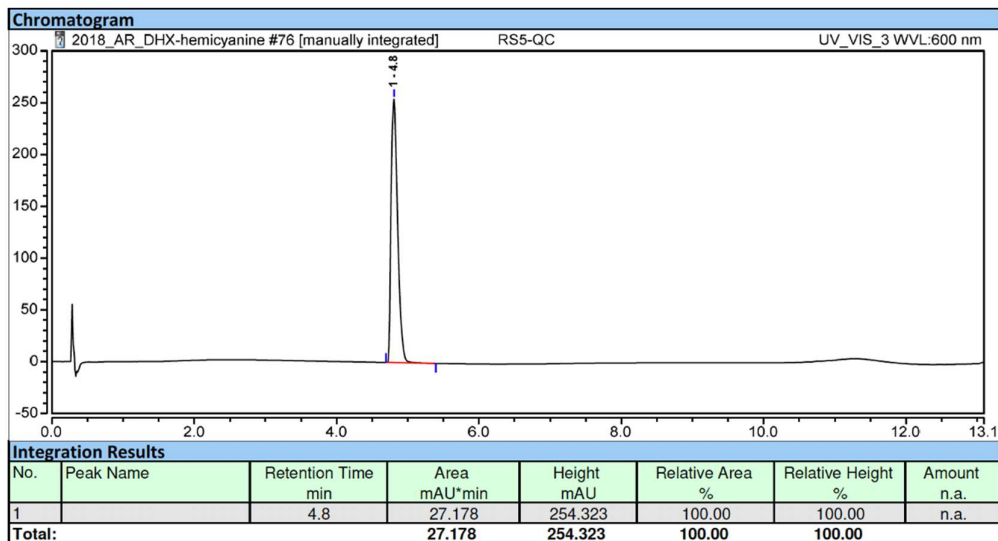
RP-HPLC elution profile of **2I** (system A, detection at 600 nm)



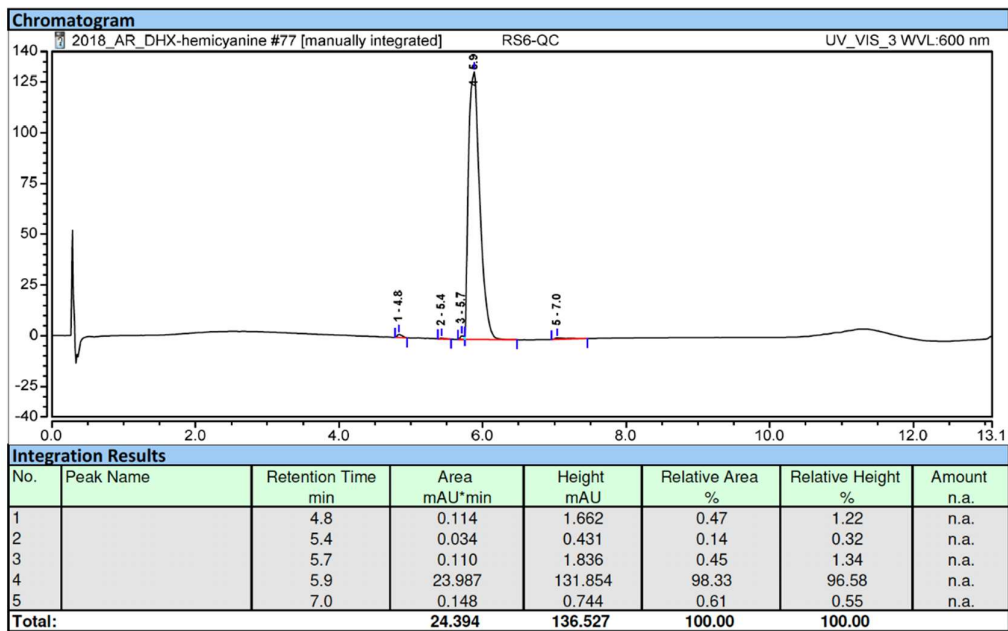
RP-HPLC elution profile of **2m** (system A, detection at 600 nm)



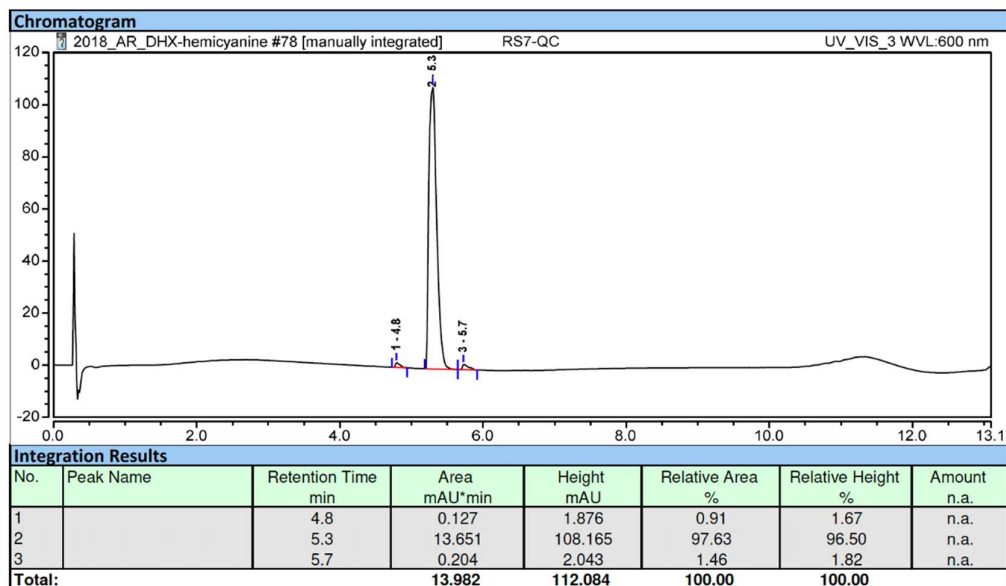
RP-HPLC elution profile of **8** (system A, detection at 600 nm)



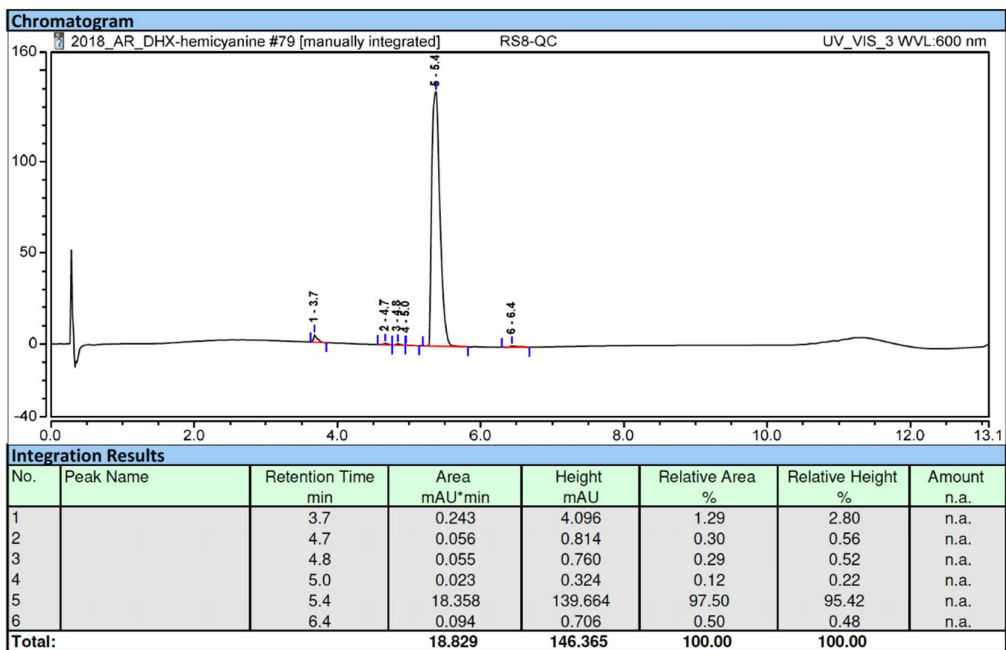
RP-HPLC elution profile of **2i** (system A, detection at 600 nm)



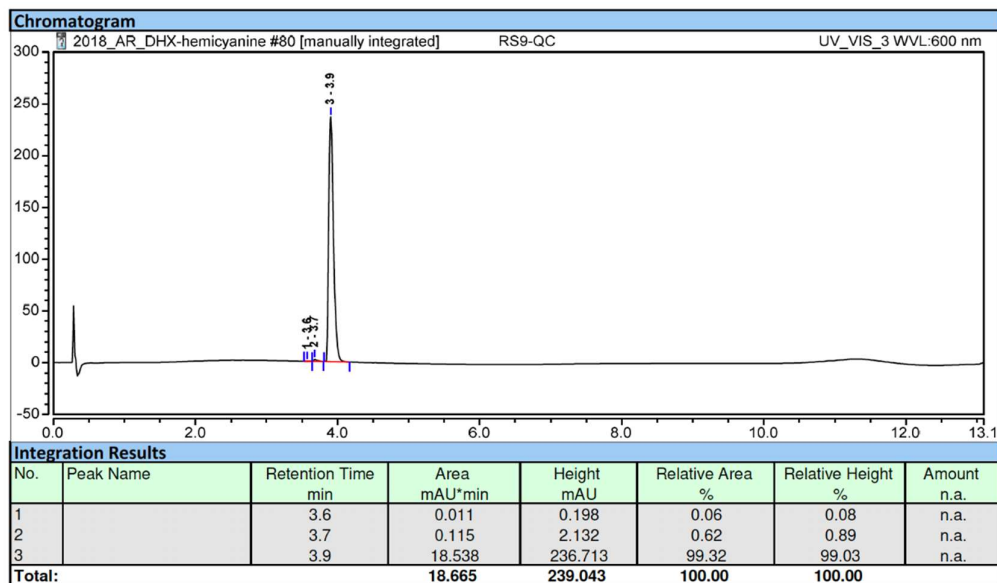
RP-HPLC elution profile of **2u** (system A, detection at 600 nm)



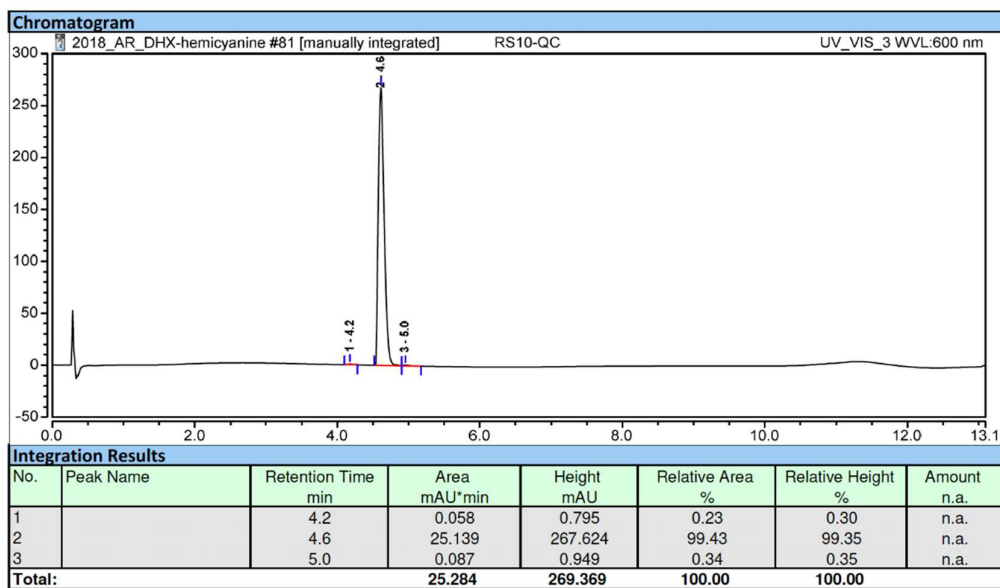
RP-HPLC elution profile of **2n** (system A, detection at 600 nm)



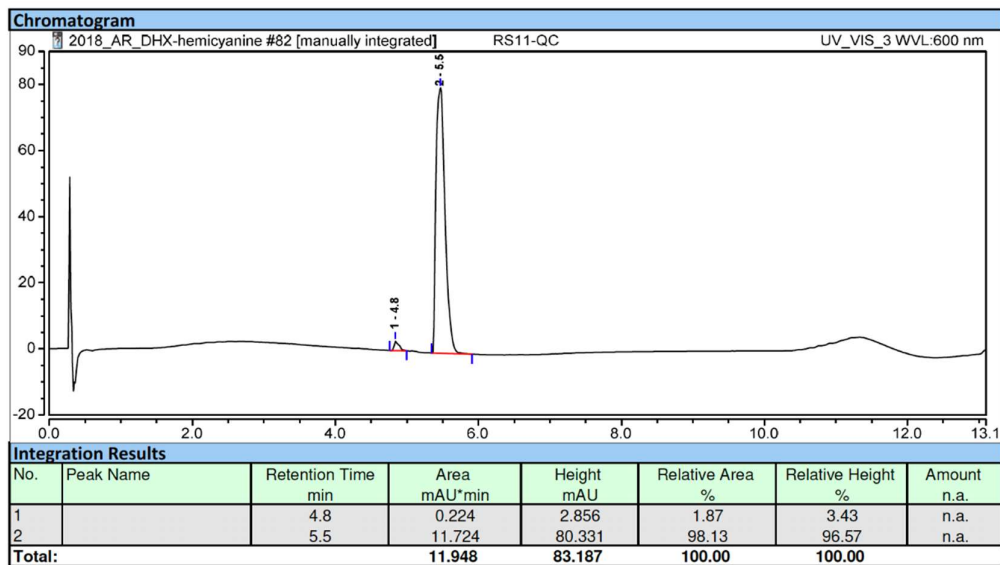
RP-HPLC elution profile of **2o** (system A, detection at 600 nm)



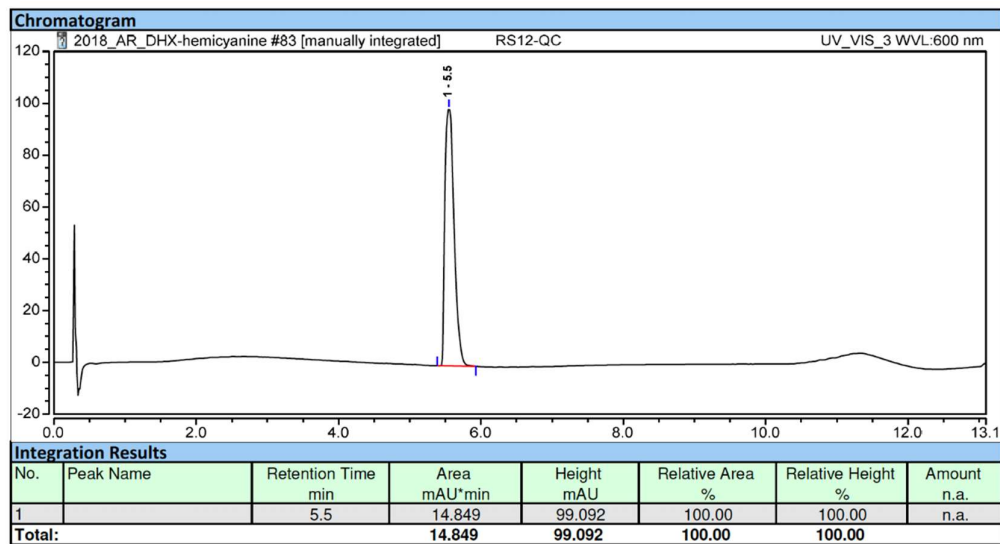
RP-HPLC elution profile of **2d** (system A, detection at 600 nm)



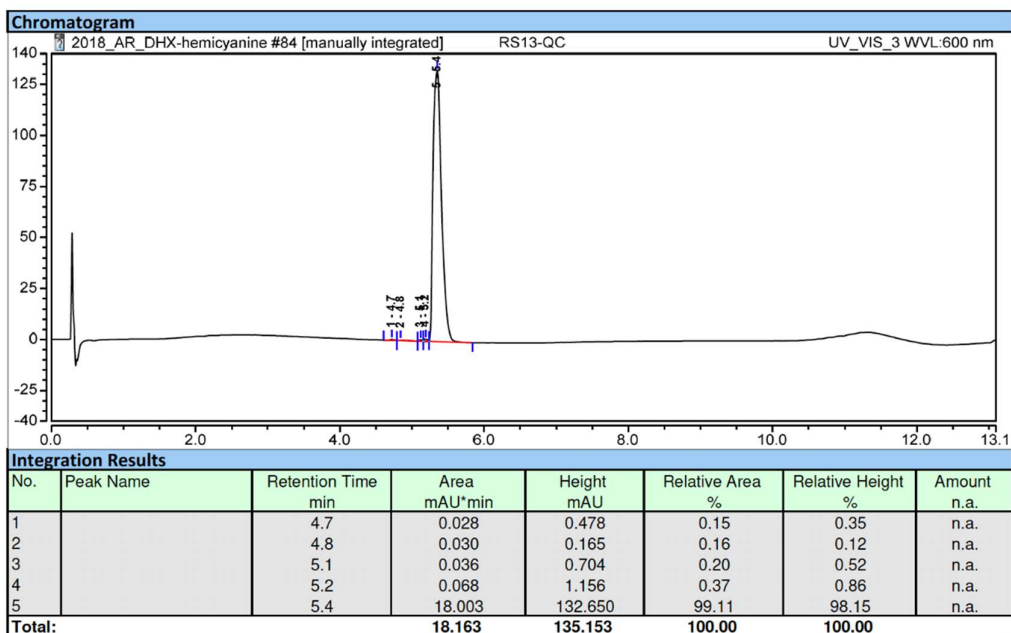
RP-HPLC elution profile of **2e** (system A, detection at 600 nm)



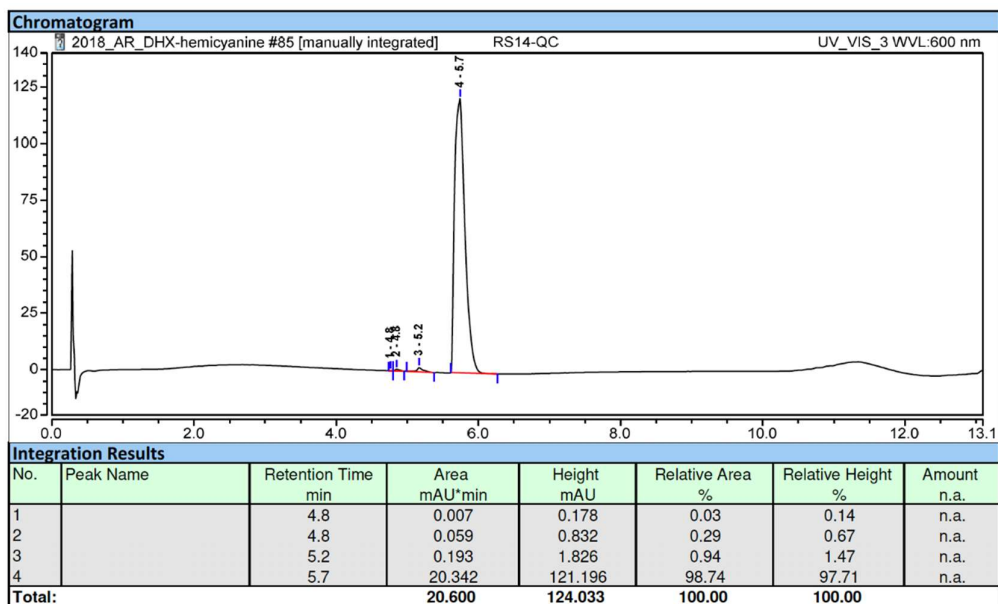
RP-HPLC elution profile of **2g** (system A, detection at 600 nm)



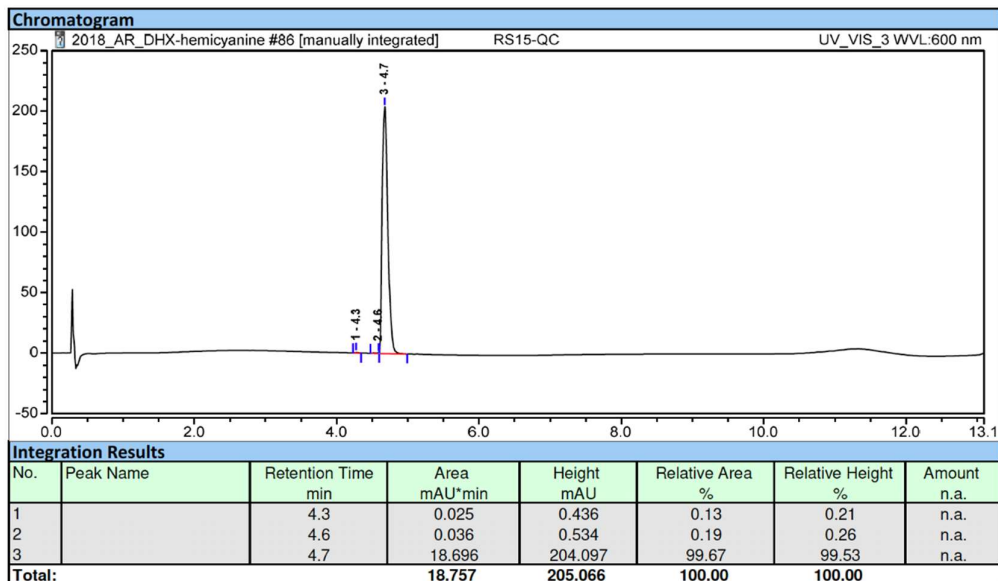
RP-HPLC elution profile of **2a** (system A, detection at 600 nm)



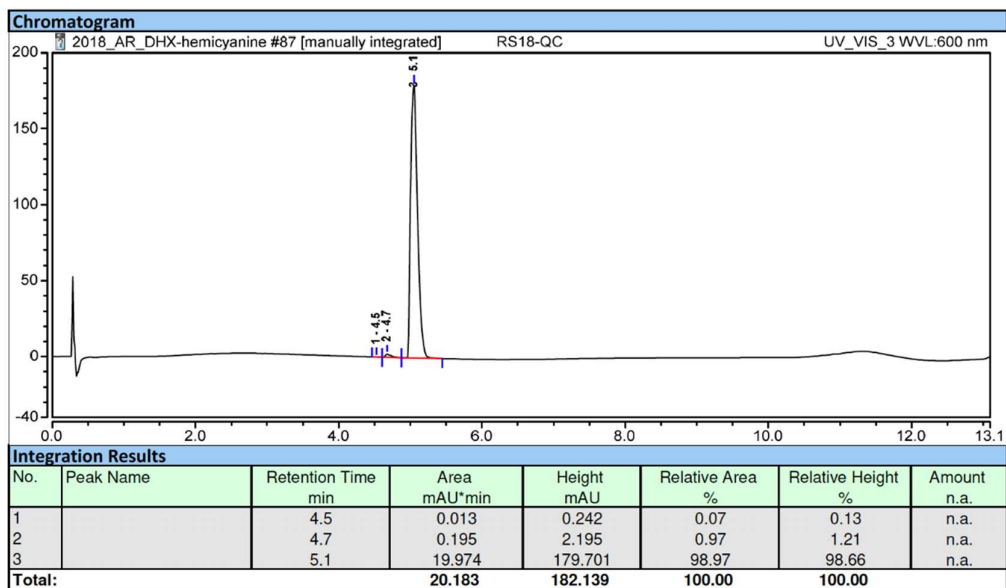
RP-HPLC elution profile of **2k** (system A, detection at 600 nm)



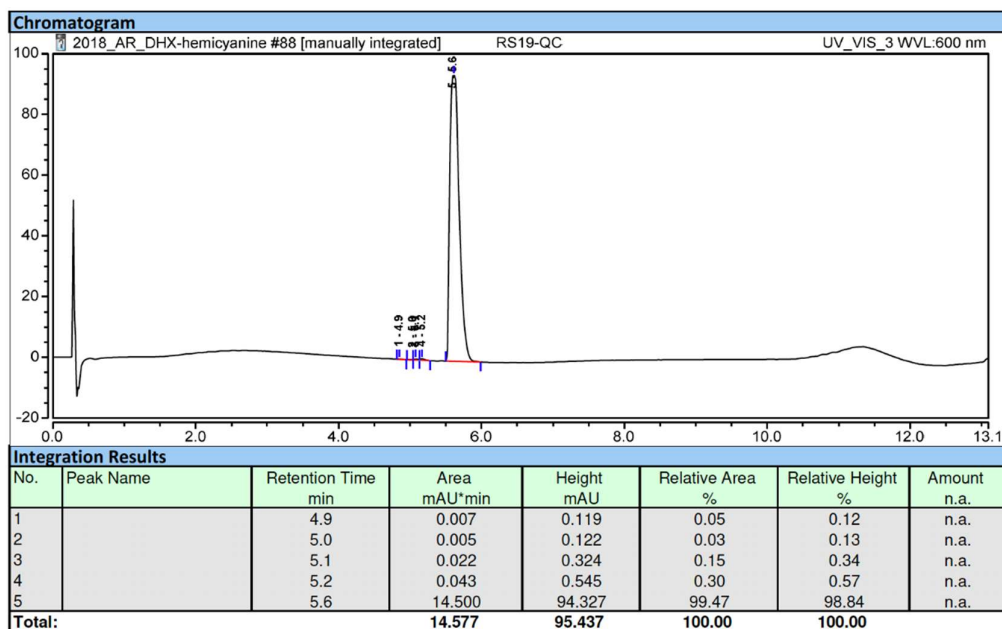
RP-HPLC elution profile of **2b** (system A, detection at 600 nm)



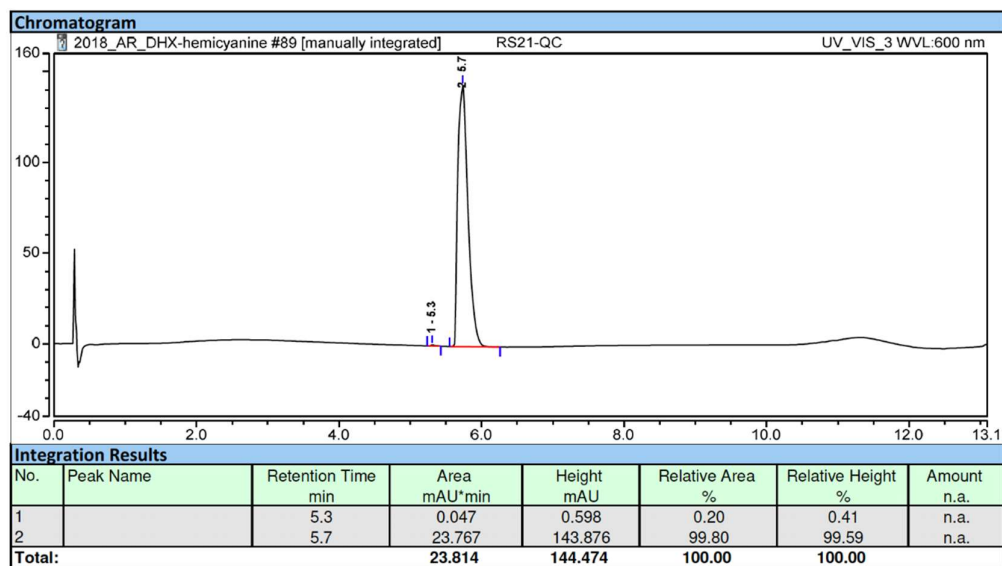
RP-HPLC elution profile of **2p** (system A, detection at 600 nm)



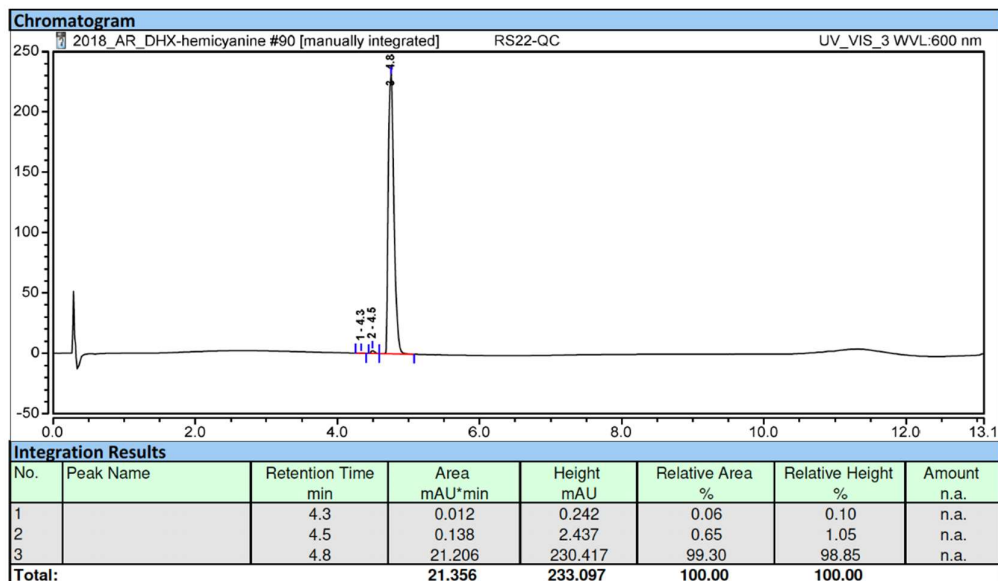
RP-HPLC elution profile of **2h** (system A, detection at 600 nm)



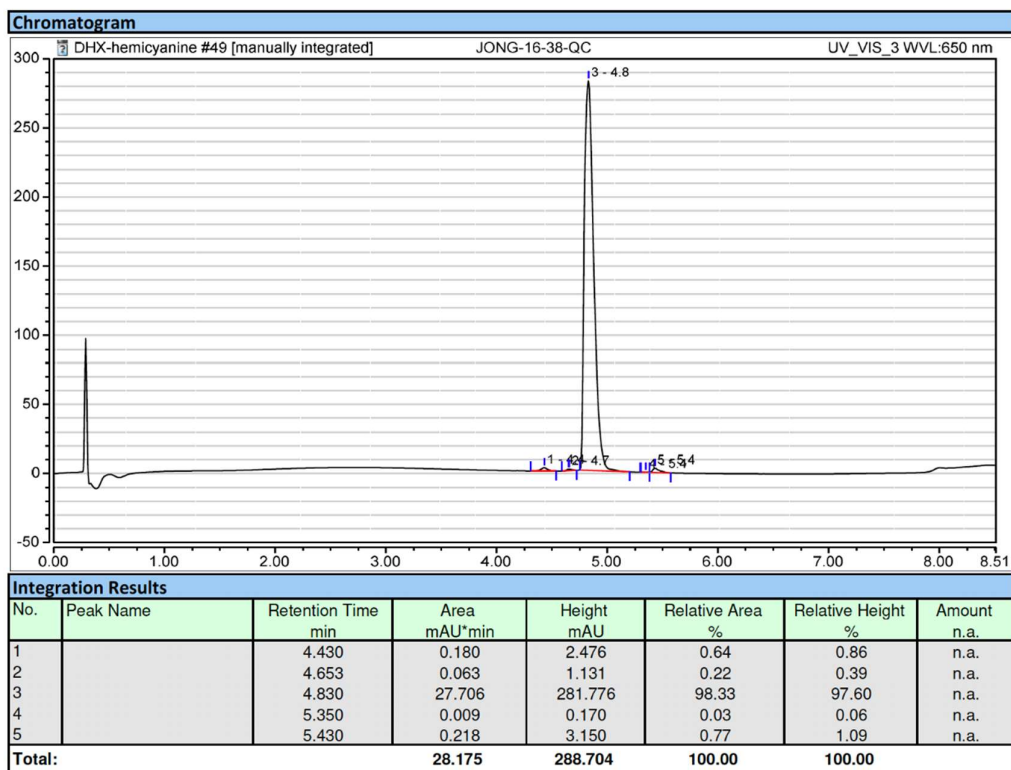
RP-HPLC elution profile of **2c** (system A, detection at 600 nm)



RP-HPLC elution profile of **2j** (system A, detection at 600 nm)

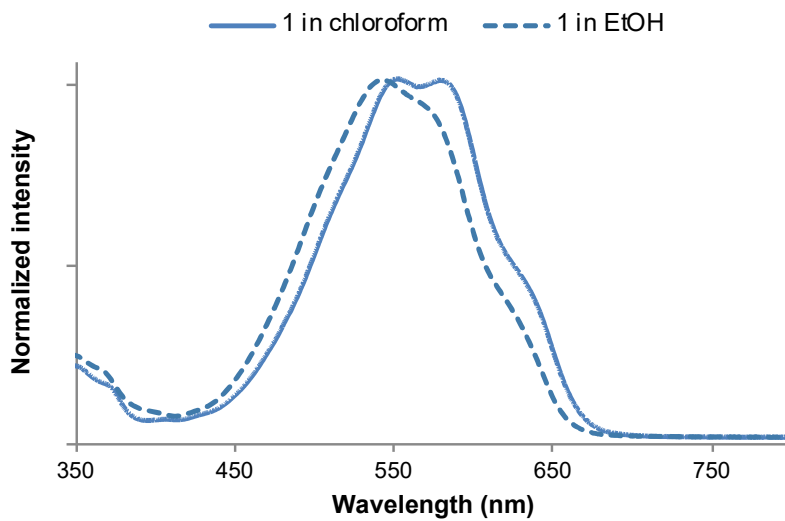


RP-HPLC elution profile of **2f** (system A, detection at 600 nm)

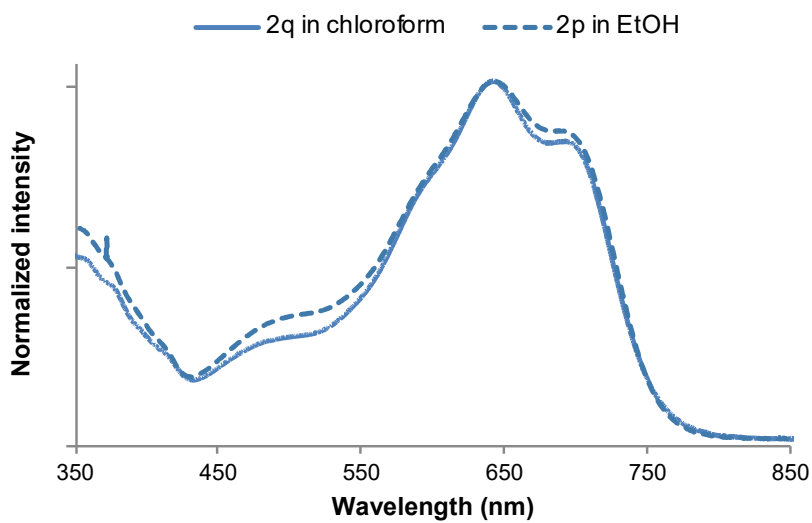


7. UV-visible absorption spectra of compound 1 and non-fluorescent 5',7'-difluoro-DHX-hemicyanine fused dyes

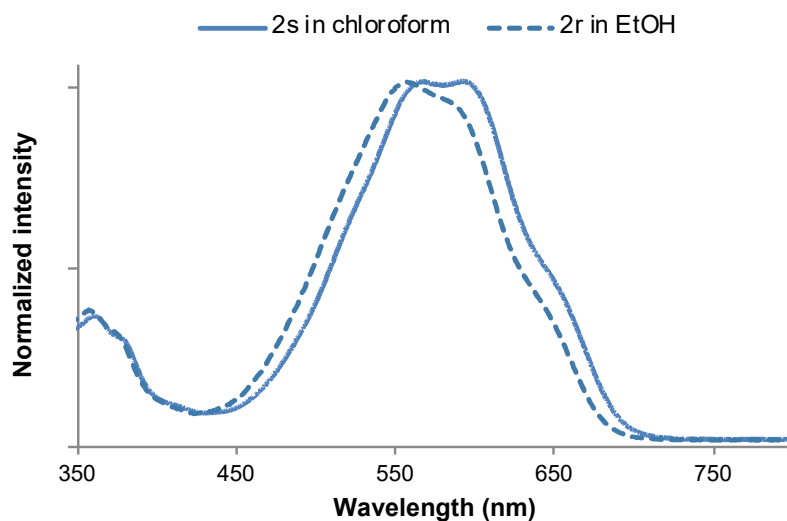
Compound 1



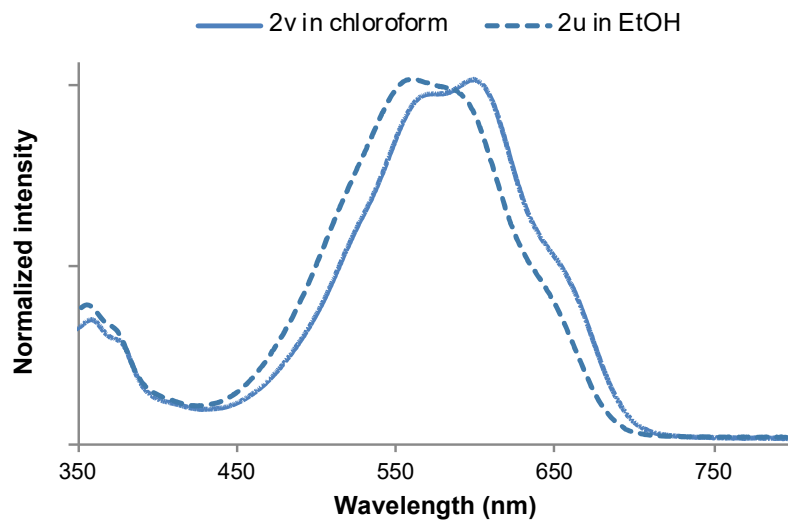
Compound 2q



Compound 2s



Compound 2v

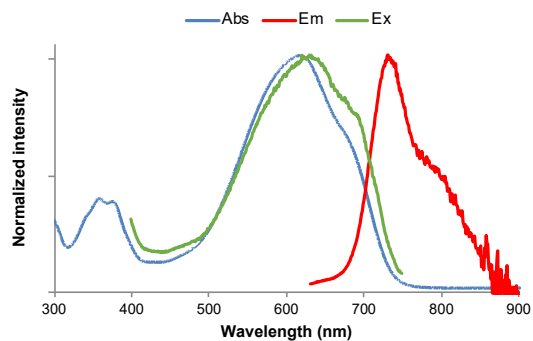


8. Absorption, excitation and emission spectra of selected 5',7'-difluoro-6'-amino-DHX-hemicyanine fused dyes

Please note: All emission spectra are corrected until 850 nm, which explains the artefact observed at this wavelength. UV-vis spectra recorded in the range 10^{-6} - 10^{-5} M for determination of molar extinction coefficients. Fluorescence Ex/Em spectra recorded in the range 10^{-7} - 10^{-6} M for QY determinations.

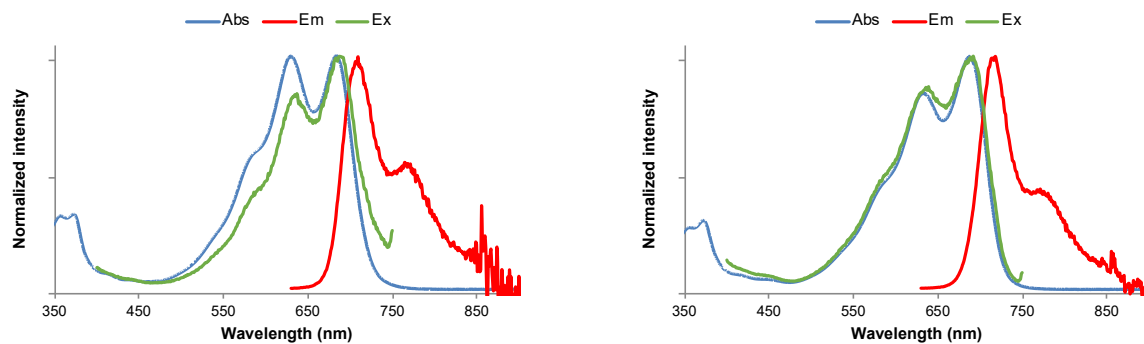
Compound 2a

EtOH, 25 °C, excitation at 615 nm, emission at 760 nm.



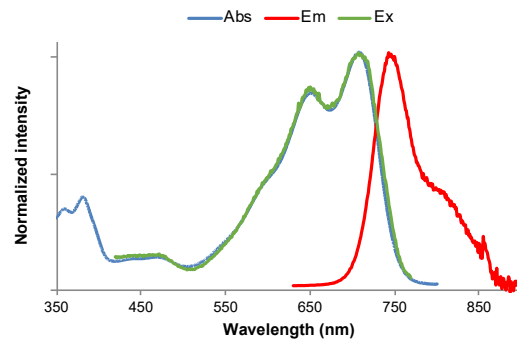
Compound 2d

CHCl₃ (left) & *EtOH* (right), 25 °C, excitation at 615 nm, emission at 760 nm.



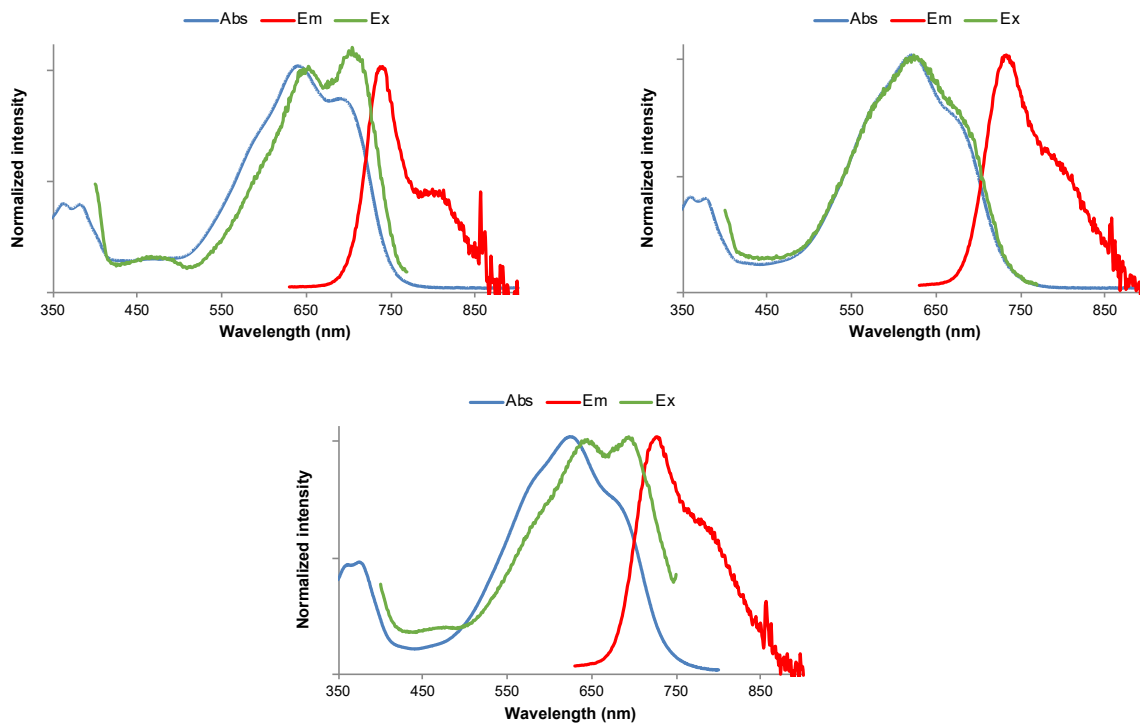
Compound 2e

EtOH, 25 °C, excitation at 615 nm, emission at 760 nm.



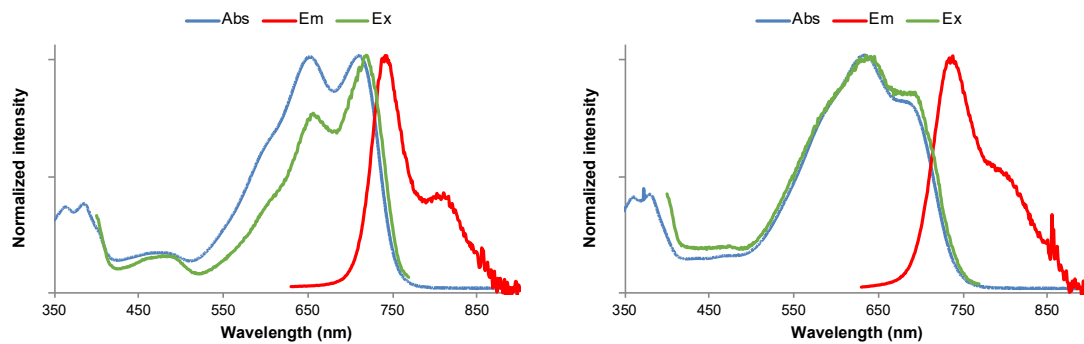
Compound 2g

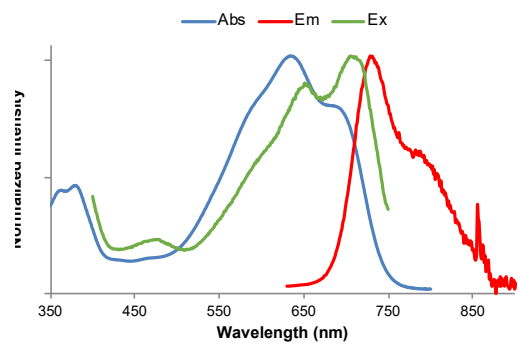
CHCl₃ (top left), *EtOH* (top right) & *PBS + 5% BSA* (bottom), 25 °C, excitation at 615 nm, emission at 800 nm (for Ex spectra in *CHCl₃* & *EtOH*), emission at 760 nm (for Ex spectrum in *PBS + 5% BSA*).



Compound 2k

CHCl₃ (top left), *EtOH* (top right) & *PBS + 5% BSA* (bottom), 25 °C, excitation at 615 nm, emission at 800 nm (for Ex spectra in *CHCl₃* & *EtOH*), emission at 760 nm (for Ex spectrum in *PBS + 5% BSA*).





Compound 8

CHCl₃ (left) & EtOH (right), 25 °C, excitation at 615 nm, emission at 760 nm.

